JAERI-M
8569

ANNUAL REPORT OF THE OSAKA LABORATORY FOR RADIATION CHEMISTRY JAPAN ATOMIC ENERGY RESEARCH INSTITUTE

(No. 12)

April 1, 1978-March 31, 1979

November 1979

Osaka Laboratory for Radiation Chemistry

日 本 原 子 力 研 究 所
Japan Atomic Energy Research Institute

Osaka Laboratory for Radiation Chemistry
Japan Atomic Energy Research Institute
25-1 Mii-minami machi, Neyagawa
Osaka, Japan

JAERI-M 8569

ANNUAL REPORT OF THE

OSAKA LABORATORY FOR RADIATION CHEMISTRY

JAPAN ATOMIC ENERGY RESEARCH INSTITUTE

(No. 12)

April 1, 1978 - March 31, 1979

(Received October 25, 1979)

This report describes research activities of Osaka Laboratory for Radiation Chemistry, JAERI during one year period from April 1, 1978 through March 31, 1979. The latest report, for 1978, is JAERI-M 7949.

Detailed descriptions of the activities are presented in the following subjects: studies on reactions of carbon monoxide, hydrogen and methane; polymerization under the irradiation of high dose rate electron beams; modification of polymers, degradation, cross-linking, and grafting.

Previous reports in this series are:

Annual Report, JARRP, Vol. 1	1958/1959*
Annual Report, JARRP, Vol. 2	1960
Annual Report, JARRP, Vol. 3	1961
Annual Report, JARRP, Vol. 4	1962
Annual Report, JARRP, Vol. 5	1963
Annual Report, JARRP, Vol. 6	1964
Annual Report, JARRP, Vol. 7	1965
Annual Report, JARRP, Vol. 8	1966
Annual Report, No. 1, JAERI 5018	1967
Annual Report, No. 2, JAERI 5022	1968
Annual Report, No. 3, JAERI 5026	1969
Annual Report, No. 4, JAERI 5027	1970
Annual Report, No. 5, JAERI 5028	1971
Annual Report, No. 6, JAERI 5029	1972
Annual Report, No. 7, JAERI 5030	1973
Annual Report, No. 8, JAERI-M 6260	1974
Annual Report, No. 9, JAERI-M 6702	1975
Annual Report, No. 10, JAERI-M 7355	1976
Annual Report, No. 11, JAERI-M 7949	1977

*Year of the activities

Keywords: Electron Beam Irradiation, γ-Irradiation, Carbon Monoxide-Hydrogen Reaction, Methane, Radiation-Induced Reaction, Polymerization, Grafting, Polymer Modification, Cross-Linking, Vinyl Monomer, Dienes, Polystyrene, Polyvinyl Chloride Fiber, Wood Plastic Combination, Cellulose Triacetate Film Dosimeter, Radiation Chemistry

JAERI－M 8569

昭和53年度日本原子力研究所 大阪研究所年報

日本原子力研究所 大阪研究所

（1979年10月25日受理）

本報告は、大阪研究所において昭和53年度に行なわれた研究活動を述べたものである。主な研究題目は、一酸化炭素、水素およびメタンの反応ならびにそれに関連した研究、高線量率電子線照射による重合反応の研究、ポリマーの改質および上記の研究と関連して重合反応、高分子分解、架橋ならびにクラフト重合に関する基礎的研究などである。

日本放射線高分子研究協会年報 Vol. 1			1958／1959
日本放射線高分子研究協会年報 Vol. 2			1960
日本放射線高分子研究協会年報 Vol. 3			1961
日本放射線高分子研究協会年報 Vol. 4			1962
日本放射線高分子研究協会年報 Vol. 5			1963
日本放射線高分子研究協会年報 Vol. 6			1964
日本放射線高分子研究協会年報 Vol. 7			1965
日本放射線高分子研究協会年報 Vol. 8			1966
日本原子力研究所大阪研における放射線化学の基礎研究 No.1	JAERI	5018	1967
日本原子力研究所大阪研における放射線化学の基礎研究 No.2	JAERI	5022	1968
日本原子力研究所大阪研における放射線化学の基礎研究 No.3	JAERI	5026	1969
日本原子力研究所大阪研における放射線化学の基礎研究 No.4	JAERI	5027	1970
日本原子力研究所大阪研における放射線化学の基礎研究 No.5	JAERI	5028	1971
日本原子力研究所大阪研における放射線化学の基礎研究 No.6	JAERI	5029	1972
日本原子力研究所大阪研における放射線化学の基礎研究 No.7	JAERI	5030	1973
Annual Report, Osaka Lab., JAERI, No.8	JAERI－M	6260	1974
Annual Report, Osaka Lab., JAERI, No.9	JAERI－M	6702	1975
Annual Report, Osaka Lab., JAERI, No.10	JAERI－M	7355	1976
Annual Report, Osaka Lab., JAERI, No.11	JAERI－M	7949	1977

CONTENTS

目　　次

I. INTRODUCTION

Osaka Laboratory was founded in 1958 as a laboratory of the Japanese Association for Radiation Research on Polymers (JARRP), which was organized and sponsored by some fifty companies interested in radiation chemistry of polymers. The JARRP was merged with Japan Atomic Energy Research Institute (JAERI) on June 1, 1967, and the laboratory changed its name from Osaka Laboratory, JARRP to Osaka Laboratory for Radiation Chemistry, JAERI. The research activities of Osaka Laboratory have been oriented towards the fundamental research on applied radiation chemistry.

The results of the research activities of the Laboratory were published from 1958 until 1966 in the Annual Reports of JARRP which consisted essentially of original papers. During the period between 1967 and 1973, the publication had been continued as JAERI Report which also consisted mainly of original papers. From 1974, the Annual Report has been published as JAERI-M Report which contains no original papers, but presents outlines of the current research activities in some detail. Readers who wish to have more information are advised to contact with individuals whose names appear under subjects.

The present annual report covers the research activities of the Laboratory between April 1, 1978 and March 31, 1979.

Most of the studies carried out in the Laboratory are continuation from the previous year, emphasis being laid on two fields; one is "Effect of radiation on the reaction of carbon monoxide, methane and hydrogen" and the other, "Radiation -induced polymerization by high dose rate electron beams".

Our high dose rate electron accelerator (HDRA) has been operated since May 31, 1975, and many results have been obtained using the HDRA.

The studies have been carried out on radiation chemistry of gas mixture of carbon monoxide and hydrogen in the presence of various solids such as Fe-Cu-diatomaceous earths, silica

gel, alumina, chromia-zinc oxide, or silver using electron beams from the HDRA.

Extensive studies on the reaction with Fe-Cu-diatomaceous earths reveal that the distribution of the products can be explained as contributions of radiation chemical reaction and catalytic reaction of gas mixture giving products, a part of which further reacts on the catalyst or with radiations. The presence of silica gel, which is inactive to the gas mixture below 350°C without radiation, gives hydrocarbon products when the gas mixture is irradiated at 300°C. Further, branched saturated hydrocarbons of C_4 and C_5 were found to form, indicating that the acidity of the silica gel was increased by irradiation.

The presence of chromia-zinc oxide or silver was found to give small effects on the radiation chemical reactions of the gas mixture.

The studies on radiation chemical reactions without the presence of solid have continued with attention laid particularly to the formation of acetaldehyde. The effects of temperature on G values of the products have been studied at 1000 Torr and 25 mole% carbon monoxide content under gas circulation, and at 5000 Torr and 15 mole% carbon monoxide content under static condition.

It was revealed that G(acetaldehyde), G(methanol), and G(formaldehyde) increased with increasing temperature at 5000 Torr.

The G values of the products were obtained as a function of pressure up to 10000 Torr under gas circulation condition using a new apparatus designed for this purpose. Preliminary results obtained for gas mixture containing 25 mole% carbon monoxide indicate that the G values of acetaldehyde, formaldehyde, and methanol increased with increasing pressure.

As a continuation from the study on radiation chemistry of methane initiated in the previous year, studies have been carried out on methane and binary gas mixture containing methane and nitrous oxide or carbon dioxide. The G value of ethylene formation was increased by 30% with the presence of

1 mole% nitrous oxide, but decreased by addition of carbon dioxide. Various oxygen containing organic compounds are found to be produced and the formation of acetic acid from gas mixture of methane and carbon dioxide is particularly interesting from our purpose.

Measurements of W values have been made on gas mixture of argon and ethane of different compositions at elevated pressures up to 7 atm. and a small increase of ionization efficiency was found for the gas mixture containing more than 80% ethane by increasing the pressure.

Coloration mechanism of cellulose triacetate (CTA) film has been studied. The coloration of CTA film containing triphenyl phosphate (TPP) was classified into two components: one formed during irradiation and the other built-up gradually after irradiation. The former is considered to be a contribution from color center formed in CTA, which is identical to that formed in cellulose, and that from phenol and biphenyl formed by radiolysis of TPP. The latter may arise from reaction of NO_2 produced by irradiation of air with CTA and TPP.

Studies on radiation-induced polymerization of styrene in carbontetrachloride and ethylene dichloride were continued. Somewhat unusual expression adopted last year for the discussion of the experimental results was revised and kinetic analysis of radical and cationic polymerization advanced. One of the important results concerning the radical polymerization in a wide range of dose rate is that several orders of magnitude greater number of initiating radicals are formed in radiation polymerization than in conventional catalytic polymerization and consequently termination by mutual reaction of growing radicals occur so frequently that the transfer to solvent molecules, which is important in the catalytic polymerization, can not be detected.

It is well known that in the case of ionic polymerization of styrene in bulk, termination with water and transfer to monomer are dominant factors to influence the rate and degree of polymerization. It is also the case in the solution

polymerization of styrene in carbontetrachloride and ethylene dichloride; however, it is probable that in the case of carbontetrachloride, solvent molecules also participate in termination.

In the course of the experiments on solution polymerization of styrene, a small amount of n-butylamine, an inhibitor to cationic polymerization, was added to the polymerization mixture, and a very interesting effect was observed that the rate of polymerization was not decreased but increased by the addition of n-butylamine. Though it was clear that the presence of carbontetrachloride is an important factor to the effect, studies on the binary mixture of styrene/n-butylamine were taken up. So long as it is concerned with the rate of polymerization, the results were not so dramatic in the absence of carbontetrachloride. It was found, however, some interesting phenomena, for example, formation of super polymer of styrene with molecular weight about 10^6, and the existence of two types of radical polymers.

Kinetic investigations have been carried out in bulk polymerization of butadiene. The rate of polymerization increased proportionally to dose rate in the wide range of dose rate from 5 rad/sec to 2×10^5 rad/sec. Molecular weight distribution of the products was independent of dose rate giving a number average molecular weight of about 2500. The products contain 75% 1,4- trans, 25% vinyl and no cis structure and contain about 80% residual double bonds. Cross-linking was found to occur in the polymer when the conversion exceeded 10%.

These results indicate that the polymerization proceeds with cationic mechanism without contribution of radical mechanism, and cyclization and cross-linking occur concurrently with the polymerization by cationic mechanism. It was also found that copolymerization with styrene and vinyl chloride occurs, suggesting that improvement of some properties of the butadiene oligomer may be possible by the copolymerization.

In an attempt to prepare fiber of general use by giving heat resistance and flame retardancy to polyethylene, studies have been carried out on grafting of acrylic acid (AA) onto

high density polyethylene filament by irradiating the polymer immersed in the monomer. The rate of grafting was small at room temperature, but by raising the irradiation temperature, fiber of high degree of grafting can be obtained. Microscopic observation of the cross section of the grafted fiber revealed that the graft percent increased gradually from outer to center part of the fiber with increasing degree of grafting.

It was found that the heat resistance of the grafted fiber was improved by the grafting of AA, but by converting to poly(acrylic acid) calcium salt, the grafted fiber of sufficient heat resistance was obtained for the fiber of smaller degree of grafting.

Studies in an attempt to prepare polymer having hydrophilic and hydrophobic parts have been continued. This year, the rate of grafting of AA onto polyvinyl chloride powder has been studied under various reaction conditions, especially, the composition of monomer solution (water/ethylene dichloride (EDC)/acrylic acid (AA)), and the adsorbability of metal ions has been also investigated for the grafted powder obtained under different reaction conditions mentioned above.

The relationship between adsorbability and the reaction conditions in which the grafted powder was obtained was discussed in relation to distribution of PAA in the PVC particle. The adsorbabilities were also examined for grafted powder obtained from trunk polymers having different molecular weights.

Administrative changes were made in the Laboratory on October 1, 1978. Tomomichi Kasamatsu moved to Takasaki Radiation Chemistry Research Establishment as the establishment director and Yunosuke Oshima was appointed Head of the Laboratory.

August 31st, 1979

Dr. Yunosuke Oshima , Head
Osaka Laboratory for Radiation Chemistry
Japan Atomic Energy Research Institute

II. RECENT RESEARCH ACTIVITIES

[1] Radiation-Induced Reactions of Carbon Monoxide, Hydrogen, and Methane

1. Irradiation of Gas Mixtures of Carbon Monoxide and Hydrogen under Circulation

In the last annual report, some experimental results were described on the product yields under various conditions such as composition of the reactants, pressure, and the presence or absence of cold traps. As a continuation of this study, experiments are carried out in order to know the product yields as a function of irradiation temperature. The irradiations are carried out using electron beams from the HDRA (0.4 MeV, 0.5 mA, 400 sec) and dose rate determined by N_2O is 5.22×10^{-4} eV·mole^{-1}·sec^{-1}. The temperature during irradiation was kept at desired temperature by using coolant of appropriate temperature. The concentration of carbon monoxide, reactant pressure, and irradiation time are 25 mole%, 1000 Torr, and 400 sec, respectively. Two cold traps cooled by dry ice-ethanol bath were inserted in the gas circulation system to remove condensable products from the reactant to avoid further irradiation.

Non-condensable products in a circulating gas were analyzed with a gaschromatograph on a Porapak Q column by intermittent sampling during and after irradiation using a gas sampler which is a part of the gas circulation system. Condensable products were found in the cold traps after irradiation together with those collected in a series of cold traps (-78°C and -196°C) through which the irradiated gas was evacuated from the irradiation vessel after the final gas sampling. The condensable products were subjected to gaschromatography and mass spectrometry.

The G values of the products are shown as a function of irradiation temperature in Figs 1A, 1B, 2A, 2B, and 3 for

hydrocarbons, aldehydes and other oxygen containing products, respectively.

As shown in Figs. 1A and B the G value of methane decreases with increasing temperature, while those of ethylene increases with increasing temperature. The G value of ethane is independent of temperature. The G values of formaldehyde and its polymers, trioxane (TOX) and tetraoxane (TEOX), decrease quite

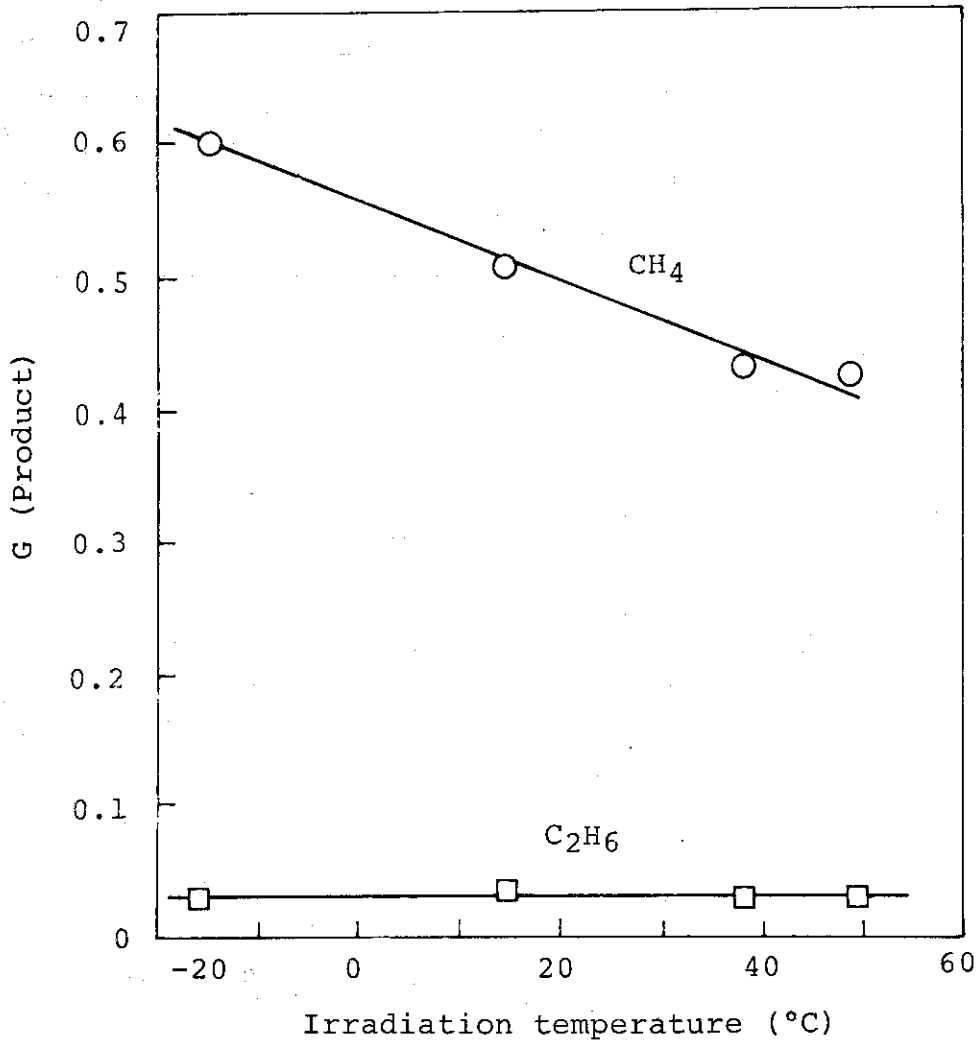

Fig. 1A. G values of hydrocarbon products as a function of temperature: CO content, 25%; reactant pressure, 1000 Torr; electron energy, 0.4 MeV; beam current, 0.5 mA; dose rate, 5.22×10^{-4} eV·N_2O molec^{-1}·sec^{-1}; irradiation time, 400 sec; volume of the irradiation vessel, 7.1 ℓ.

similarly when the irradiation temperature increased from -20°C to 15°C, (Fig. 2A and B) possibly indicating that precursors for these compounds are the same. The G value of acetaldehyde seems to be independent of temperature. The G values of the other products (Fig. 3) are almost independent of temperature, except for methyl formate, the G value of which scatters, and therefore no definite temperature dependence can be seen.

The temperature dependences of G values of some products found in the present study are different from those of earlier study using static method in the condition that the products were further irradiated in the reactant gas because no effort was made to remove products from reactant gas by cold traps.

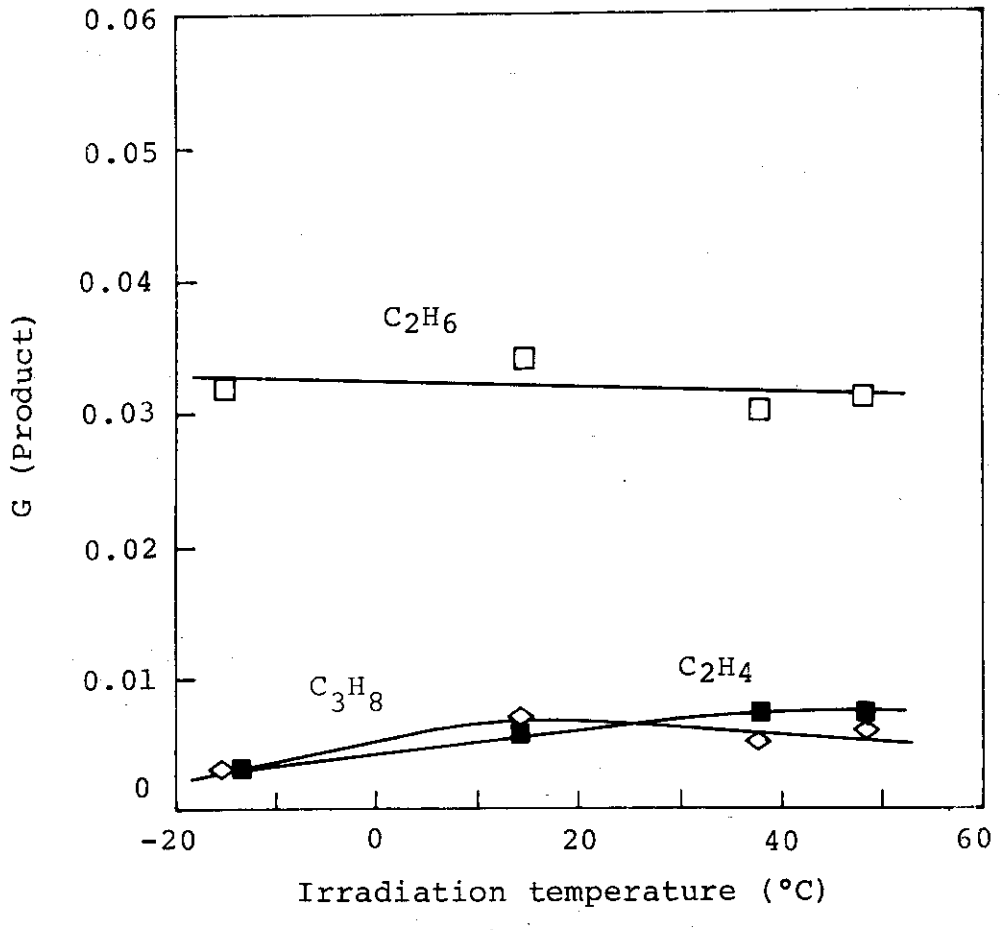

Fig. 1B. G values of hydrocarbon products as a function of temperature: the reaction conditions are given in the caption of Fig. 1A.

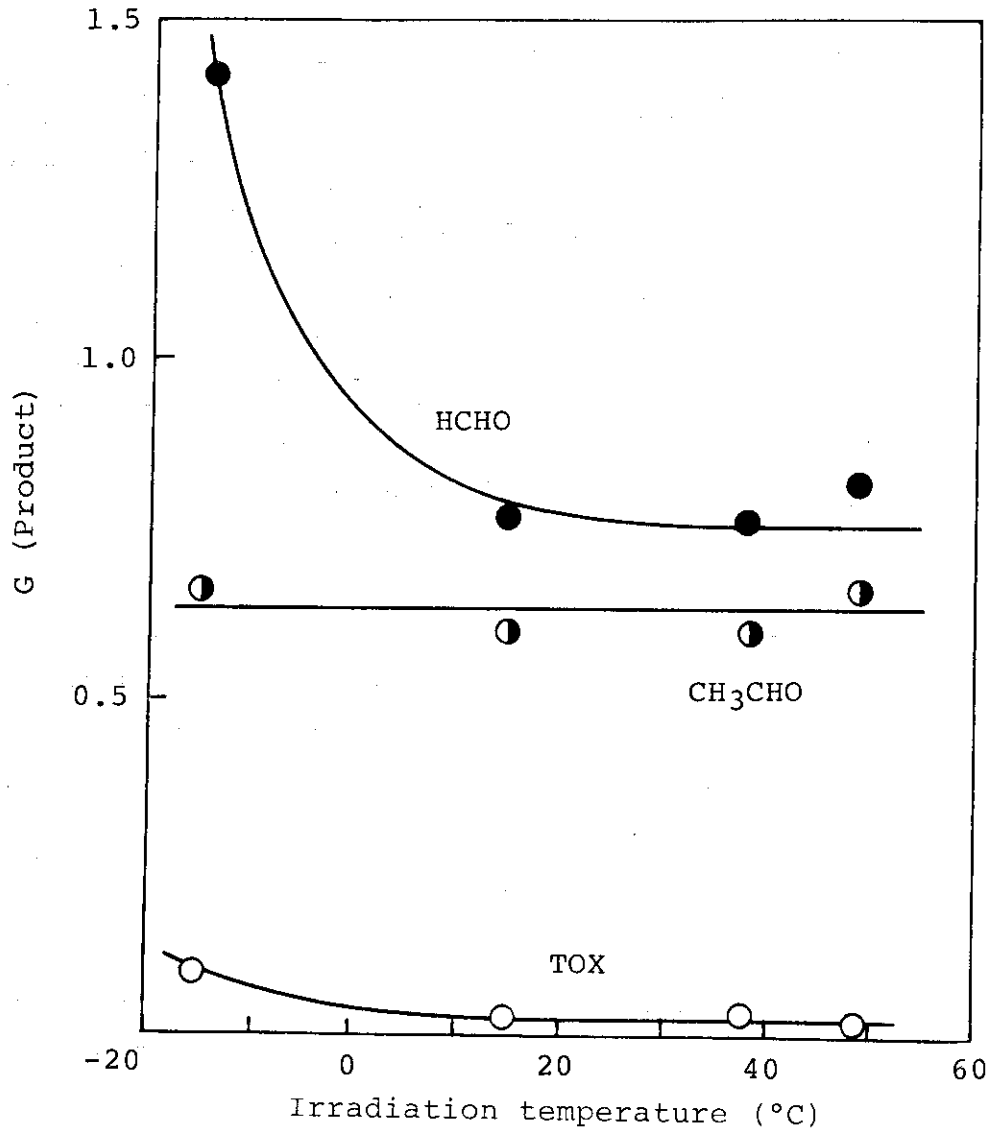

Fig. 2A. G values of aldehydes as a function of temperature: the reaction conditions are given in the caption of Fig. 1A.

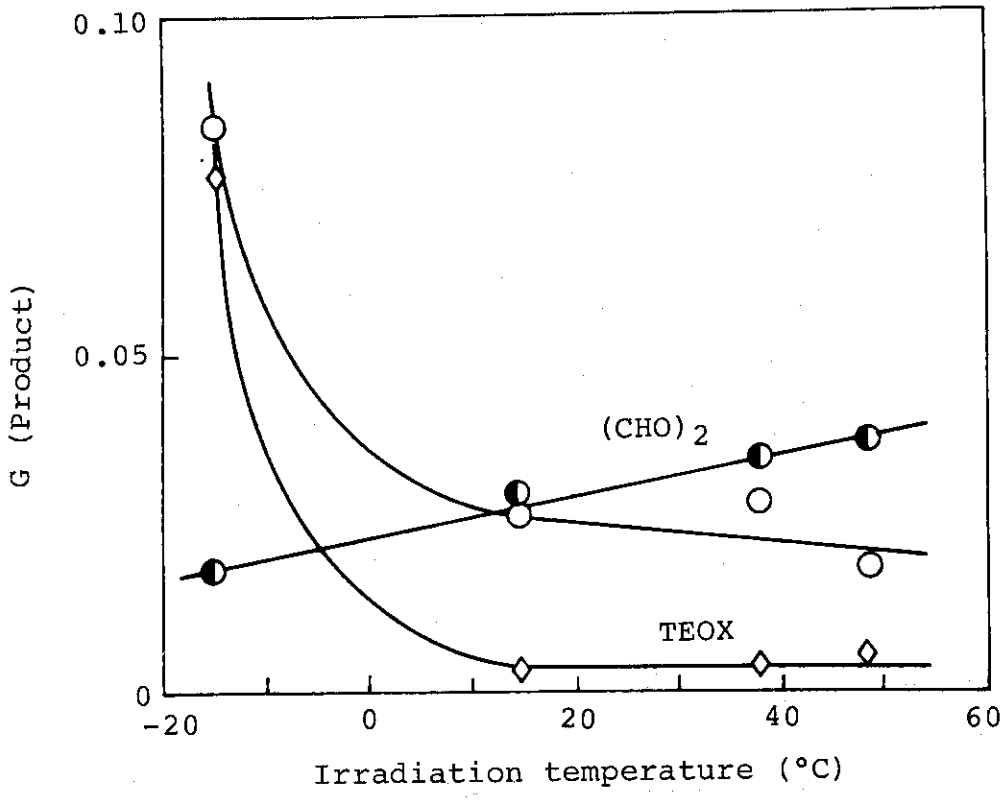

Fig. 2B. G values of aldehydes as a function of temperature: the reaction conditions are given in the caption of Fig. 1A.

(See Fig. 17, JAERI-M 7899, p. 65.) For example, the G values of formaldehyde showed positive temperature dependence, which appears reversely in the present study.

The G value of acetaldehyde in the earlier study decreased markedly with increasing temperature, probably due to the fact that the acetaldehyde produced as converted to other compounds by further reaction.

The temperature dependences of other compounds such as methanol or TOX are the same with those obtained at earlier work. No data are available for hydrocarbons in the earlier work to be compared with the results obtained in the present research.

The effect of addition of methane has been examined in an attempt to improve selectivity of the radiation chemical

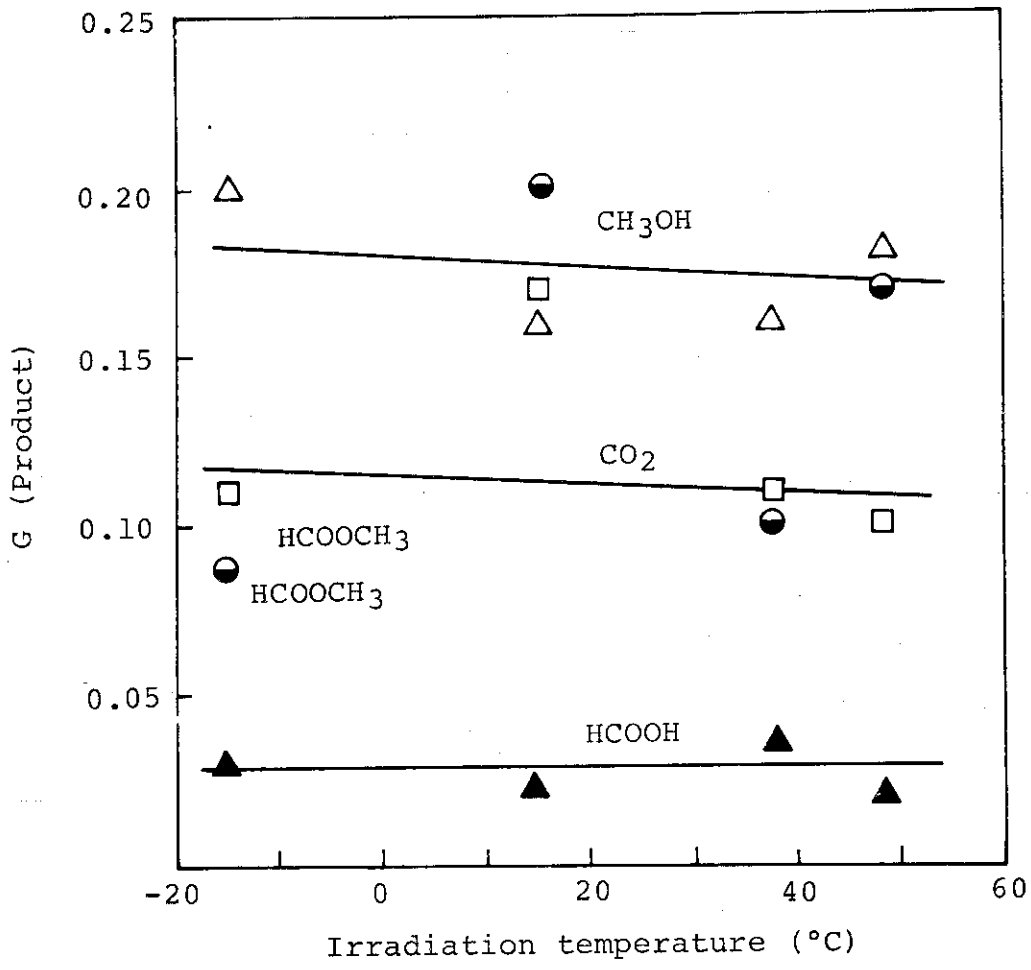

Fig. 3. G values of oxygen containing products as a function of temperature: the reaction conditions are given in the caption of Fig. 1A.

reaction. When the concentration of methane was increased up to 2.1 mole%, the G values of hydrocarbons increased by 50% whereas the G values of formaldehyde, tetraoxane, water, and carbon dioxide decreased. The G values of other compounds did not change by the addition of methane.

(S. Sugimoto and M. Nishii)

2. Irradiation of Gas Mixtures of Carbon Monoxide and Hydrogen at Elevated Pressure at Static Condition

We have examined the effect of electron energy on the product yields and the product yields as a function of carbon monoxide content in the reactant using electrons of 0.8 MeV incident energy at elevated pressure of 5000 Torr.

For this purpose we used the irradiation vessel of 2.66 ℓ, the details of which were described in the last annual report.

Irradiations are performed by electron beams from the HDRA (0.4 ∿ 0.8 MeV, 0.1 mA) for 1000 seconds on the gas mixtures containing hydrogen and carbon monoxide of various compositions at -30°C. Dose rates absorbed by N_2O gas in the vessel are estimated to be 0.60×10^{-4} and 1.77×10^{-4} eV·molecule^{-1}·sec^{-1} for 0.4 MeV and 0.8 Mev electrons, respectively.

After irradiation, the reactants and products in the reaction vessel were pumped off through cold traps in which condensable products were collected. The products recovered from the cold traps were subjected to gaschromatography and mass spectrometry. The products which are not condensed in the traps were not analyzed.

The product yields from gas mixture containing 15 mole% CO are plotted as a function of electron accelerating voltage in Figs. 1A and 1B, where all the yields of the products are shown to increase with increasing accelerating voltage. This result mainly comes from the fact that the range of electrons in the gas mixture becomes longer to irradiate the gas more uniformly as the incident electron energy becomes higher from 0.4 MeV to 0.8 MeV. Another factor to increase the yields with increasing accelerating voltage is that the temperature of the gas mixture increases since more energy is absorbed by vessel wall when the incident electron energy increases. The calculation of G values from this result revealed that the changes of G values of these products due to the incident electron energy are small, however.

The G values of the products obtained by irradiation at

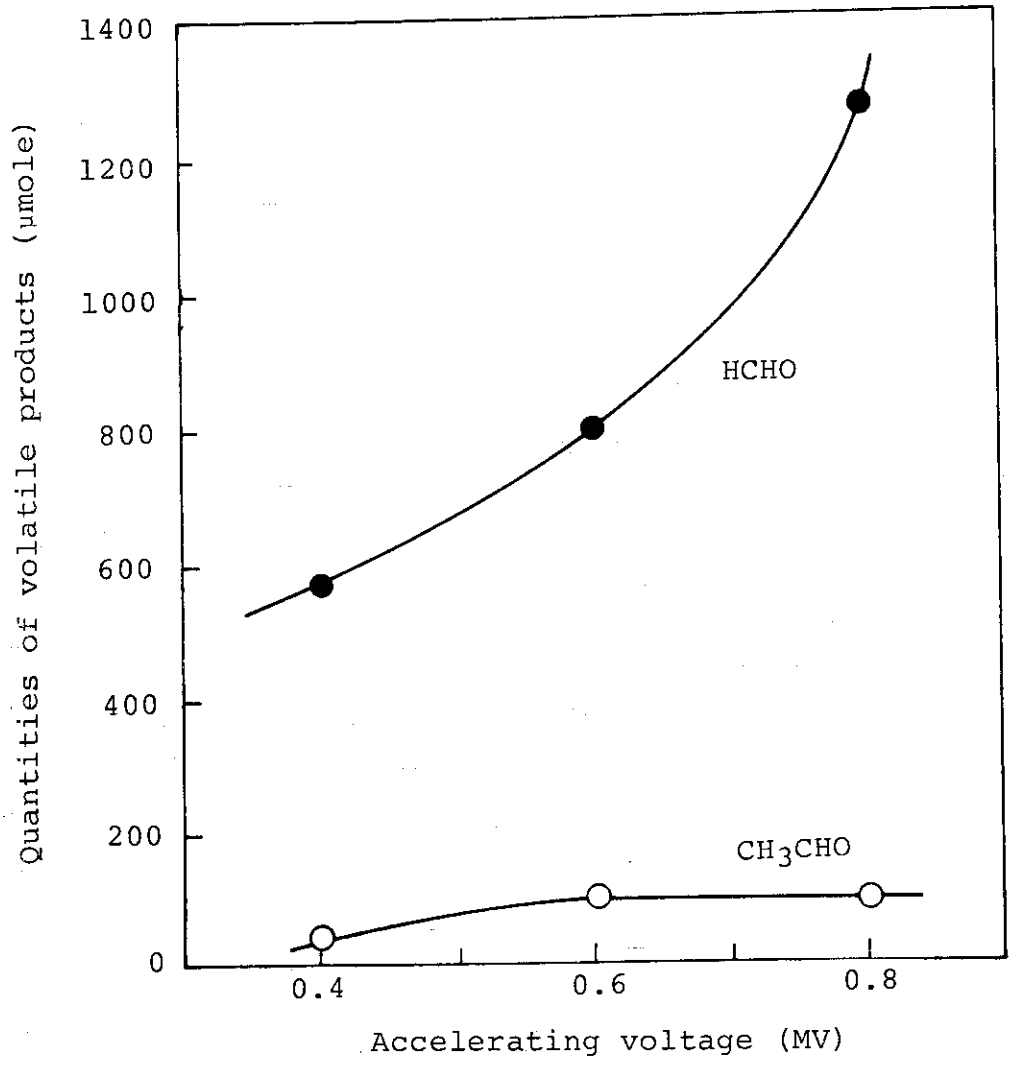

Fig. 1A. The yields of the products as a function of electron accelerating voltage: CO content, 15 mole%; reactant pressure, 5000 Torr; temperature, -30°C; beam current, 0.1 mA; irradiation time, 1000 sec.

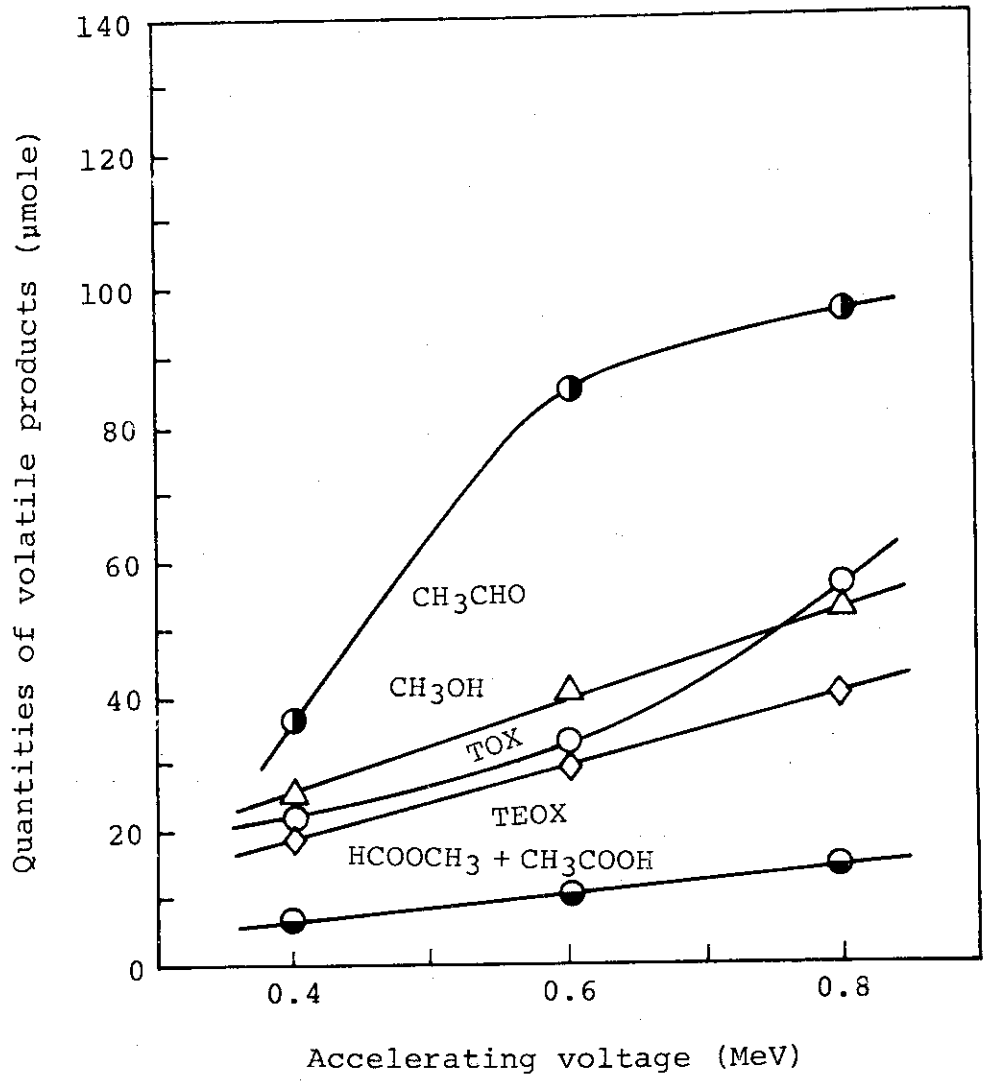

Fig. 1B. The yields of the products as a function of electron accelerating voltage: the reaction conditions are given in the caption of the Fig. 1A.

5000 Torr gas pressure are plotted against CO content in the gas mixture in Figs. 2 and 3 for aldehydes and cycloethers and for other oxygenated products, respectively.

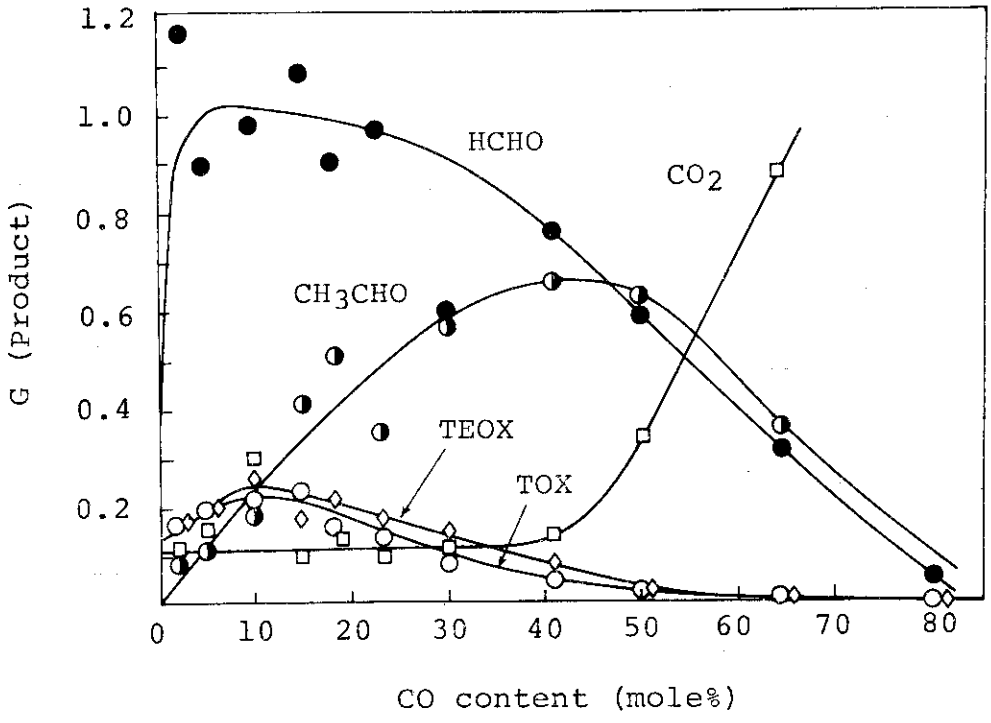

Fig. 2. G values of the products as a function of CO content: pressure, 5000 Torr; temperature, -30°C; incident electron energy, 0.8 MeV; beam current, 0.1 mA; irradiation time, 1000 sec.

The CO contents which give highest G values of the products are 10% (all in mole%) for trioxane (TOX) and tetraoxane (TEOX), 45% for acetaldehyde and below 5% for formaldehyde. The maximum G values of methanol and methylformate + acetic acid appear below 5% and at 50% respectively. The G value of carbon dioxide becomes larger above 50%. Some of these results, for example, G_{max} (CH_3CHO), are different from the previous results obtained at the same pressure but with the incident electron energy of 0.4 MeV, probably because of poor penetrating power of 0.4 MeV electrons for gas mixture

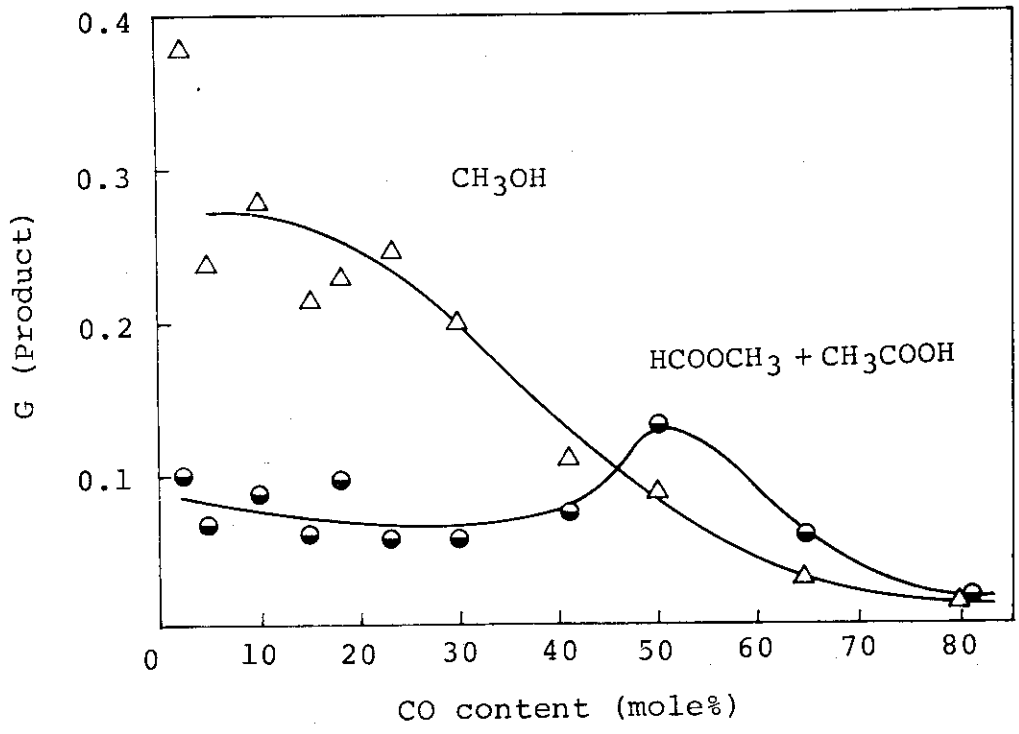

Fig. 3. G values of the products as a function of CO content: the reaction conditions, see the caption of Fig. 2.

containing carbon monoxide at higher concentrations.

(S. Sugimoto and M. Nishii)

3. Irradiation of the Circulated Gas Mixtures of Carbon Monoxide and Hydrogen under Elevated Pressure

In the previous studies, it was found that the raise of gas pressure was effective to increase space time yields of the products, and the use of cold traps was also effective to increase some products by preventing decomposition of the products by repeated irradiation of the products. Therefore, we made a new irradiation system which can irradiate circulating gas mixture under elevated pressures up to 10,000 Torr.

The irradiation vessel contains 8 ℓ gas mixture and has a titanium window (dimensions, 4 cm x 40 cm; thickness, 100 μm)

on top and a pressure sensor (Rose Mount Co., Alphaline type 1151GP and 1151 DP). The gas mixture is circulated by a circulation pump (Aoki Mfg. Co., SG-2A-135) through the irradiation vessel, two cold traps and a flow meter sensor (Hasting H3M AHL-25P). A part of gas stream flows through a gas sampler to the gaschromatograph. All equipments can be remote-operated during irradiation from the operation room of the accelerator which is 20 m away from the irradiation area. The whole system is composed of stainless steel and was evacuated below 10^{-5} Torr before charging the gas mixture.

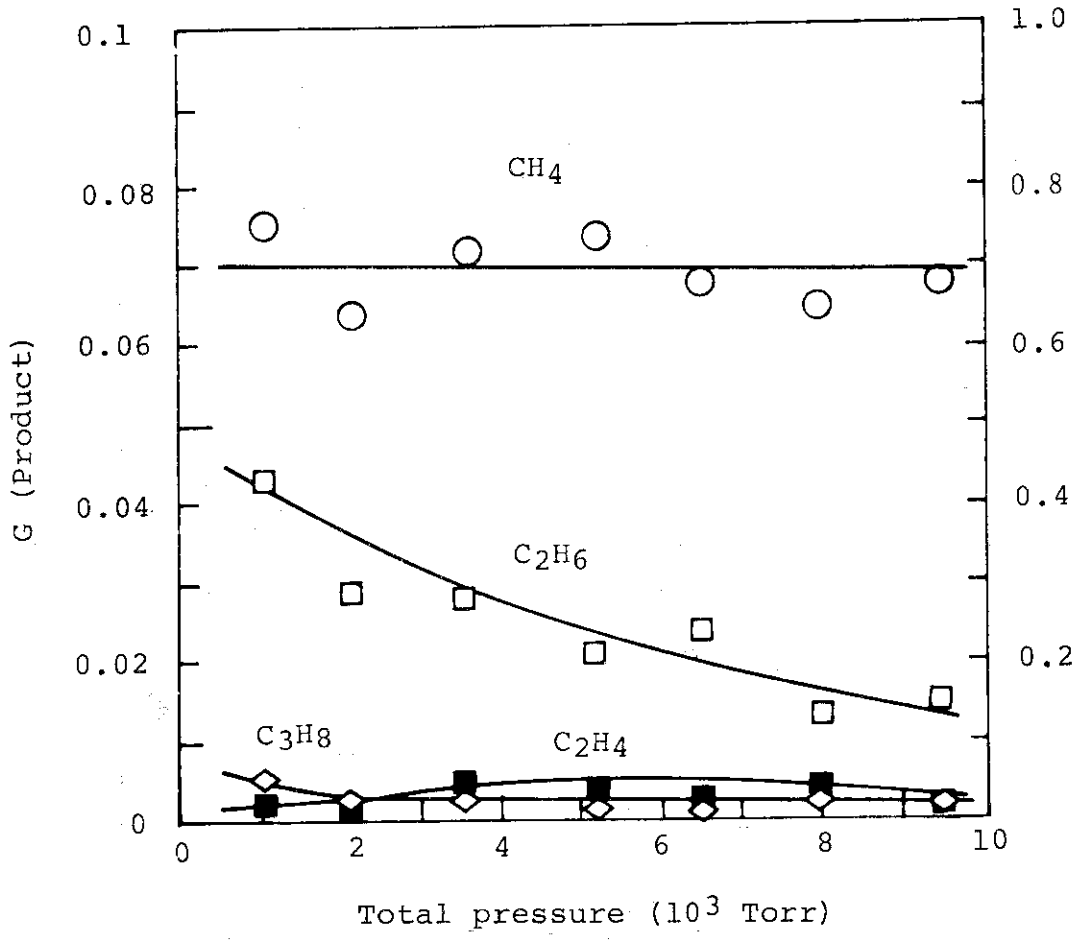

Fig. 1. G values of the products as a function of reactant pressure: concentration of CO, 25 mole%; temperature, -30°C; electron accelerating voltage, 0.8 MV; beam current, 2 mA; irradiation time, 400 sec.

Irradiations are performed by electron beams from the HDRA (0.8 Mev, 2 mA) for 400 seconds on the gas mixtures containing hydrogen and carbon monoixde of various compositions at -30°C. Dose rate absorbed by N_2O gas in the vessel is estimated to be 7.88×10^{-4} eV·molecule^{-1}·sec^{-1}.

After the irradiation, the reactants and products in the reaction vessel were pumped off through cold traps in which condensable products were collected. The products recovered from the cold traps were subjected to gaschromatography and

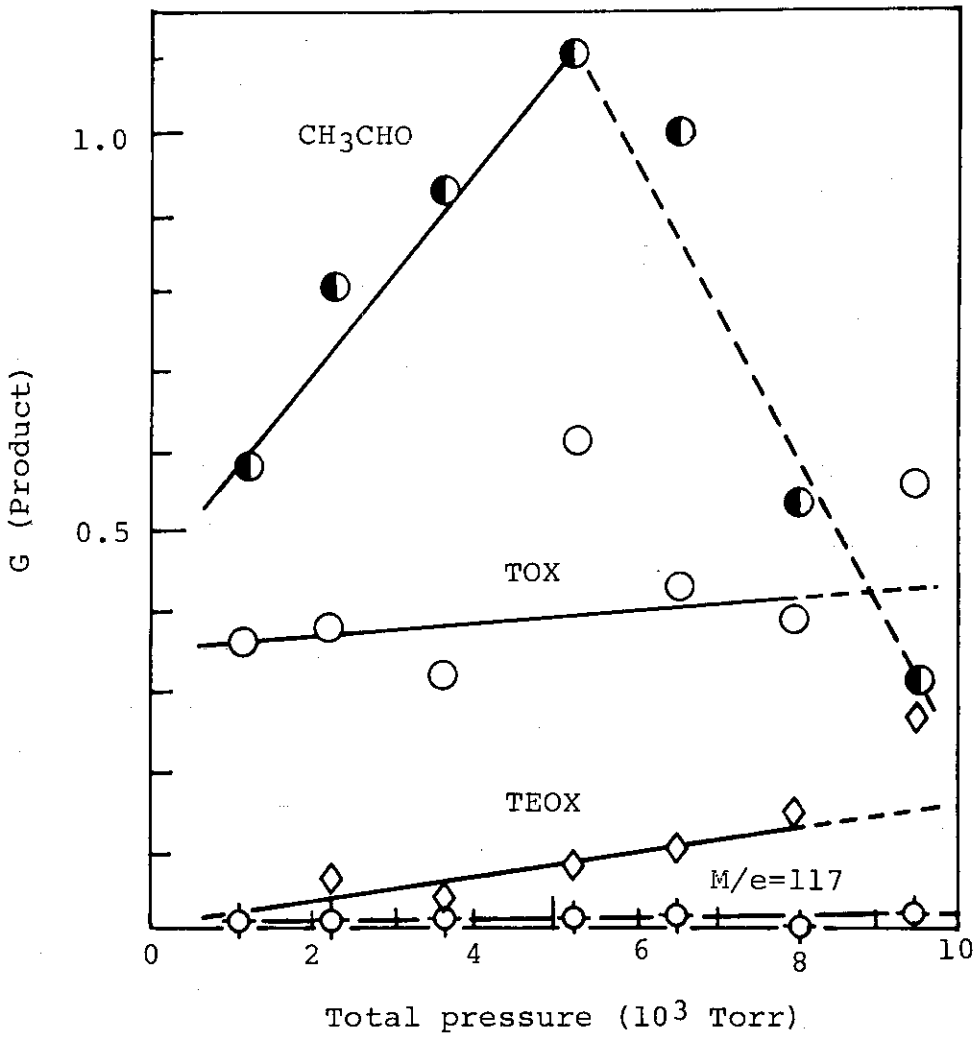

Fig. 2A. G values of the products as a function of reactant pressure: for the reaction conditions, see the caption of Fig. 1.

mass spectrometry.

The G values of the products from the reactant containing 25 mole% CO are plotted against pressure of the reactant in Figs. 1, 2 and 3 for hydrocarbons, aldehydes and cyclic ethers, and other oxygen containing products, respectively.

As shown in Fig. 1, the G values of methane, ethylene and propane are independent of the pressure, while the G value of ethane decreases with increasing pressure. The G values of formaldehyde TOX and TEOX increase with increasing pressure (Figs. 2A and 2B); the G value of formaldehyde increases to approach a certain value, while that of TEOX linearly increases.

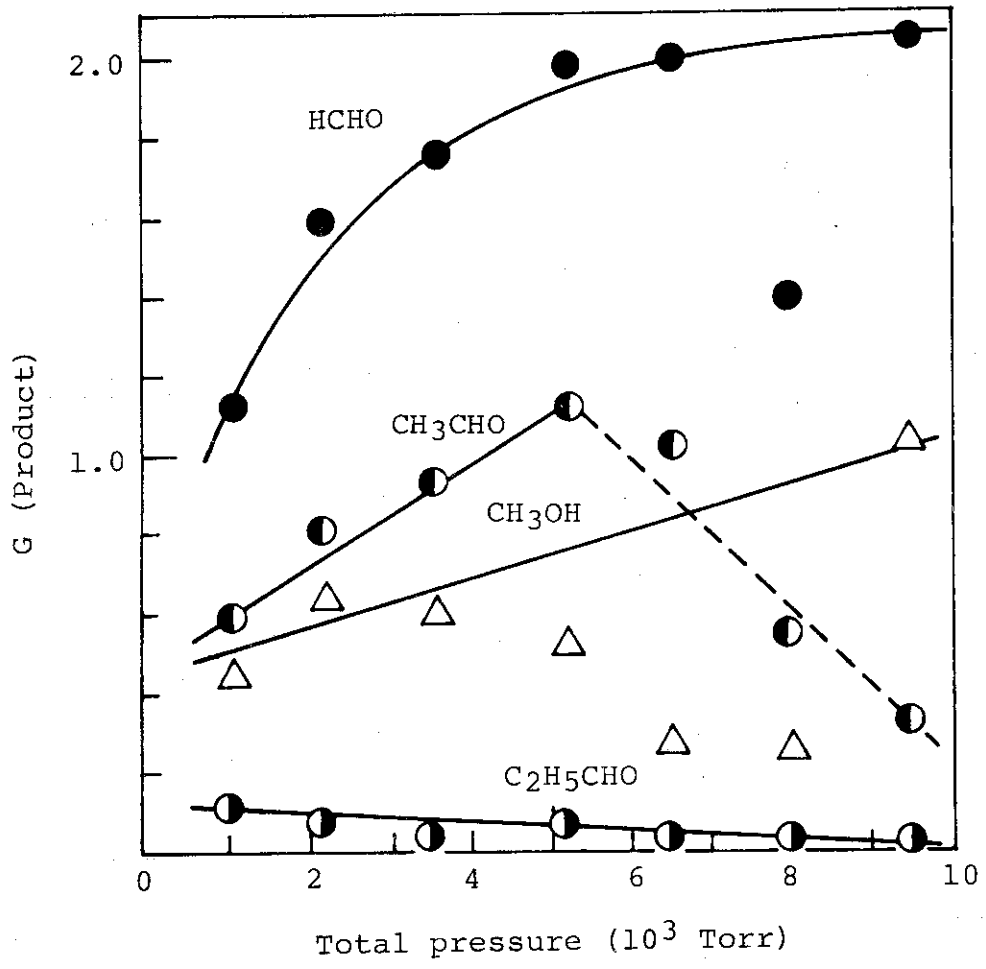

Fig. 2B. G values of the products as a function of reactant pressure: for the reaction conditions, see the caption of Fig. 1.

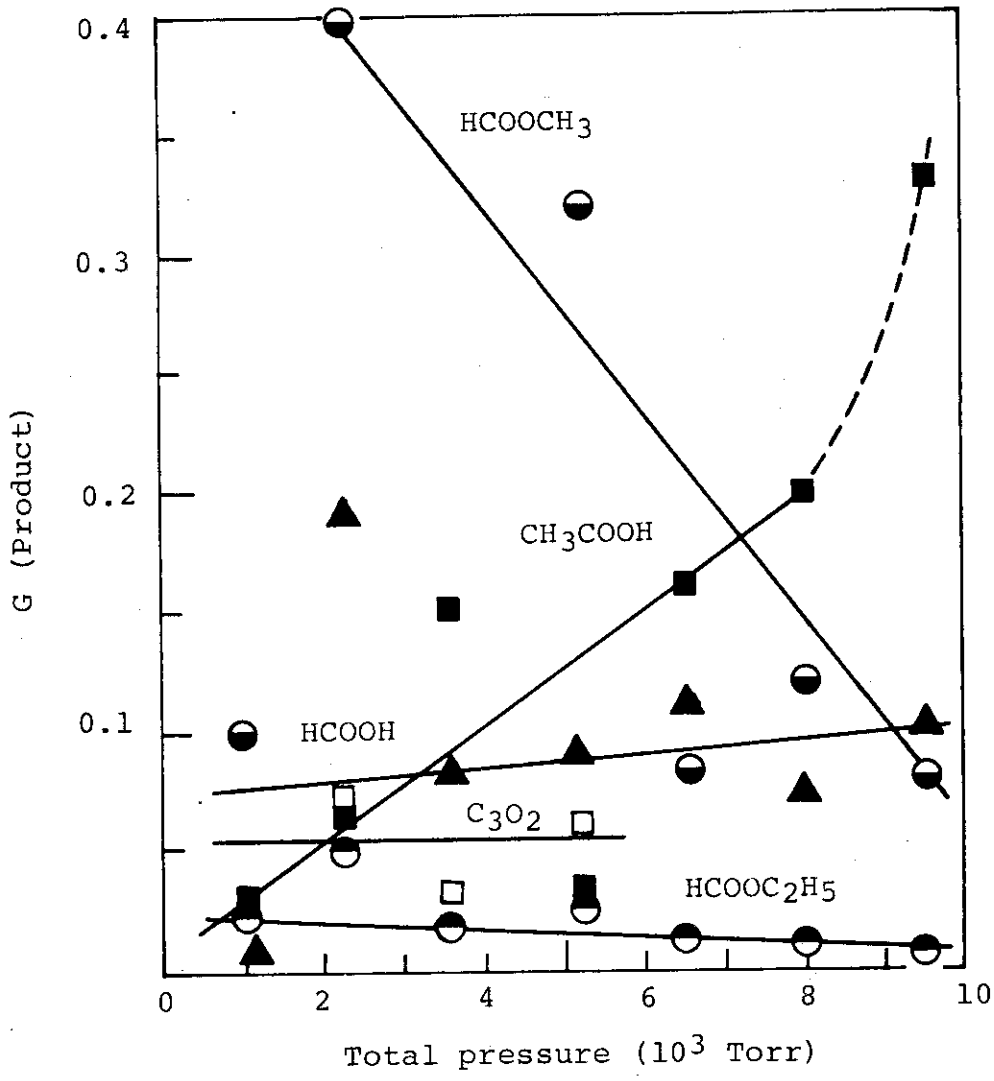

Fig. 3. G values of the products as a function of reactant pressure: for the reaction conditions, see the caption of Fig. 1.

The G value of acetaldehyde increases with the pressure but decreases above 6000 Torr (Fig. 2B), probably because the irradiation temperature decreases above this pressure due to recycled cold gas mixture from the cold traps, and it is known that the G value of acetaldehyde decreases at lower temperatures. The G value of methyl formate decreases and instead, that of acetic acid increases with increasing pressure. The G values of other compounds do not show apparent pressure

dependence. (S. Sugimoto and M. Nishii)

4. Irradiation of the Gas Mixtures of Carbon Monoxide and Hydrogen in a Flow System

This section describes the radiation chemical reactions of the $CO-H_2$ mixtures in the absence of solid catalyst, studied as a blank experiment of the reactions in the presence of solid catalyst. In the previous studies[1] carried out along the same line, the analysis system employed did not allow accurate determination of the yield of formaldehyde which is now known as a dominant product from $CO-H_2$[2]. In addition, effect of temperature on the product yields has not been studied yet.

The present study was carried out using a flow reactor, FIXCAT-II. Product yields were determined as functions of reactant-gas composition (14 ∿ 50 CO mole%), electron beam current (1, 2 and 5 mA), and temperature of irradiation (65 ∿ 300°C; beam current, 2 mA). In addition to the gaschromatographic analysis on Porapak Q columns employed in the previous studies, the simultaneous analysis was made on Porapak N columns equipped in a Shimadzu GC 7A gaschromatograph to obtain accurate yield of formaldehyde. The response of formaldehyde to the peak area recorded in the gaschromatogram by a thermal conductivity detector was determined using an aqueous solution of formaldehyde, the concentration of which has been determined by the hydrogen bisulfite method[3].

The G values of the products obtained at electron beam currents of 1, 2 and 5 mA are plotted against gas composition in Figs. 1, 2, and 3, respectively, and the corresponding product yields are listed in Tables 1, 2, and 3. It may be seen from Fig. 1, that the G values of formaldehyde, methane, and methanol have maximum values at 25, 30, and 10 mole CO %, respectively. The G values of carbon dioxide and acetaldehyde increase with increasing CO content up to 50%, above this CO content the experiment being difficult because of clogging of a transfer tubing connecting the reaction vessel and the gas

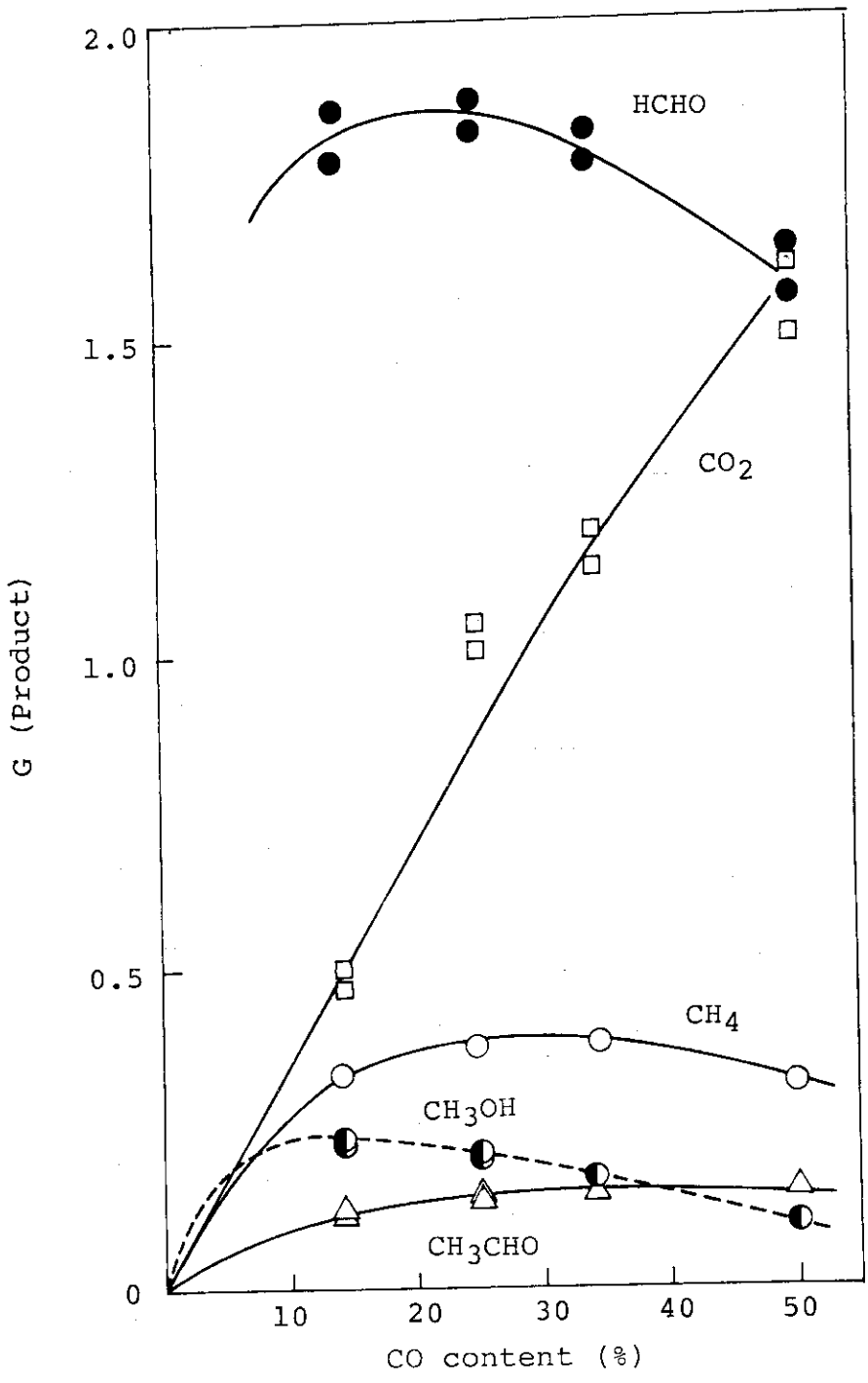

Fig. 1. G values of the products as a function of CO content: electron accelerating voltage, 0.6 MV; beam current, 1 mA; scanning width, 16 cm; temperature, 66 ∿ 68°C; flow rate of the reactant, 100 ml/min.

samplers by unidentified solid products. Similar relationships between the G values of the products and gas composition can be seen at the electron beam currents of 2 and 5 mA as seen from Figs. 2 and 3, although the G values of most products decrease with increasing beam current. Fig. 4 shows the G

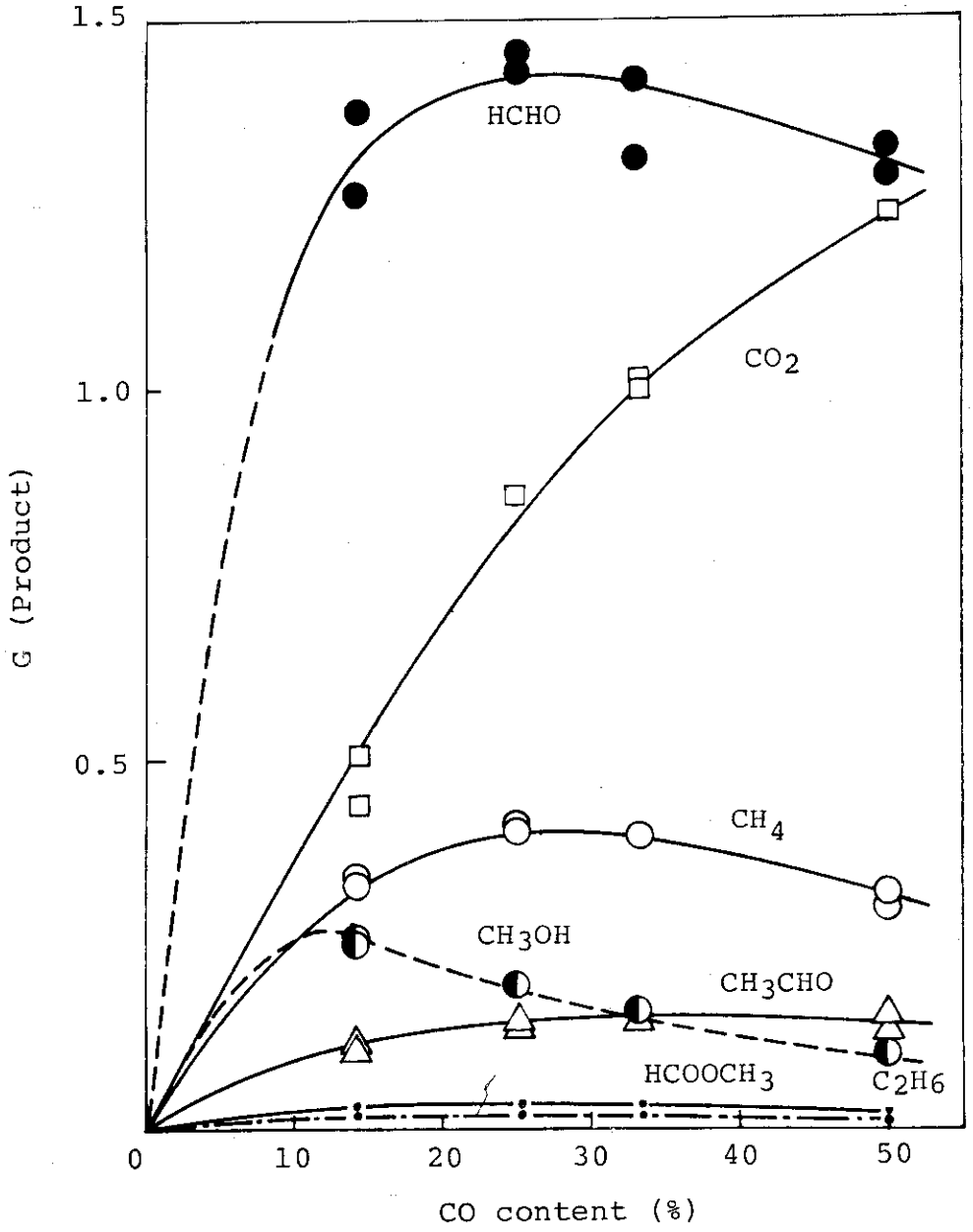

Fig. 2. G values of the products as a function of CO content: beam current, 2 mA; temperature, 92 ∿ 98°C; for other reaction conditions, see the caption of Fig. 1.

values of the products as a function of the electron beam current for the 1:6 CO-H_2 mixture. As may be seen from Fig. 4, the G value of formaldehyde decreases markedly with increasing beam current. Although the dependence of the G values of other products is not so great as that of the G value of formaldehyde,

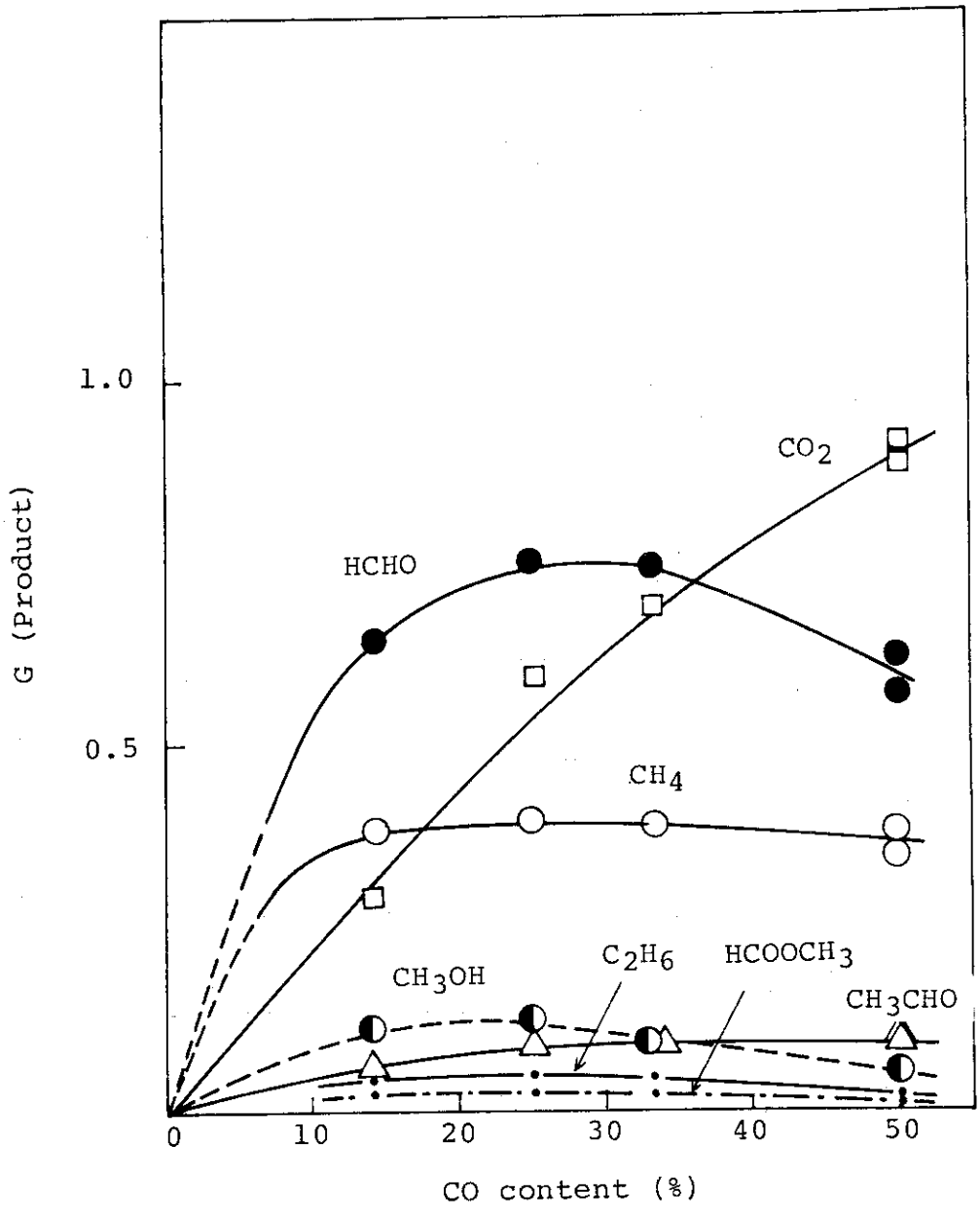

Fig. 3. G values of the products as a function of CO content: beam current, 5 mA; temperature, 148 ∿ 159°C, for other reaction conditions, see the caption of Fig. 1.

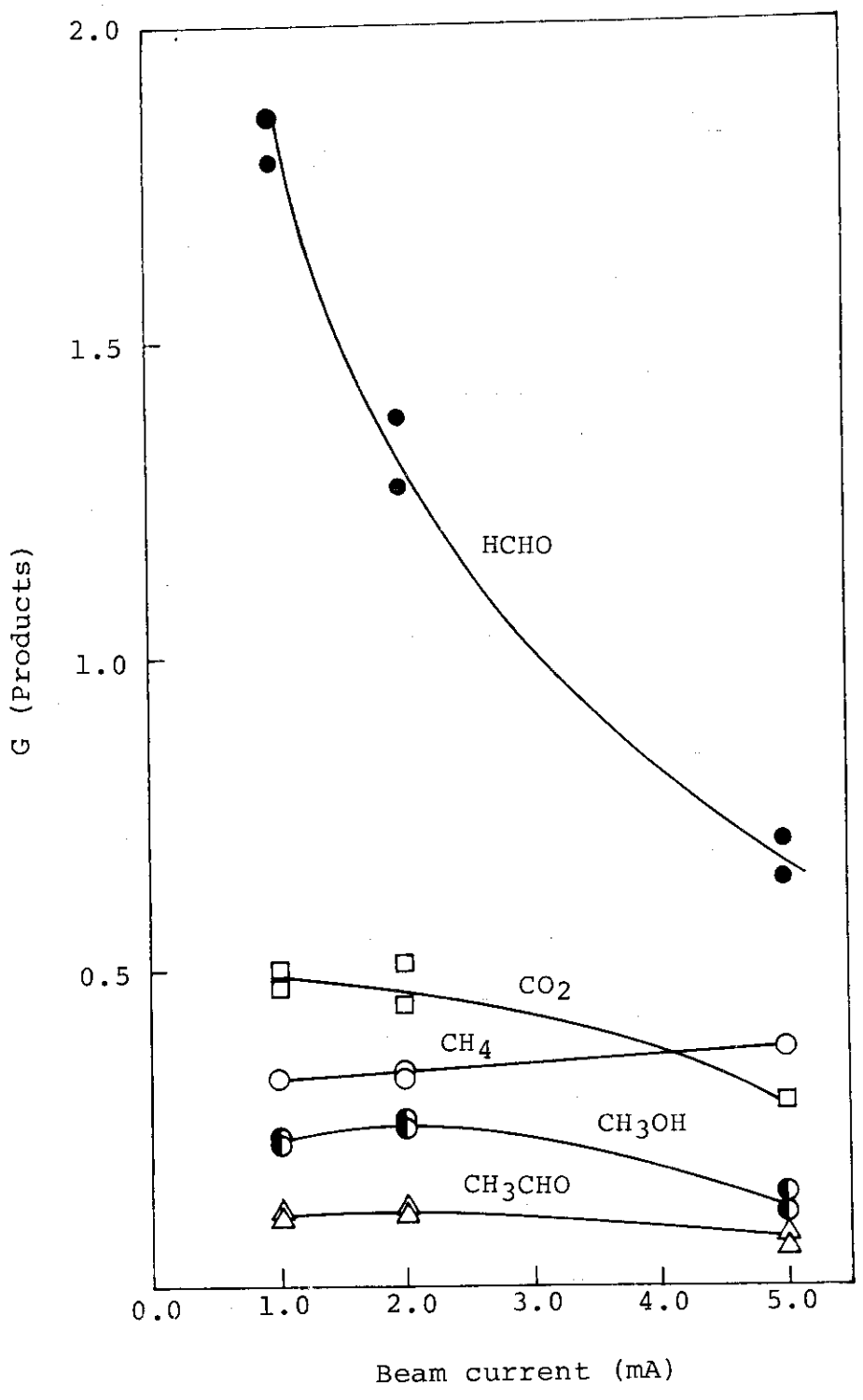

Fig. 4. G values of the products as a function of beam current: CO/H_2 mole ratio, 1/6; data in Figs. 1 through 3 are replotted.

Table 1. Effect of the Component on the Product Yields in g/m^3 Reactant

Identification	1523	1549	1615	1141	1707	1734	1800	1826
Flow rates H_2	85.7		75		66.7		50	
(ml/min) CO	14.3		25		33.3		50	
Temp. (°C)	66		67		68		68	
CH_4	0.0226	0.0225	0.033	0.034	0.039	0.040	0.044	0.044
C_2H_4	0.0005	0.0008	0.0009	0.0009	0.001	0.001	0.002	0.002
C_2H_6	0.0022	0.002	0.003	0.003	0.003	0.003	0.005	0.005
C_3H_6	0.	0.	0.0001	0.0002	0.0002	0.0002	0.0002	0.0002
C_3H_8	0.0009	0.0008	0.0007	0.001	0.0009	0.001	0.001	0.001
HCHO	0.219	0.230	0.315	0.307	0.361	0.353	0.427	0.409
CH_3OH	0.0295	0.032	0.035	0.037	0.035	0.036	0.029	0.030
CH_3CHO	0.0225	0.021	0.036	0.034	0.043	0.044	0.058	0.057
$HCOOCH_3$	0.0022	0.004	0.003	0.003	0.006	0.004	0.005	0.006
C_2H_5OH+n-C_4H_{10}	0.0078	0.008	0.008	0.009	0.008	0.008	0.009	0.008
C_2H_5OH	0.0081	0.009	0.009	0.008	0.009	-	0.008	0.010
CO_2	0.094	0.089	0.248	0.257	0.332	0.351	0.617	0.575
H_2O	1.202	1.024	0.890	0.816	0.713	0.754	0.678	0.640

Beam current, 1 mA; Electron accelerating voltage, 0.6 MeV; Scanning width, 16 cm; Flow rate, 100 ml/min.

Table 2. Effect of the Component on Product Yields in g/m^3 Reactant

Identification	1945	2011	1013	1040	1106	1159	1853	1919
Flow rates H_2	85.7		75		66.7		50	
(ml/min) CO	14.3		25		33.3		50	
Temp. (°C)	92		90		95		98	
CH_4	0.045	0.047	0.073	0.071	0.085	0.084	0.089	0.085
C_2H_4	(0.0009)	(0.0009)	0.001	0.002	0.002	0.002	0.003	0.003
C_2H_6	0.008	0.008	0.012	0.011	0.014	0.014	0.015	0.014
C_3H_6	(0.0003)	-	(0.0004)	(0.0003)	(0.0004)	(0.0004)	(0.0004)	(0.0004)
C_3H_8	0.004	0.005	0.007	0.006	0.006	0.007	0.005	0.005
HCHO	0.353	0.326	0.489	0.484	0.564	0.521	0.676	0.695
CH_3OH	0.068	0.071	0.067	0.069	0.069	0.070	0.055	0.058
CH_3CHO	0.040	0.045	0.073	0.069	0.087	0.086	0.114	0.101
$HCOOCH_3$	0.009	0.009	0.011	0.011	0.013	0.014	0.012	0.014
C_2H_5OH+n-C_4H_{10}	0.013	0.014	0.018	0.015	0.017	0.015	0.016	0.014
C_2H_5OH	0.016	-	0.016	0.015	0.018	-	0.015	0.016
CO_2	0.192	0.166	0.421	-	0.589	0.584	-	0.948
H_2O	1.09	0.987	1.927	1.610	1.462	1.325	-	1.125

Beam current, 2 mA; Electron accelerating voltage, 0.6 MeV; Scanning width, 16 cm; Flow rate, 100 ml/min.

Table 3. Effect of the Component on the Product Yields in g/Nm^3 Reactant

Identification	1444	1539	1703	1756	1848	1822
Flow rates H_2	120	85.7	75	66.7	50	50
(ml/min) CO	20	14.3	25	33.4	50	50
Temp. (°C)	148	148	152	155	159	159
CH_4	0.092	0.130	0.179	0.205	0.267	0.247
C_2H_4	(0.0008)	0.001	0.002	0.003	0.005	0.005
C_2H_6	0.019	0.027	0.039	0.044	0.067	0.061
C_3H_6	(0.0003)	(0.0004)	(0.0005)	0.001	0.001	0.001
C_3H_8	0.012	0.019	0.023	0.025	0.036	0.031
HCHO	0.321	0.409	0.628	0.735	0.753	0.807
CH_3OH	0.066	0.077	0.106	0.100	0.073	0.075
CH_3CHO	0.057	0.055	0.110	0.138	0.178	0.185
$HCOOCH_3$	0.020	0.031	0.036	0.036	0.052	0.045
C_2H_5OH+n-C_4H_{10}	0.023	0.031	0.039	0.033	0.034	0.035
C_2H_5OH	-	-	0.023	0.025	0.017	0.019
CO_2	0.197	0.271	0.720	1.01	1.75	1.71
H_2O	0.989	1.404	1.602	1.864	2.00	1.89

Beam current, 5 mA; Electron accelerating voltage, 0.6 MeV; Scanning width, 16 cm; Flow rate, 100 ml/min.

the G value of methane increases whereas the G values of the oxygen-containing products decrease with the increase of the beam current. It should be noted, however, that the G values of the products at different beam current in Fig. 4 were determined at different temperature of irradiation. Therefore, the result in Fig. 4 should be regarded as a combined effect of the beam current, i.e., dose rate, and temperature of irradiation.

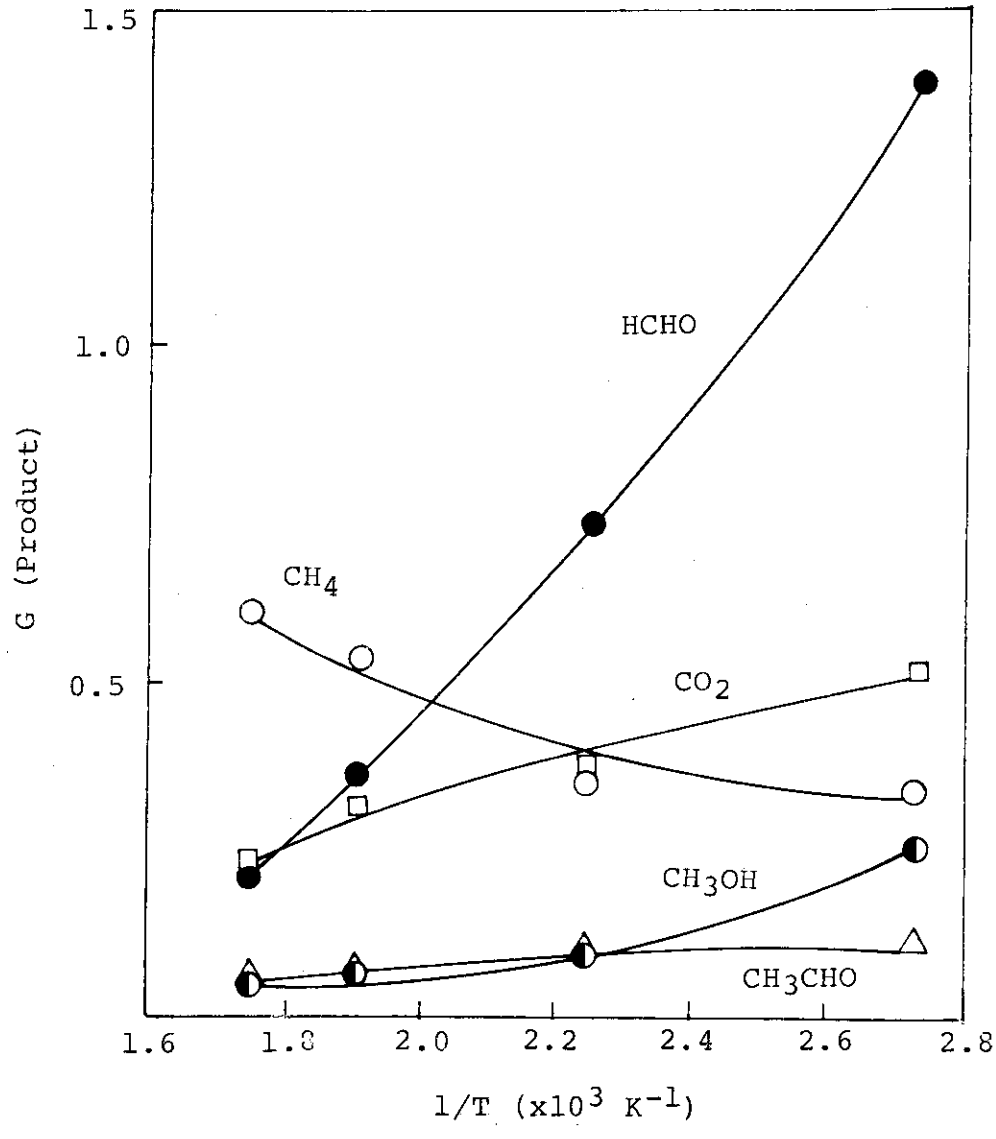

Fig. 5. G values of the products as a function of irradiation temperature: CO/H_2 mole ratio, 1/6; beam current, 2 mA; flow rate of the reactant, 100 ml/min.

Figure 5 shows the effect of temperature on the G values of the dominant products by irradiation of the 1:6 $CO-H_2$ mixture with the beam current of 2 mA. The details of the yields at three temperatures are shown in Table 1 in section 6. It is apparent that the G value of methane increases whereas the G values of the oxygen-containing products decrease with increasing temperature. These trends qualitatively agree well with those observed by increasing the beam current as shown in Fig. 4. The effect of temperature observed may be due to the fact that the reactions of $CO-H_2$ producing hydrocarbons and oxygen-containing products take place less favorablly at higher temperature. The increase in the G value of methane, on the other hand, may be ascribed to dehydrogenation or dehydration reactions of the oxygen-containing products.

(S. Nagai, K. Matsuda, H. Arai and M. Hatada)

1) K. Matsuda, S. Nagai, H. Arai and M. Hatada, JAERI-M, 7355, 11 (1977).
2) S. Sugimoto, M. Nishii and T. Sugiura, JAERI-M 7898 (1978).
3) S. Sigga, Quantative Organic Analysis, 2nd Ed., John Wiley & Sons, Inc., New York (1954).

5. Radiation Effects on the Reaction of Carbon Monoxide - Hydrogen Gas Mixture in the Presence of Fischer-Tropsch Catalyst

Irradiation of $CO-H_2$ mixtures over Fischer-Tropsch (F-T) catalyst would induce various reactions such as radiation chemical reactions both in gas phase and adsorbed state. Catalytic reactions over the catalyst would also occur due to a temperature rise by irradiation with electron beams of such a high dose rate as employed in our studies. In addition, secondary reactions may be expected to occur, as shown previously[1] in the conversion of formaldehyde and acetaldehyde produced in gas phase by radiation to methanol and ethanol,

respectively, over F-T catalyst. The present study was carried out in an effort to elucidate the radiation effects on the $CO-H_2$ mixture over F-T catalyst by comparing the product yields with those by the catalytic reactions of the gas mixture over the same catalyst and those by irradiation of the gas mixture in the absence of solid catalyst.

The catalyst, reactor, flow system and product analysis system used in this study are the same as described before[1].

Irradiation of $CO-H_2$ mixture (1 : 5) over F-T catalyst produced hydrocarbons, methanol and acetaldehyde in addition to CO_2 and H_2O. Formaldehyde was not produced in a detectable amount, in marked contrast to the radiolysis in the absence of solid catalyst. Fig. 1 shows the yields of dominant products as a function of time after initiating irradiation with electron beams of 1 mA, 2 mA and 5 mA. The maximum temperatures of the catalyst recorded during the irradiation were 86°C for 1 mA, 142°C for 2 mA, and 308°C for 5 mA, respectively.

As may be seen from Fig. 1 a, the yield of CO_2 decreases rapidly, while the yield of methanol increases with time. The yields of hydrocarbons, on the other hand, increase gradually with time. Similar behavior in the yield of each product is also seen by irradiation with 2 mA (Fig. 1 b). When irradiation was carried out with 5 mA (Fig. 1 c), the yields of hydrocarbons and CO_2 become two orders of magnitude higher than those by irradiation with 2 mA.

Catalytic reactions of the same gas mixture over F-T catalyst which were examined for comparison, produced the products same as those by irradiation described above except that organic oxygenates were detected only at reaction temperatures below 200°C. In Fig. 2 are shown the product yields vs. time after initiating the flow of the gas mixture over F-T catalyst kept at three different temperature ranges.

Table 1 compares the product yields obtained with and without irradiation. The yields in each case were determined by analysis of the effluent at ca. 2 hour after initiating the reaction.

By comparing the data by irradiation with 2 mA with those

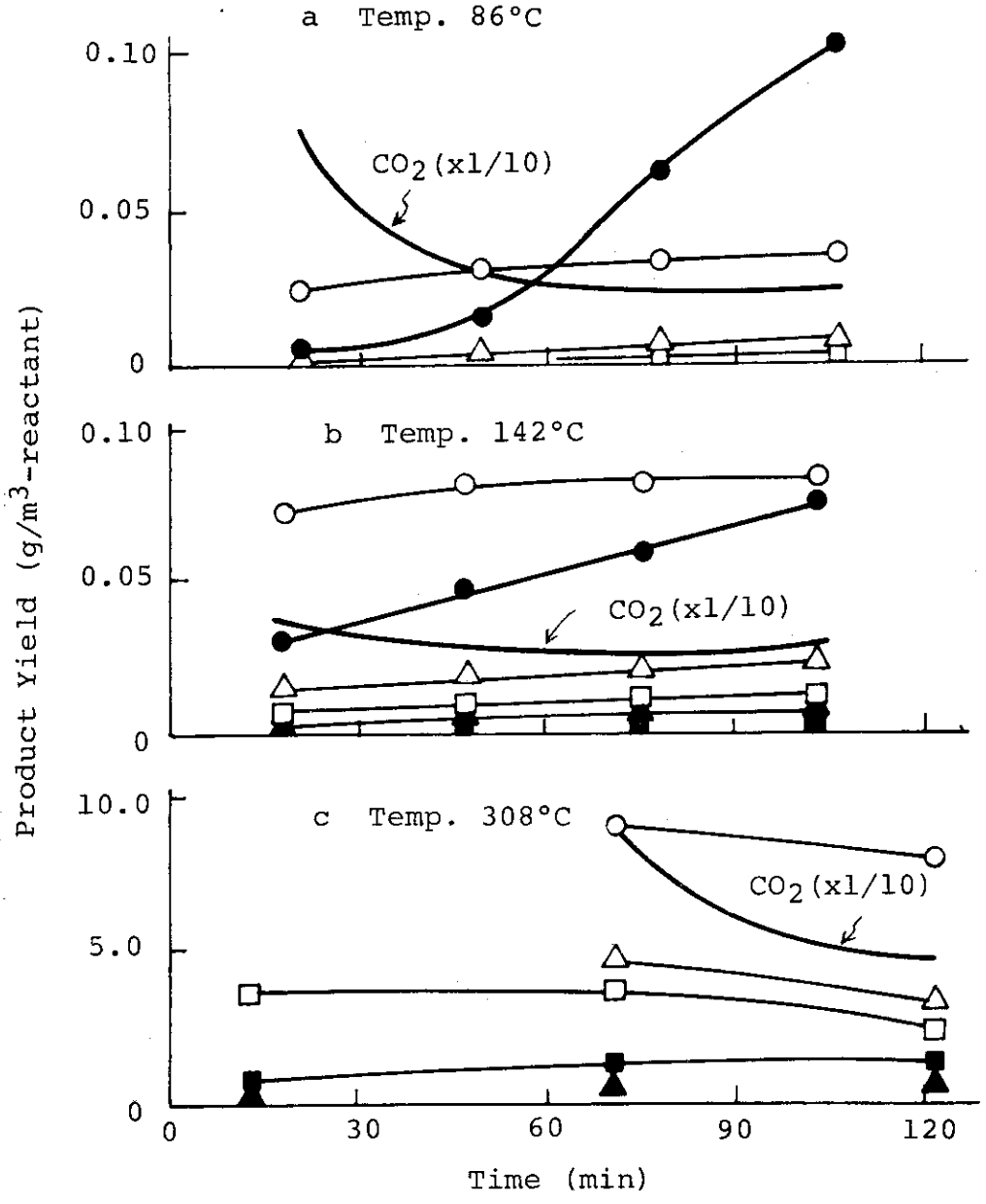

Fig. 1. Product yields vs. time after initiating irradiation on the CO-H_2 mixture in the presence of Fe-Cu-KG catalyst. Irradiations were carried out with 600 keV and (a) 1 mA, (b) 2 mA, and (c) 5 mA. (o) CH_4, (Δ) C_2H_6, (▲) C_2H_4, (□) C_3H_8, (■) C_3H_6, and (●) CH_3OH.

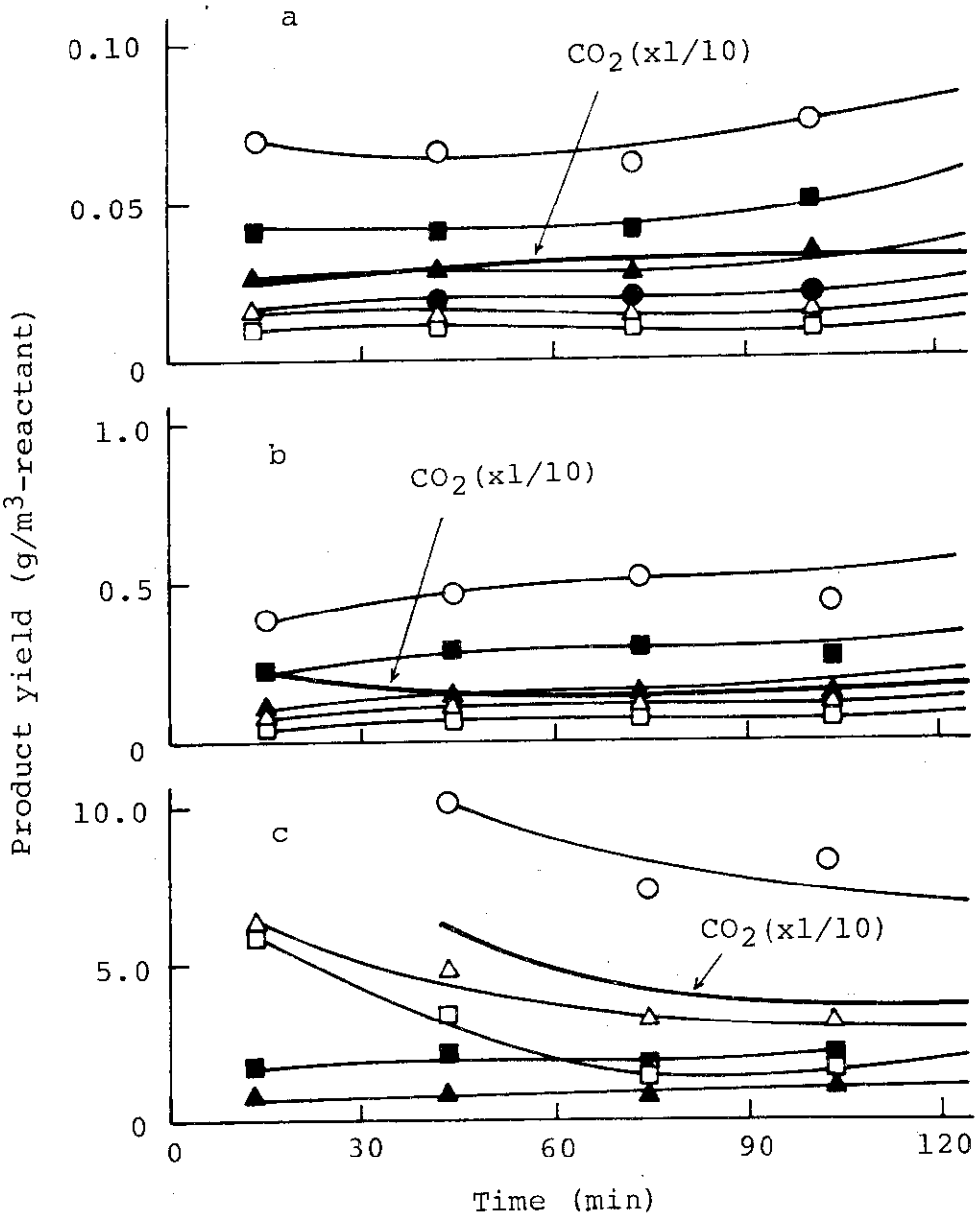

Fig. 2. Product yields vs. time after initiating the CO-H_2 flow over Fe-Cu-KG catalyst. Maximum temperatures of the catalyst were (a) 148°C, (b) 184°C, and (c) 312°C. See legend to Fig. 1 for product notations.

Table 1 Comparison of the Product Yields* by Electron Irradiation of 1 : 5 Mixture of $CO-H_2$ in the Presence of Fe-Cu-KG Catalyst with Those by Catalytic Reactions of the Same Mixture over the Same Catalyst

	Electron Irradiation			Thermal Reaction		
	1 mA	2 mA	5 mA			
Temp. of Catalyst, max.	86	142	308	148	184	312
(°C) min.	52	68	139	136	158	214
CH_4	0.034	0.083	7.79	0.083	0.640	6.56
C_2H_4	0.002	0.004	0.52	0.037	0.196	1.03
C_2H_6	0.005	0.022	3.25	0.019	0.181	2.32
C_3H_6	(0.0002)	0.001	1.01	0.054	0.357	1.75
C_3H_8	0.001	0.011	2.13	0.013	0.089	0.94
CH_3OH	0.101	0.077	0.03	0.025	0.081	-
CH_3CHO	0.002	0.011	0.03	-	0.021	-
$HCOOCH_3$	-	0.003	-	-	-	-
iso-C_4H_{10}	-	-	0.21	-	trace	-
1-C_4H_8	-	-	0.23	0.021	0.137	0.40
C_2H_5OH+n-C_4H_{10}	-	0.016				
n-C_4H_{10}	-	-	1.39	0.026	0.181	0.84
C_2H_5OH	-	-		0.023		
iso-C_5H_{12}	-	-	} 0.69			
1-C_5H_{10}	-	-		0.013	0.089	0.24
n-C_5H_{12}	-	-	1.20	0.026	0.201	0.56
CO_2	0.215	0.280	44.2	0.339	1.70	30.4

* Product yields were determined after ca. 2 hr on-stream, and are given in g/m^3-reactant.

by catalytic reactions at 136 - 148°C, it may be seen that the yields of methane, ethane and propane agree well, respectively, in both reactions. The yields of olefins by radiolysis are much lower than those by catalytic reactions. The yield of methanol by radiolysis, on the other hand, is three times higher than that produced catalytically, which may be explained by the hydrogenation of formaldehyde produced in gas phase by radiation to methanol over F-T catalyst[1].

A comparison between the product yields by irradiation with 5 mA and those by catalytic reactions at 214 - 312°C shows that radiation favors the formation of paraffins and reduces the yields of olefins. In addition, organic oxygenates are detected only in the radiolysis.

The agreement in the yields of paraffins between radiolysis and catalytic reactions indicates that most of the paraffins produced by radiolysis may arise from the catalytic reactions over F-T catalyst due to a temperature rise by irradiation. The olefins produced catalytically would be hydrogenated to paraffins by radiation, which may explain the low yield of olefins obtained by radiolysis. On the other hand, the yields of oxygenates by radiolysis are higher than those by the catalytic reactions but do not exceed those produced by radiolysis of $CO-H_2$ in the absence of solid.

In conclusion, radiation effects on $CO-H_2$ mixture in the presence of F-T catalyst may be accounted for by radiation-induced reactions in gas phase, catalytic reactions due to temperature rise by irradiation, and the secondary hydrogenation reaction of aldehydes and olefins over the catalyst. In other words, the presence of F-T catalyst does not enhance the yields of products from $CO-H_2$ mixture.

(S. Nagai, H. Arai, K. Matsuda, M. Hatada)

1) S. Nagai, H. Arai, K. Matsuda, JAERI-M 7949, 14 (1978).

6. Radiation Effect on the Reactions of Carbon Monoxide-Hydrogen Gas Mixture in the Presence of Silica Gel

Our studies of radiation effects on $CO-H_2$ mixtures in the presence of solid catalyst have been carried out to find if it is possible to maximise the yield of some desirable products and the selectivity in the radiation-induced reaction by using an appropriate catalyst. These studies, therefore, rely very much on choice of solid catalyst to be employed. Previous studies of radiolysis in the adsorbed state[1] demonstrate that enhancement in the radiolysis yield is most prominent when molecules to be studied are adsorbed on insulators such as silica and alumina rather than metals or semiconductors. This fact has been accounted for by energy transfer from irradiated solid to adsorbed molecules[1], the efficiency of the process being determined by the band gap of the solid. Accordingly, it seemed of interest to study radiation-induced reactions of $CO-H_2$ mixtures over silica gel and alumina.

Experiments were carried out in the same flow system as employed in our previous studies[2]. Silica gel (Mallinkrodt, 100 mesh) was outgassed at 450°C in vacuo for several hours before use. The mixture of $CO-H_2$ (1 : 6) was introduced at 100 ml/min to the reactor (FIXCAT-II) in which 2 grams of silica gel were placed. Irradiation was carried out with electron beams of 600 KeV and 2 mA from the HDRA.

Product analysis was made by two gaschromatographs equipped with Porapak Q and Porapak N columns, respectively. Product yields were determined from the concentration of the products detected during irradiation and those desorbed by argon gas stream passed over the irradiated solid after irradiation. For comparison, studies were also carried out on reactions over alumina (Nakarai Chemicals Co., 200 mesh).

In the absence of radiation, only small amounts of methane, ethylene, ethane and propylene were detected in the gas stream of the $CO-H_2$ mixture passed over silica gel kept at 350°C, but were still lower than those produced by reactions of the gas mixture over the walls of the reactor at the same temperature.

This finding indicates that silica gel exhibits no catalytic activity for the reactions of the $CO-H_2$ mixture without radiation.

Reactions over silica gel were studied at two temperatures of irradiation, 140°C and 295°C. The dominant products by irradiation of the $CO-H_2$ mixture over silica gel were low molecular weight hydrocarbons together with carbon dioxide and water. Table 1 shows the product yields in gram produced by irradiation of 1 m^3 reactant over silica gel together with those produced in the absence of silica gel. It may be seen from Table 1 that the yield of each hydrocarbon over silica gel is more than an order of magnitude higher than that in the homogeneous radiolysis, whereas the yields of formaldehyde, methanol and acetaldehyde are much lower in the reaction over silica gel.

The high yield of hydrocarbons is accompanied with the high yield of CO_2 as may be seen by comparison of the data in the homogeneous radiolysis and those by reactions over silica gel in Table 2. This provided evidence that CO_2 is indeed one of the by-products in the radiation-induced reactions producing hydrocarbons. However, over silica gel the amount of CO_2 produced is higher when the temperature of reaction is lower, contrary to the amounts of hydrocarbons produced. That is, a high yield of CO_2 does not necessarily mean a high yield of hydrocarbons.

Table 2 shows a comparison of products obtained by reactions of $CO-H_2$ mixtures. The hydrocarbon yield over silica gel is much higher than the sum of the yields of hydrocarbons and oxygen containing products in the absence of solid. Therefore, it is not likely that most of the hydrocarbons produced over silica gel would be formed by decomposition of organic oxygen containing products produced in gas phase. The high yield of hydrocarbons, instead, would be due to longer residence time of reactant gases in the irradiation zone by adsorption on silica gel, which results in higher irradiation dose compared with the radiolysis in the absence of solid. Alternatively, it would be due to efficient energy transfer from the irradiated

Table 1. Product Yields[1] by Irradiation of the 1:6 $CO-H_2$ Mixture

Solid	-	-	-	Silica Gel	
Temperature (± 5°C)	92	171	297	140	295
CH_4	0.045	0.047	0.080	0.693	2.616
C_2H_4	0.0009	0.0007	0.0004	0.014	0.043
C_2H_6	0.008	0.011	0.015	0.203	0.665
C_3H_6	0.0003	0.0003	0.0002	0.024	0.068
C_3H_8	0.004	0.008	0.009	0.103	0.529
HCHO	0.353	0.187	0.051	trace	-
CH_3OH	0.068	0.024	0.010	0.008	0.009
CH_3CHO	0.040	0.035	0.015	0.010	0.017
$HCOOCH_3$(+iso-C_4H_{10})	0.009	0.011	0.013	-	-
C_2H_5OH(+n-C_4H_{10})	0.013	-	-	-	-
CH_3COOH	0.107	-	-	-	-
CO_2	0.192	0.140	0.084	14.5	9.34

1) Yields in gram produced by electron beam irradiation of 1 m^3 reactant.

Table 2. Comparison of Products by Reactions of the CO-H_2 Mixtures

H_2/CO ratio	6	6	6	6	6	6	6
Solid	-	-	-	Alumina	Silica gel	Silica gel	F-T catalyst
Reaction	Irrad.	Irrad.	Irrad.	Irrad.	Irrad.	Irrad.	Thermal
Temp. (°C)	92	171	297	297	140	295	214 ∿ 312
Yield[1]							
Total hydrocarbons	32	35	58	500	275	1055	890
Total organic oxygenates	170	80	26	5	6	7	-
Mole ratio							
C_2H_4/C_2H_6	0.13	0.07	0.03	0.17	0.07	0.07	0.44
C_3H_6/C_3H_8	0.07	0.03	0.02	0.23	0.24	0.13	1.86
$\Sigma C_4H_8/\Sigma C_4H_{10}$	-	-	-	0.21	0.40	0.12	0.48
iso-C_4H_{10}/n-C_4H_{10}	-	-	-	0.65	0.39	1.94	-
iso-C_5H_{12}/n-C_5H_{12}	-	-	-	1.19	0.82	2.55	-

(1) In 10^{-6} mol per 10 ℓ reactant (per gram of solid).

solid to adsorbed molecules, which has often been invoked[1] to explain enhancement in the radiolysis yield in the adsorbed state.

One of the characteristics in the reaction producing hydrocarbons over silica gel is the low yield of olefins as seen from the values of mole ratio, olefin/paraffin in Table 2. Similar values were obtained in the presence of alumina. In addition, we have found that the olefin/paraffin ratio decreases markedly when $CO-H_2$ mixture was irradiated in the presence of Fischer-Tropsch catalyst which in the absence of radiation, is an excellent catalyst producing olefins in high yield as may be seen from Table 2. Accordingly, the observed low values of the mole ratio may be ascribed to hydrogenation reaction of olefins over the solid surfaces.

Another point to be noted in the reaction over silica gel is the high yield of isobutane and isopentane. This finding parallels the predominant formation of branched hydrocarbons observed in the radiolysis of pentane adsorbed on silica gel[3]. It has already been found that radiation generates acidity of silica gel[4] which is known to play an important role in the isomerisation reaction of hydrocarbons.

(S. Nagai, H. Arai, M. Hatada)

1) J. G. Rabe, B. Rabe and A. O. Allen, J. Phys. Chem., 70 1098 (1966); G. M. Zhabrova, V. I. Vladimirova, B. Kadenatsi, V. B. Kazanskii and G. B. Pariiskii, J. Catal., 6, 411 (1966).
2) S. Nagai, H. Arai, K. Matsuda and M. Hatada, JAERI-M 7949, 14 (1978).
3) J. W. Sutherland and A. O. Allen, J. Amer. Chem. Soc., 83, 1040 (1961).
4) C. Barter and C.D. Wagner, J. Phys. Chem., 68, 2381 (1964).

7. Radiation Chemical Reaction of Carbon Monoxide-Hydrogen Gas Mixture in the Presence of Chromia-Zinc Oxide Catalyst

It was reported that ionizing radiation affects the catalytic reaction of carbon monoxide and hydrogen or decomposition of methanol over chromia-zinc oxide or zinc oxide[1),2)]. It is of interest to know whether the presence of these semiconducting solid catalysts affects the radiation chemical reactions of the gas mixture of carbon monoxide and hydrogen in comparison with the studies on the effect of insulating or conducting solid catalysts.

Chromia-zinc oxide catalyst was prepared from chromic acid and zinc oxide supplied by Merck, A.G. (purity, >99%) and Nakarai Chemicals Co. (G.R.; purity, >99%), respectively, by the method described by Y. Ogino[3)].

A known amount of catalyst was placed in a flow reactor, FIXCAT-II, described in the previous sections[4)], the length of the catalyst bed in the reactor being about 16 cm for chromia-zinc oxide (ca. 7.3 g) and for zinc oxide (ca. 2.3 g). Carbon monoxide and hydrogen were introduced into the reactor and the flow rate of each gas was monitored separately with two thermal mass flow meters (Ueshima-Brooks type 5810). The flow rate ratio of hydrogen to carbon monoxide was kept constant at 2:1 throughout this experiment. The gas mixture was irradiated with electron beams (0.6 MeV, 2 mA) from the HDRA. The bottom of the reactor was cooled by running water (10°C) during irradiation.

The method of analysis was the same as that described in the previous sections: two gaschromatographs, Shimadzu GC7A and Yanagimoto G80, equipped with 2 m Porapak N and 3 m Porapak Q, respectively, were used simultaneously to allow the analysis of the irradiated gas within 30 min.

The data obtained at various reaction conditions are listed in Table 1. Since adsorption and desorption of the reactant and products gave slow change of the product concentration in the reacted gas with time, the data given in the table

Table 1 Product Yields from $CO-H_2$ Gas Mixture by Electron Irradiation with or without Solid Catalyst

Identification	1106*	1551	1617	2125	2135	2127
Time after Change of Reaction Condition (min)		162	188	75	20	54
Beam Current (mA)	2	0	0	2	2	2
Temp. (°C)	90	209	209	235	235	190
Flow Rates (ml/min) H_2	66.7	66.7	66.7	66.7	33.7	66.7
CO	33.3	33.3	33.3	33.3	16.7	33.3
Residence Time (sec)***	3.8	3.8	3.8	3.8	7.7	3.8
Catalyst	no	Cr_2O_3-ZnO	Cr_2O_3-ZnO	Cr_2O-ZnO	Cr_2O_3-ZnO	ZnO
Product Yields (mg/Nm^3 reactant)						
CH_4	85	0.37	0.42	104.7	227.8	127
C_2H_4	2	1.27	1.27	1.2	2.1	1.62
C_2H_6	14	0.06	0.12	37.7	98.9	38.9
C_3H_6	0.4	0.11	0.	0.3	0.54	0.34
C_3H_8	6	0.	0.	6.1	15.3	14.2
HCHO	564	0.	0.	131	262.1	327.2
CH_3OH	69	51.96	68.9	96.5	148.5	109.8
CH_3CHO	87	0.	0.	15.0	30.0	4.5
C_2H_5OH	18	0.	0.	0.	0.	0.
$HCOOCH_3$	13	0.	0.	4.4	11.3	6.9
CH_3COOH	733**	0.	0.	603.7	780.1	726
CO_2	589	468	449	692	888	483
H_2O	1462	136	—	724	346	796

*) S. Nagai, et al., This report, p. 27.

**) Data interpolated to the composition ($H_2/CO = 2$) from the data obtained by Arai, et al.

***) No correction was made for volume of irradiation area occupied by solid.

were taken from the data at steady state or at condition close to steady state as possible. The yields of the products by irradiation in the absence of solid catalyst are also listed in the table from the data described previously.[4)]

Methanol is a main product from the gas mixture when chromia-zinc oxide catalyst is present at 209°C without irradiation. Ethylene was also found to be produced catalytically under this conditions, but the amount of this product is small. By the irradiation of this system, various products which were found in the radiation chemical reactions of the gas mixture without solid were found to be formed.

The effects of the presence of the solid catalysts on the radiation chemical reaction of the gas mixture were not large, but it can be mentioned that the yields of hydrocarbons and methanol were increased by the presence of the solid catalysts, while those of formaldehyde and acetaldehyde were decreased.

When the residence time of the reactant in the reaction zone was increased in the case of chromia-zinc oxide, most product increased roughly proportionally to the residence time. The amounts of acetic acid and carbon dioxide also increased with increasing residence time, but in a way that the increased amounts are less than those expected from the proportionality. The amount of water produced seems to decrease with the residence time, but this can not permit to conclude that longer residence time is effective to reduce this unwanted by-product, because the determination of water content in the reacted gas is always accompanied by large error.

The presence of zinc oxide produced similar effects as that of chromia-zinc oxide on the radiation chemical reactions of the gas mixture. This result suggests that zinc oxide in the chromia-zinc oxide catalyst plays an important role in the "solid effect". This may be confirmed by comparison of the above results to those which will be obtained in the further studies on chromia catalyst.

(M. Hatada, S. Nagai, H. Arai, K. Matsuda)

1) T. I. Barry and R. Roberts, Nature, 4692, 1061 (1959).

2) A. J. Teller, F. L. Poska, and H. A. Davies, Int. J. Appl. Radiation and Isotopes, 11, 123 (1961).
3) Y. Ogino, Bull. Chem. Soc. Japan, 32, 288 (1959).
4) S. Nagai, H. Arai, K. Matsuda, and M. Hatada, This report.

8. The Reaction of a Carbon Dioxide and Hydrogen Gas Mixture by Electron Irradiation with or without the Presence of Chromia-Zinc Oxide Catalyst

Carbon dioxide is one of the products having large G values in some of the past studies of radiation chemical reactions of gas mixture of carbon monoxide and hydrogen when a solid catalyst is present. Carbon dioxide thus formed in large quantity may further react with hydrogen. Therefore, it is important to know the reaction of carbon dioxide and hydrogen in the presence or in the absence of the solid catalyst. Chromia-zinc oxide was selected in this study because this catalyst was reported to promote the formation of methanol from the gas mixture containing carbon dioxide and hydrogen.

The method of experiment was exactly the same as the previous study. Carbon dioxide was obtained from Osaka Suiso Ind. Co., and used without further purification.

Table 1 summarizes the results of product yields and G values from gas mixtures of carbon dioxide and hydrogen by electron irradiation without solid catalyst. The main products are methane, ethane, propane, carbon monoxide and water, and G values of the latter two are larger than those of the others. The G values of hydrocarbons are smaller than those reported for gas mixture of carbon monoxide and hydrogen, and decrease when the carbon dioxide content increases. The oxygen containing compounds found in the gas mixture of carbon monoxide and hydrogen were not detected except for methanol.

The G value of methane obtained for the 1 : 1 mixture in the present study is close to that obtained by Mitsui, et al.[1] under similar reaction conditions but with the use of γ-rays.

Table 1 Product Yields and G Values from CO_2-H_2 Gas Mixtures by Electron Irradiation*)

Beam Current (mA)	2	5	γ**)	2	2	3
Dose Rate (Mrad/sec)	3.72	9.3	0.023	3.4	3.4	3.22
Dose (Mrad)	26.8	67.0	20.0	24.5	24.5	23.2
Temperature (°C)	100	150	150	45	45	68
CO_2 Content (mole%)	25	25	20	50	50	90
Flow Rate (ml/min)	100	100	-	100	100	100
Product Yields (mg/Nm^3 Reactant) and G Values in Brackets						
CH_4	46. [0.18]	153. [0.25]	[0.24]	45.1[0.12]	42.9[0.12]	18.4[0.026]
C_2H_4	0.	0.		0.	0.	0.
C_2H_6	3. [0.007]	21. [0.018]	[0.02]	1.9[0.003]	2.0[0.003]	0.3[0.0002]
C_3H_6	0.	0.		0.	0.	0.
C_3H_8	1. [0.001]	16. [0.01]	[0.00]	0.	0.	0.
HCHO	0.	0.		0.	0.	0.
CH_3OH	0.	0.7[0.0005]	[0.00]	1.2[0.0002]	0.	0.
CH_3CHO	0.	0.		0.	0.	0.
CO	670. [1.54]	1830. [2.08]	[0.51]	1960. [3.01]	1865. [2.86]	2968. [2.38]
H_2O	3320. [11.85]	5770. [8.23]	[1.07]	9468. [23]	5886. [14]	8712. [11.0]

*) Electron Accelerating Voltage, 600 kV; Scanning Width, 30 cm; Residence Time, 3.6 sec.

**) H. Mitsui and Y. Shimidzu, JAERI-M 7993, p. 8 (1978).

Table 2 Product Yields of Thermal and Radiation Chemical Reactions of CO_2-H_2 Gas Mixture over Cr_2O_3·ZnO Catalyst

Beam Current (mA)		0	0	0	0	5
Temperature (°C)		100	150	270	295	275
Flow Rates (ml/min)	H_2	75	75	75	75	75
	CO_2	25	25	25	25	25
Product Yields (mg/Nm^3 Reactant)						
	CH_4	0.	0.	0.68	1.33	81.0
	C_2H_4	0.	0.	0.	0.	0.4
	C_2H_6	0.	0.	0.26	0.24	13.
	C_3H_6	0.	0.	0.	0.	0.
	C_3H_8	0.	0.	0.	0.	8.
	HCHO	0.	0.	0.	0.	11.
	CH_3OH	0.	0.	2.0	5.3	18.
	CH_3CHO	0.	0.	0.	0.	5.
	$HCOOCH_3$	0.	0.	0.	0.	4.
	CO	0.	0.	1070.	5640.	4700.
	CO_2	0.	0.	4680.	42600.	15910.

Electron Accelerating Voltage, 600 keV; Scanning Width, 30 cm; Residence Time, 3.6 sec.

However, higher G value was obtained for carbon monoxide in the present sutdy.

Table 2 shows the yields of the products obtained by the reaction over chromia-zinc oxide with or without irradiation. It is evident that zinc oxide has no catalytic activity for the gas mixture below 150°C, but above 270°C, promotes reactions to form lower saturated hydrocarbons, methanol, carbon monoxide, and water. The irradiation with electrons (5 mA, 600 keV) further promotes the reaction, but it is noted that the irradiation produces formaldehyde, acetaldehyde, and methyl formate, which were found neither in radiation chemical reactions of the mixutre without chromia-zinc oxide, nor in the catalytic reactions over chromia-zinc oxide without radiation. (H. Arai, S. Nagai, M. Hatada)

1) H. Mitsui and Y. Shimidzu, JAERI-M 7993,8(1978).

9. Radiation Chemical Reaction of Methane

As a continuation from the study initiated in the previous year[1], the radiation chemical reactions of methane have been studied over wide range of the dose.

The irradiation of methane produces hydrogen and higher hydrocarbons, while the irradiation of the latter is known to produce methane and to form cross-linked structure or double bond structure. Therefore, it is interesting to know the composition of the irradiated gas when methane is irradiated with an extremely large dose of radiation. The G value was calculated from the yield and radiation dose absorbed by the system by usual method.

Takachiho "research" grade methane (>99.95 mole%) was used without further purification. Irradiation of methane was carried out using electron beams from the HDRA (0.6 MeV, 0.01∿10 mA) either under flow condition or, for extremely large dose irradiation, under static condition.

In the irradiation under flow condition, a flow reactor,

FIXCAT-II, which was used for irradiation of gas mixture of CO and H_2 in the previous sections. The bottom of the reactor was cooled by running water. Electron beam current employed was altered from 0.01 to 10 mA, and correspondingly, the dose rate and temperature as measured at the bottom of the reactor changed from 0.018 to 18 Mrad·sec^{-1} (from 3.56 x 10^{-5} to 3.56 x 10^{-2} eV·molec^{-1}·sec^{-1}), and from 23 to 260°C respectively. The temperature was below 60°C at a beam current below 1 mA, however (Table 1). The flow rate was also altered from 10 to 100 ml·min^{-1}, which gives the residence time in the reactor from 1.2 to 0.12 min. Analysis of the irradiated gas flowed out of the reactor was carried out using two gas chromatographs simultaneously on 3 m Porapak Q columns and on 2 m Porapak N columns.

In the irradiation under static condition, a batch type irradiation vessel of 7.1 ℓ in volume, which had been used for early irradiation studies on CO-H_2 gas mixtures [2]. The dose rate received by methane in this vessel was calculated to be 5.54 x 10^{-4} eV·molec^{-1}·sec^{-1}·mA^{-1} or 1.69 Mrad·sec^{-1}·mA^{-1} based on N_2O dosimetry assuming $G(-N_2O) = 10.0$ [3] for 0.6 MeV electrons. The largest dose received by methane was 25000 Mrads. Pressure change during the irradiation was monitored using a Univac GD-B2 type pressure gauge. The average temperature during irradiation was estimated to be 88°C by 3.5 mA electron beam irradiation from the pressure increase. The temperature of the vessel wall may not be uniform and some part of the wall may be considerably high. Little pressure change due to the irradiation was detected after the vessel was cooled down to the room temperature. After the irradiation, the irradiated gas was pumped into the gas samplers of the gas chromatographs. The rest of the gas was removed at room temperature through cold traps to collect condensable products which was analyzed by a gas chromatograph on squalane capillary columns. Then the irradiation vessel was disassembled to collect viscous liquid and solid products on the vessel wall. The products were scraped off from the vessel wall to be weighed. The solid products were subjected to infrared and MNR spectroscopy

and the liquid was subjected to gas chromatography.

The G values of hydrogen and C_2 hydrocarbons obtained by the flow technique under different beam currents and flow rates are plotted as a function of dose in Fig. 1, and those of C_3 and C_4 hydrocarbons in Fig. 2 and 3, respectively, and the yields of the products in Table 1. Since the G values of the hydrocarbons from methane are almost independent of temperature during irradiation at temperatures below 120°C, and are not strongly dependent on temperature below 130°C [1], the effect of beam current on G values is considered to be due to dose rate effect. As shown in Fig. 1, the G values of hydrogen and

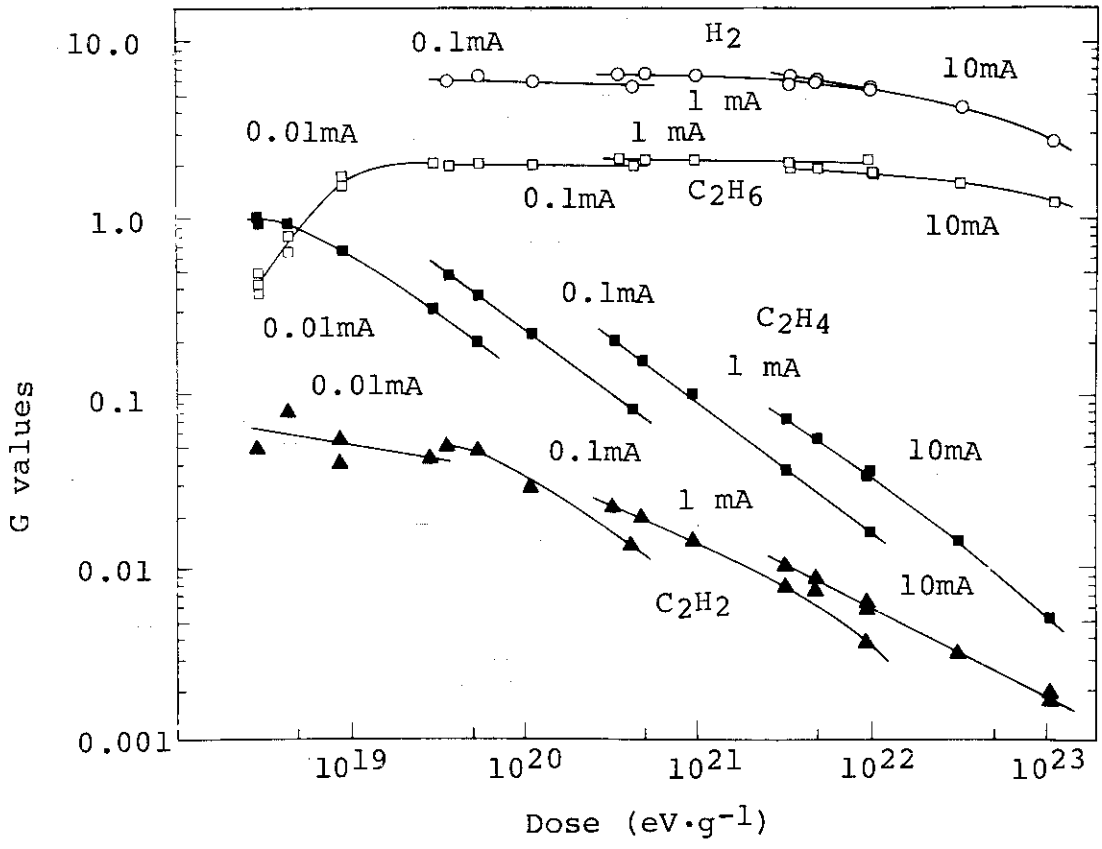

Fig. 1. G values of hydrogen and C_2 hydrocarbons as a function of dose: (○) hydrogen; (□) ethane; (■) ethylene; (▲) acetylene. Dose rate, 1.21×10^{18} eV·g^{-1}·sec^{-1} at 0.01 mA; 1.48×10^{19} eV·g^{-1}·sec^{-1} at 0.1 mA; 1.32×10^{20} eV·g^{-1}·sec^{-1} at 1 mA; 1.32×10^{21} eV·g^{-1}·sec^{-1} at 10 mA.

ethane are almost independent of dose regardless of the dose rate over the dose range studied except those obtained at the highest and lowest dose ranges. On the other hand, the G values of unsaturated products such as ethylene and acetylene decreased with increasing dose. It is noted that the curves obtained at different beam currents are discrete, showing that the G values are higher, compared at the same dose, when the irradiation is carried out with higher beam current. Similar tendency was also observed for C_3 and C_4 hydrocarbons as shown in Fig. 2 and 3.

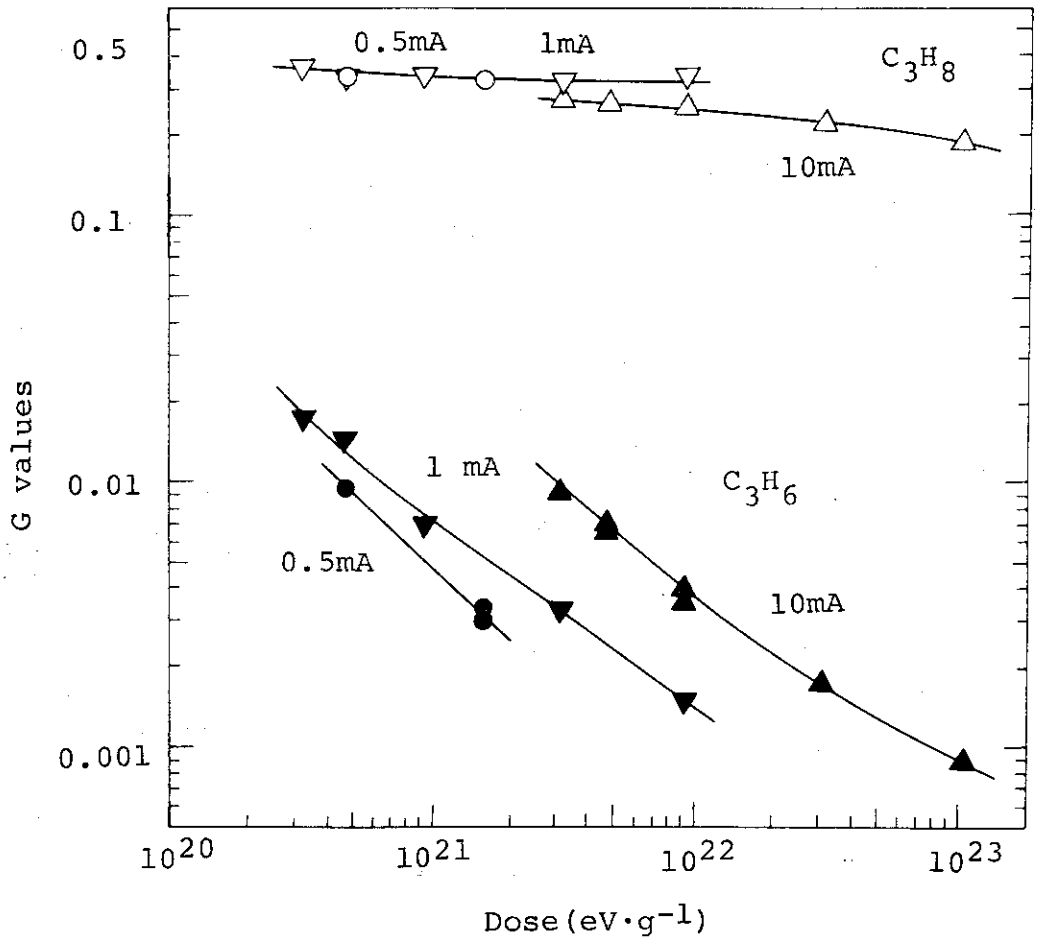

Fig. 2. G values of C_3 hydrocarbons as a function of dose: propane: (○) 0.5 mA, 6.68×10^{19} eV·g^{-1}·sec^{-1}; (▽) 1.0 mA, 1.32×10^{20} eV·g^{-1}·sec^{-1}; (△) 10 mA, 1.32×10^{21} eV·g^{-1}·sec^{-1}; propylene: (●) 0.5 mA; (▼) 1.0 mA; (▲) 10 mA.

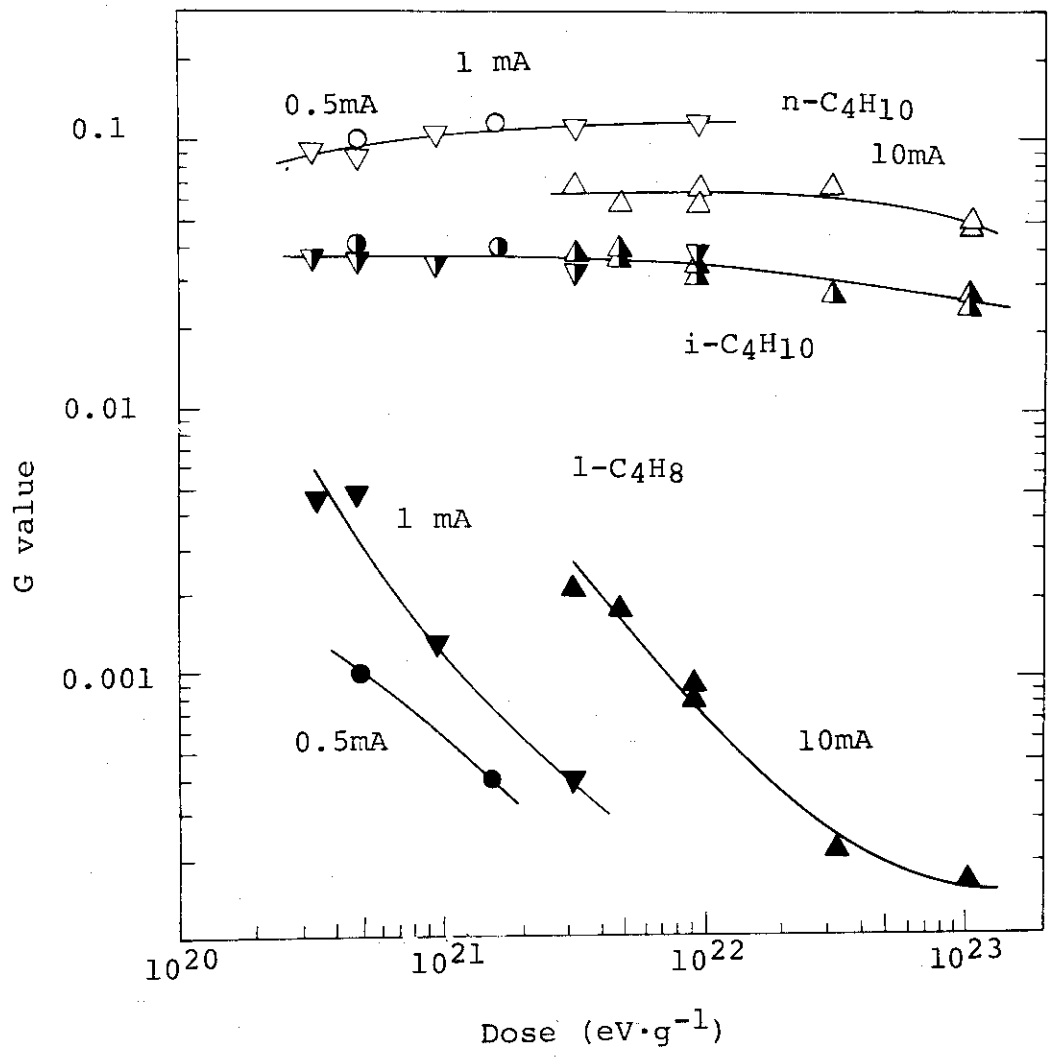

Fig. 3. G values of C_4 hydrocarbons as a function of dose: circles obtained at 0.5 mA beam current; inverse triangles, at 1.0 mA; trianges, at 10.0 mA; open symbols denote n-butane, half-filled symbols, i-butane, and filled symbols, 1-butene.

In Table 2, the concentrations of the irradiated gas under static condition are given together with those obtained with the largest dose under flow condition. The concentrations of methane and main products are plotted in Fig. 4 as a function of dose. The concentration of methane was reduced to ca. 10% of the original one by 25000 Mrad irradiation, but the concentration of hydrogen increases further at this dose. Since the G value of hydrogen from methane (5.5) is not much

Table 1. Yields of Products from Methane by Electron Irradiation

Identification	1645	1720	1550	1820	1855	1928	1952	2020	1455	1552
Beam Current (mA)	0.01	0.01	0.01	0.01	0.1	0.1	0.1	0.1	1	1
Flow Rate (ml/min)	302	201	100	30	201	202	99.5	30	292	200
Residence Time (sec)	2.4	3.6	7.2	24	2.4	3.56	7.2	24	2.46	3.6
Temperature (°C)	25	25	25	25	25	25	25	25	60	60
Energy Absorbed (eV/10ℓ)	2.01×10^{19}	3.02×10^{19}	6.08×10^{19}	2.03×10^{20}	2.3×10^{20}	3.42×10^{20}	6.94×10^{20}	2.30×10^{21}	2.08×10^{21}	3.04×10^{21}
(Mrad)	0.05	0.07	0.14	0.46	0.52	0.77	1.56	5.16	4.67	6.82
Yields (μmole/10ℓ reactant at 28°C, 1 atm)										
H_2	0.99	1.6	7.7	18	22.3	36.6	69.2	218	228	350
C_2H_2	0.02	0.04	0.06	0.14	0.19	0.28	0.35	0.55	0.80	1.05
C_2H_4	0.31	0.45	0.82	0.98	1.85	2.11	2.52	3.19	6.98	7.91
C_2H_6	0.13	0.31	1.63	6.71	7.78	11.7	24.0	78.3	77.2	110
C_3H_6	0.	0.	0.	0.	0.	0.	0.	0.	0.59	0.73
C_3H_8	0.	0.	0.	0.	0.	0.	0.	0.	12.8	16.9
$1\text{-}C_4H_8$	0.	0.	0.	0.	0.	0.	0.	0.	0.16	0.25
$2\text{-}C_4H_8$	0.	0.	0.	0.	0.	0.	0.	0.	-	-
$i\text{-}C_4H_{10}$	0.	0.	0.	0.	0.	0.	0.	0.	1.25	1.82
$n\text{-}C_4H_{10}$	0.	0.	0.	0.	0.	0.	0.	0.	3.22	4.50
$i\text{-}C_5H_{12}$	0.	0.	0.	0.	0.	0.	0.	0.	1.68	2.37
$n\text{-}C_5H_{12}$	0.	0.	0.	0.	0.	0.	0.	0.	0.09	0.20

Electron Accelerating Voltage, 600 kV; Scanning Width, 30 cm; Dose Rate, 7.33×10^{-3} eV·N_2Omolec^{-1}·sec^{-1}·mA^{-1}.

Table 1. Yields of Products from Methane by Electron Irradiation (continued)

Identification	1630	1730	1736	1245	1314	1340	1410	1510	1550	1703
Beam Current	1	1	1	10	10	10	10	10	10	10
Flow Rate (ml/min)	100	30	10	302	200	200	101	100	30	9
Residence Time (sec)	7.2	24	72	2.4	3.6	3.6	7.2	7.2	24	80
Temperature (°C)	60	60	60	260	260	260	260	260	260	260
Energy Absorbed (eV/10ℓ)	6.08×10^{21}	2.02×10^{22}	6.08×10^{22}	2.01×10^{22}	3.04×10^{22}	3.04×10^{22}	6.02×10^{22}	6.02×10^{22}	2.03×10^{23}	6.76×10^{23}
(Mrad)	13.6	45.3	136.4	45.3	68.2	68.2	135.0	136.4	455	1516
Yields (μmole/10ℓ reactant at 28°C, 1 atm)										
H_2	656	2040	5690	2210	3050	3100	5330	5520	15000	31600
C_2H_2	1.55	2.82	4.12	3.65	4.38	4.64	6.70	6.13	11.5	23.1
C_2H_4	9.90	12.4	16.4	24.8	28.6	29.0	37.5	35.5	48.3	62.5
C_2H_6	219	691	2090	701	1020	1030	1890	1950	5570	14400
C_3H_6	0.61	1.11	1.42	3.16	3.38	3.23	3.95	4.56	5.62	8.8
C_3H_8	34.4	106	342	93.5	176	133	250	242	762	2100
$1\text{-}C_4H_8$	0.13	0.14	0.05	0.7	0.45	0.88	0.91	0.82	0.74	2.0
$2\text{-}C_4H_8$	-	-	-	-	-	-	-	-	-	-
$i\text{-}C_4H_{10}$	3.57	11.2	37.7	12.6	19.4	18.2	35.4	32.4	90.6	296
$n\text{-}C_4H_{10}$	10.8	39.2	118	23.0	28.9	29.4	57.1	67.4	220	562
$i\text{-}C_5H_{12}$	4.39	13.3	40.7	11.3	18.3	20.9	38.7	35.7	92.2	24.8
$n\text{-}C_5H_{12}$	0.25	0.66	2.53	4.98	3.55	3.22	4.40	5.49	13.0	32.0

Table 2. Composition of Irradiated Mathane

Method	Flow	Flow	Static	Static
Volume of irradiation zone (ml)		12	7100	7100
Beam current (mA)		10	2.5	3.5
Electron accelerating voltage (MeV)		0.6	0.5	0.6
Dose (10^4 Mrad)	0	0.16	1.12	2.5
Temperature (°C)	25	260	65.3	88
Irradiation time (sec)	0	80	18000	28800
Pressure (Torr)	760	760	730	760
Concentration in m mole/ℓ * g/ℓ				
H_2	0	3.16	20.2	39.5
CH_4	40.6	-	12.0	4.1
$C_2H_4 + C_2H_2$	0	0.0023	0.02	0.005
C_2H_6	0	1.44	2.91	1.08
C_3H_6	0	0.008	0.004	0.001
C_3H_8	0	0.21	0.55	0.158
i-C_4H_{10}	0	0.03	0.10	0.043
1-C_4H_8	0	0.0002	-	-
n-C_4H_{10}	0	0.056	0.124	0.079
neo-C_5H_{12}	0	0.	0.015	0.008
x	0	-	-	0.0003
i-C_5H_{12}	0	0.025	0.036	0.071
n-C_5H_{12}	0	0.003	0.003	0.015
liquid product	0	0	0.034*	trace
solid wax	0	0	0	0.17*

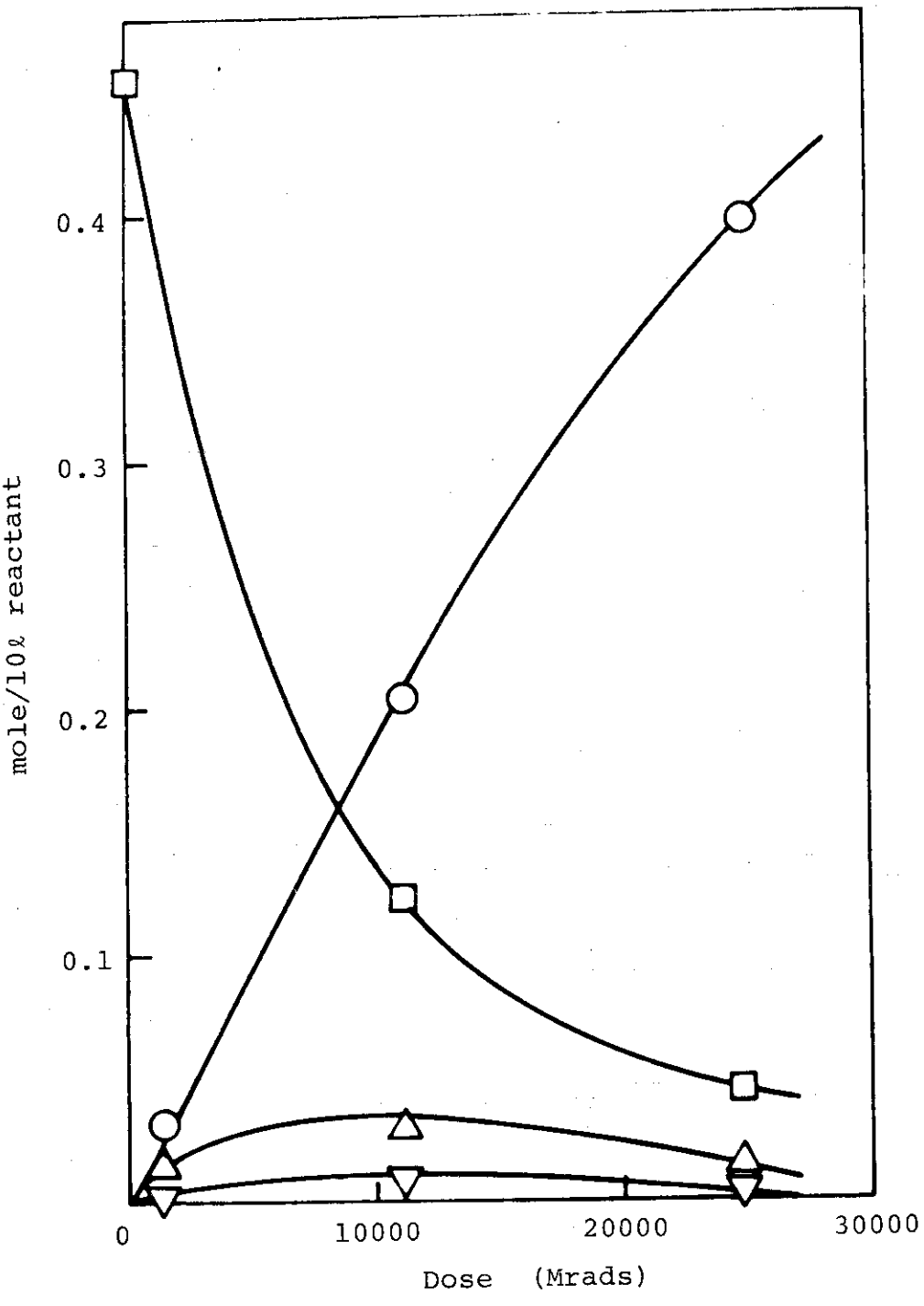

Fig. 4. Concentrations of irradiated gas as a function of dose: (□) methane, (○) hydrogen, (△) ethane, (▽) propane.

Table 3. Material Balance of the Radiation Chemical Reactions by 25000 Mrad Irradiation

Products	Weight from 10ℓ reactant (g)
H_2	1.12
C_2H_4	0.002
C_2H_6	0.46
C_3H_6	0.001
C_3H_8	0.10
iso-C_4H_{10}	0.04
n-C_4H_{10}	0.07
neo-C_5H_{12}	0.01
?	0.003
iso-C_5H_{12}	0.07
n-C_5H_{12}	0.02
Solid wax	1.74
Unreacted CH_4	0.94
	4.576
CH_4 (before irradiation)	7.14

different from those of higher hydrocarbons (∿6), this means that most hydrogen increase at this dose may come from radiolysis of higher hydrocarbons. The concentrations of ethane and propane are increased to maxima by 10000 Mrads irradiation and then decreased by further irradiation. No large discrepancies lie between the data obtained by the static technique and those obtained by the flow technique.

On careful examination of Table 2, one may find that branched C_5 hydrocarbon still increase with dose. This may suggest that hydrocarbons higher than C_5 may be still produced by sacrifice of lower hydrocarbons at this dose. It was difficult to determine the amount of solid product because of poor collection efficiency of the product, but 64% by weight of the material reacted were recovered (Table 3). The rest of the material may be assumed to be uncollected solid. The amount of solid thus roughly estimated agrees qualitatively with the value extrapolated from the data obtained by Blake, et al.[3)]

Gas chromatogram of the clear liquid indicated the presence of branched hydrocarbons of C_5 through C_7 with the lack of straight chain hydrocarbons. Infrared and NMR spectra of the liquid and the yellowish wax-like solid (m.p., 35 ∿ 50°C) also show the presence of hydrocarbons, and no signals due to compounds other than hydrocarbons were detected so far. The formation and properties of the solid products are in progress.

(H. Arai, S. Nagai, K. Matsuda, M. Hatada)

1) H. Arai, S. Nagai, K. Matsuda, and M. Hatada, JAERI-M 7949, 27 (1978).
2) S. Sugimoto, M. Nishii, and T. Sugiura, JAERI-M 7898, (1978).
3) A. R. Blake, D. A. Hilton, and I. H. Robbins, J. Appl. Chem., 17, 321 (1978).

10. Radiation Chemical Reactions of Gas Mixture of Methane and Nitrous Oxide

In the studies of radiolysis of pure methane, ethane is a dominant product over ethylene. Ethylene is assigned as a primary product formed from excited ethane produced by a reaction of two methyl radicals, but hydrogen addition to ethylene followed to convert ethylene to ethane. In an attempt to increase the yield of ethylene by scavenging hydrogen atom by additive, the studies on radiation chemical reactions of gas mixture of methane and nitrous oxide have been carried out.

The other purpose is to see whether organic oxygen containing compounds are produced from the gas mixture of methane and nitrous oxide by irradiation.

Takachiho "research" grade methane (purity, >99.95 mole%) and nitrous oxide (purity, 99.5 mole%) were used without further purification. Flow without circulation technique was employed throughout the experiment. The flow rates of the reactant were measured separately before mixing using two Ueshima-Brooks thermal mass flow meters (type 5810). The gas mixture was then introduced into a flow reactor, "FIXCAT-II", which was used in the previous studies, and irradiated with electron beams from the HDRA (0.6 MeV, 2 mA; dose rate, 7.33×10^{-3} eV·N_2O molec^{-1}·sec^{-1}·mA^{-1}). The irradiated gas was led from the reactor to two gas samplers in series of gas chromatographs through 20 m stainless steel tubing (1.5 mm inner diameter), equipped with 3 m Porapak Q columns and with 2 m Porapak N columns, respectively.

Fig. 1 shows G values of hydrocarbon products as a function of N_2O content in the gas mixture. The yields of saturated hydrocarbons decreased monotonously with increasing N_2O content, while those of unsaturated hydrocarbons increased and then decreased as the N_2O concentration increases. The small increase of the yields of unsaturated hydrocarbons may be due to the reaction of N_2O with hydrogen atom which otherwise reacts with double bond of olefins.

The G values of inorganic products are plotted in Fig. 2

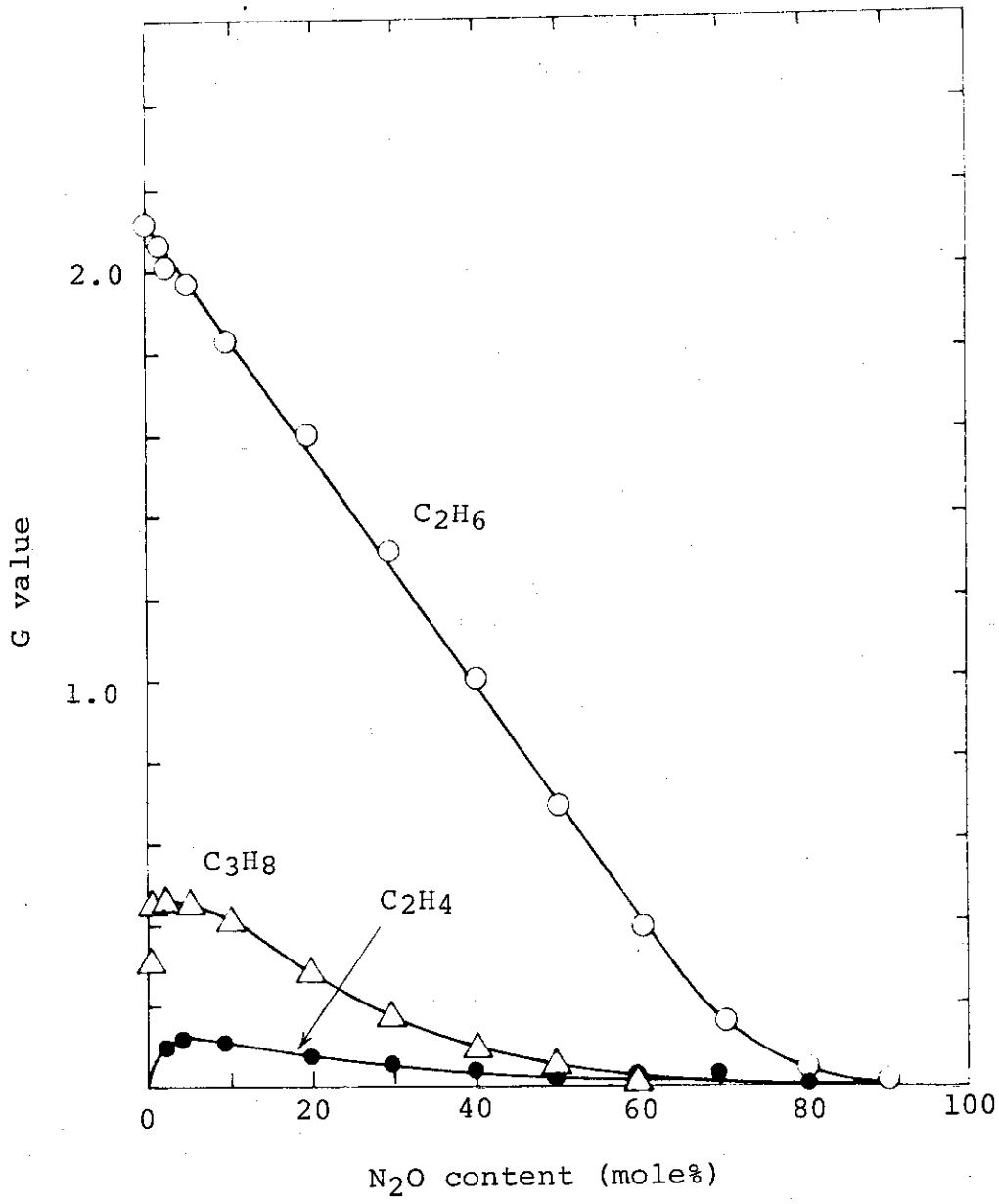

Fig. 1A. G values of hydrocarbons as a function of N_2O content: beam current, 2 mA; dose rate for the mixture containing 50 mole% N_2O, 1.51 x 10^{21} eV·g^{-1} (25 Mrad); flow rate, 100 ml/min; residence time, 0.12 min; temperature, 75°C.

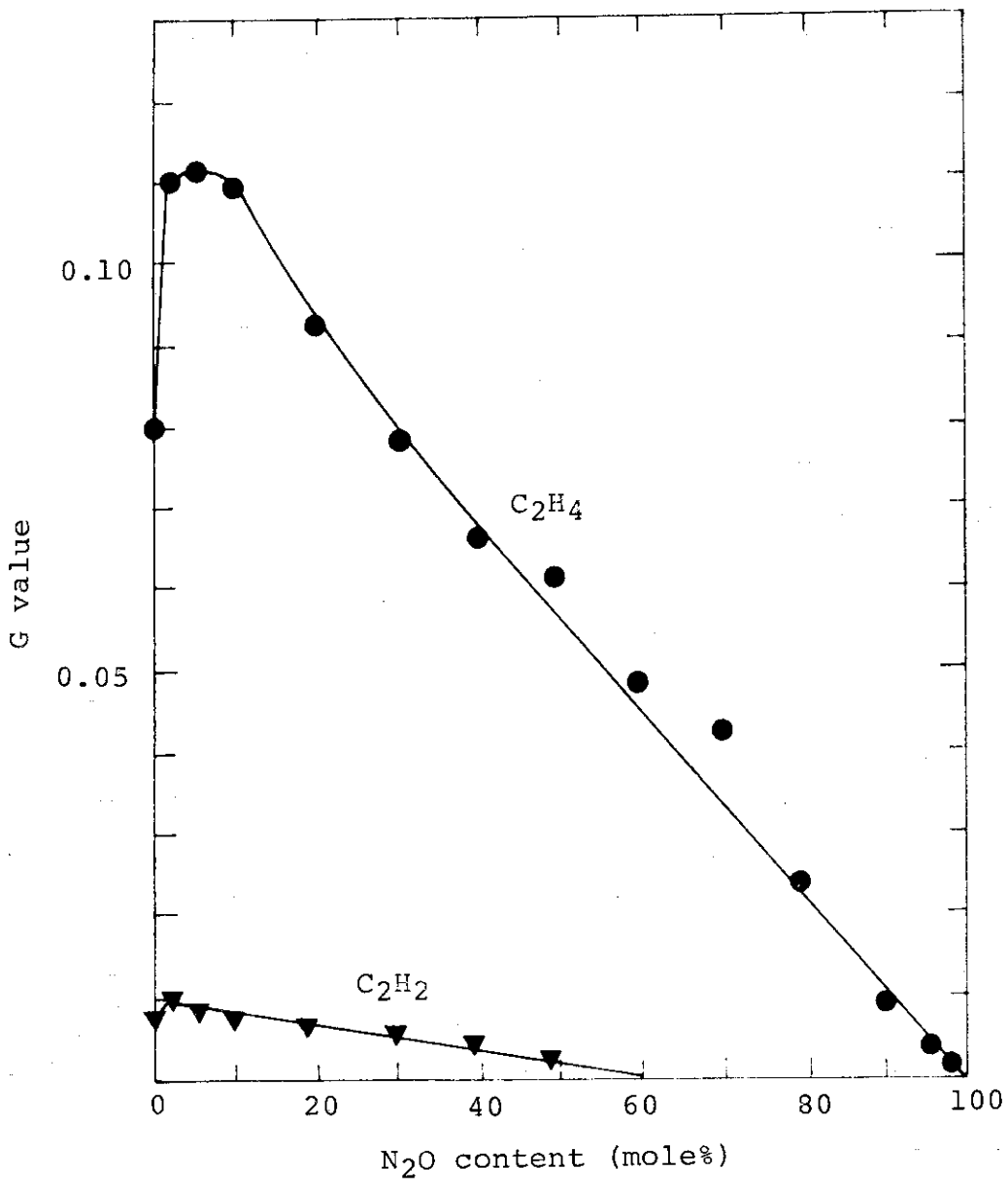

Fig. 1B. G values of hydrocarbons as a function of N_2O content: the reaction conditions are given in the caption of Fig. 1A.

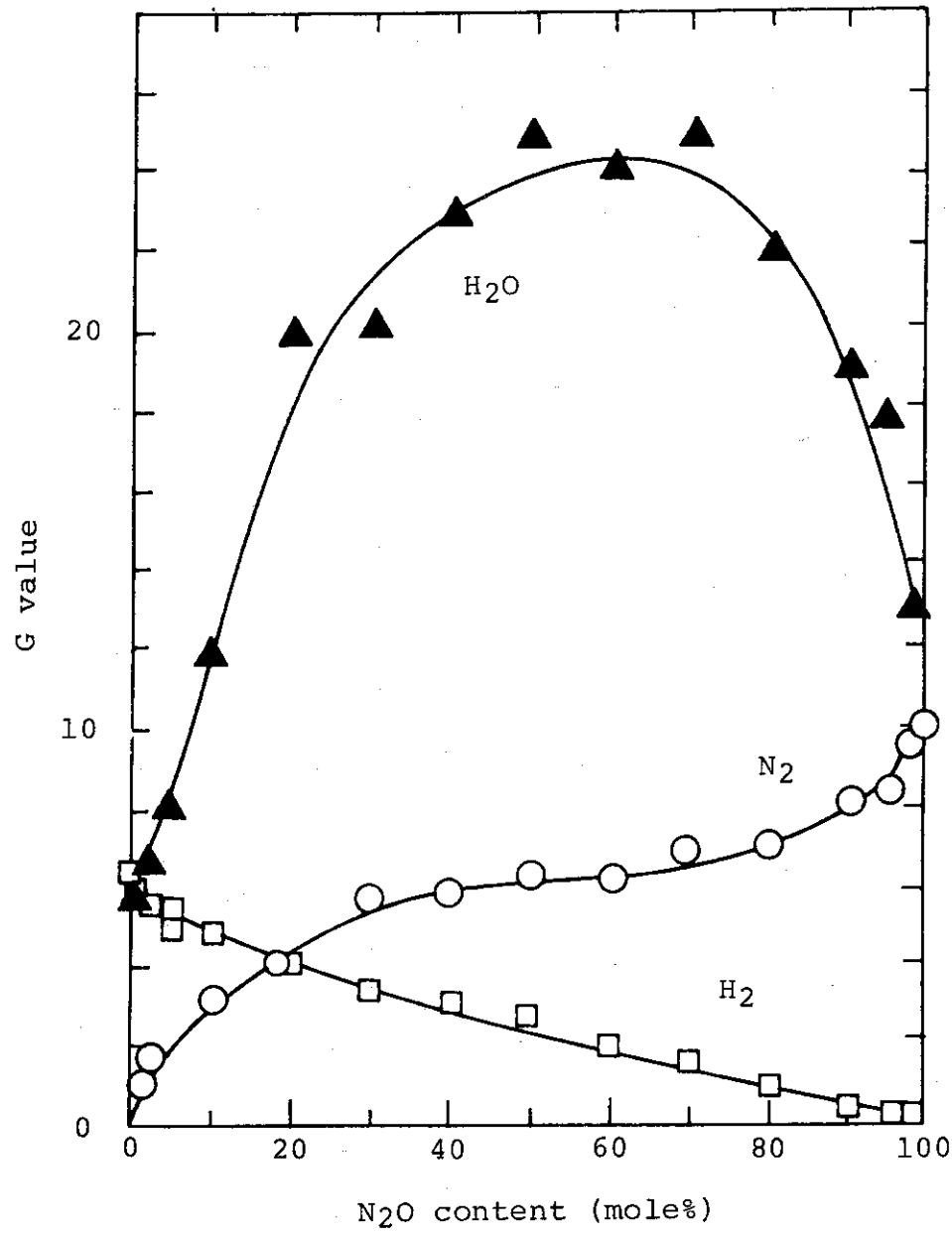

Fig. 2A. G values of inorganic products as a function of N_2O content: the reaction conditions are given in the caption of Fig. 1A.

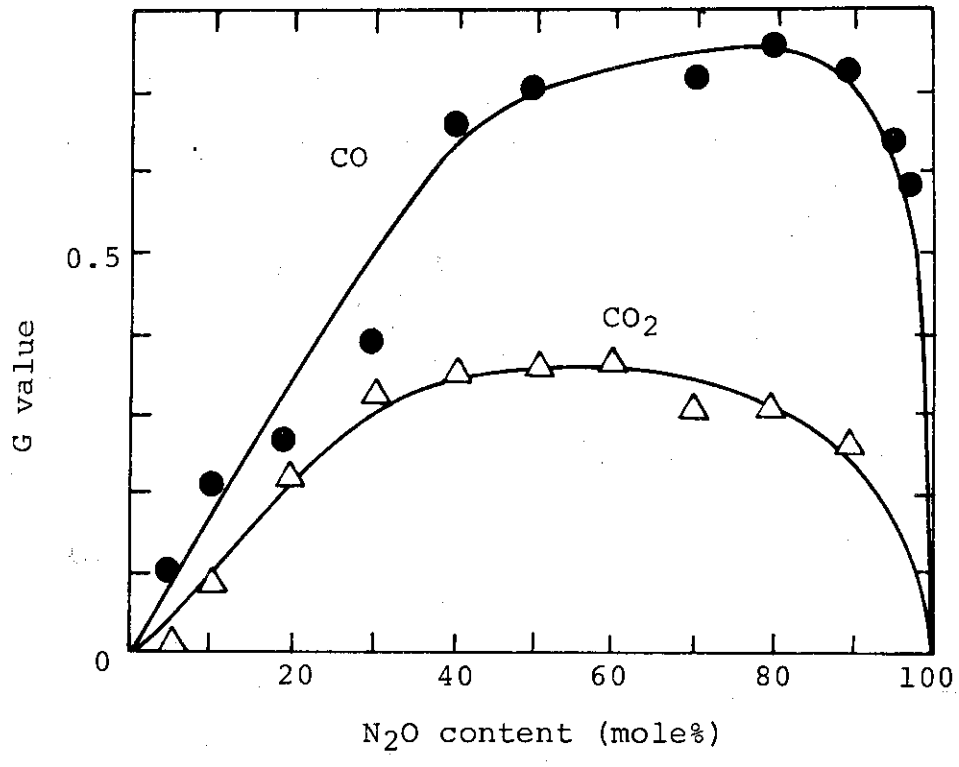

Fig. 2B. G values of inorganic products as a function of N_2O content: the reaction conditions are given in the caption of Fig. 1A.

as a function of N_2O content. The G value of H_2 decreases sharply with the addition of small amount of N_2O, indicating that N_2O reacts with hydrogen atom contributing to the increase of yields of olefins described above. The following linear decrease with increasing N_2O concentration may be due to dilution of methane as the hydrogen source. Sharp rise of $G(N_2)$ at small concentration of N_2O corresponds to the sharp decrease of $G(H_2)$ supporting the above observations.

G values of other inorganic products have maxima at certain N_2O concentrations and become zero at both 0 and 100% N_2O.

Various oxygen containing products such as acetic acid, methyl acetate, methanol and ethanol are formed in the gas mixture by irradiation. The G values of these products are plotted against N_2O content in Fig. 3. The maximum G value appears at 30 mole% N_2O for acetic acid, at 80% for methanol,

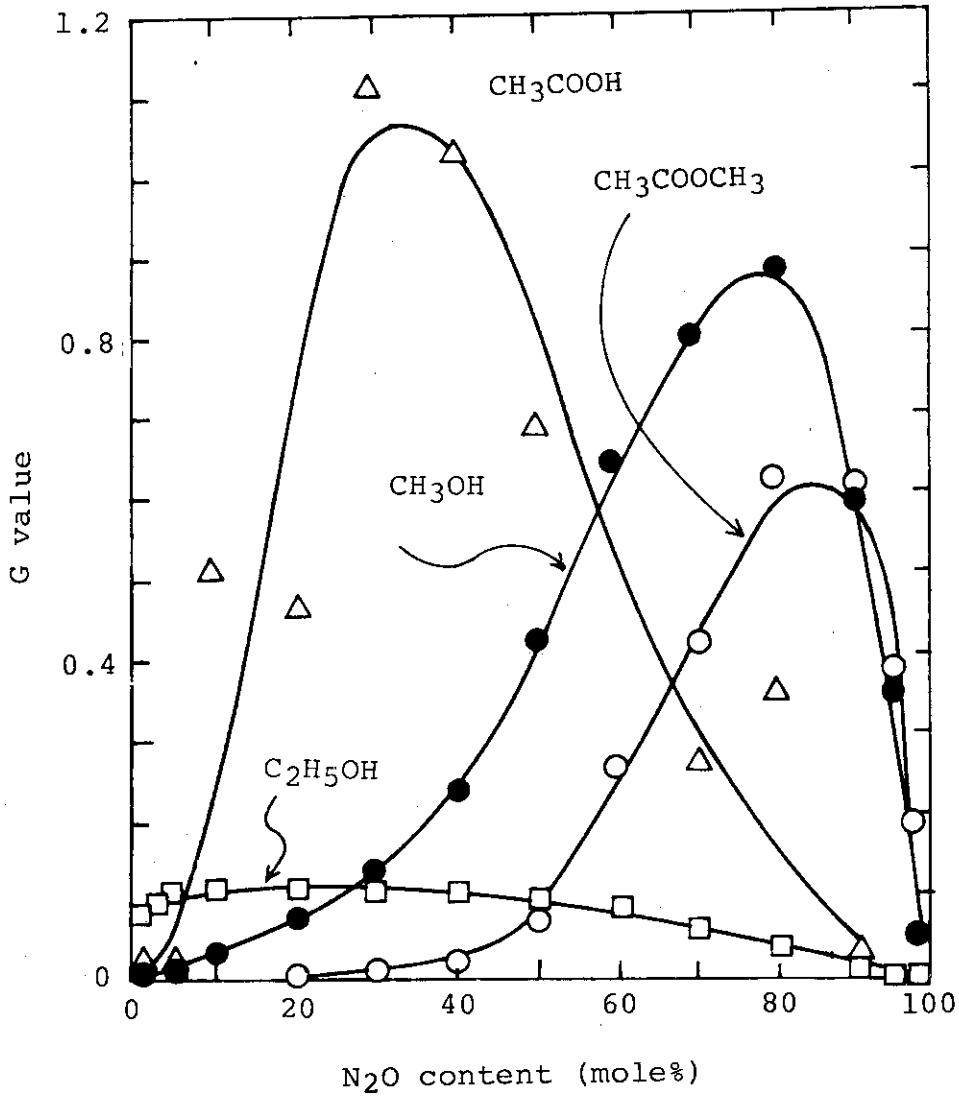

Fig. 3. G values of organic oxygen containing products as a function of N_2O content: (○) methyl acetate, (●) methanol, (△) acetic acid, (□) ethanol; the reaction conditions are given in the caption of Fig. 1A.

Table 1 The Yields of Products per One kWh Energy Input from CH_4-N_2O Gas Mixture

N_2O content (mole%)	30	80
Products	Yields (g)	
Acetic Acid	24.7	7.9
Methyl Acetate	0.0	16.6
Methanol	1.43	10.5
Ethanol	1.9	0.5
Carbon Monoxide	4.2	8.0
Ethane	14.6	0.2
Ethylene	0.8	0.2

at 85% for methyl acetate and at 15% for ethanol.

The G values of the products can be converted to the yield in $g \cdot kWh^{-1}$ unit by multiplying 0.374 and molecular weight. The maximum yields of the organic products are shown in Table 1 in order to give rough indication of energy balance.

The reaction mechanism which explains the relationships between G values and N_2O concentration is not known at present and will be considered systematically later when data will be accumulated for gas mixtures containing other oxygen containing additives.

(H. Arai, S. Nagai, K. Matsuda, M. Hatada)

11. Radiation Chemical Reactions of Gas Mixture of Methane and Carbon Dioxide

Studies have been carried out on the irradiation of gas mixture of methane and carbon dioxide. The first purpose is to know if it is able to enhance the yield of ethylene by scavenging hydrogen atom formed as a primary product of the methane radiolysis. The second one is to synthesize C_2 and still higher oxygen containing compounds from the gas mixture of methane and carbon dioxide.

The method and technique are the same as the previous section. Carbon dioxide is obtained from Osaka Suiso Industry (purity, 99.9 mole%). Methane is obtained from Takachiho Chemical Co. (purity, >99.95%).

In this study, beam current, electron energy and flow rate were kept constant at 2 mA and 100 ml/min, respectively,

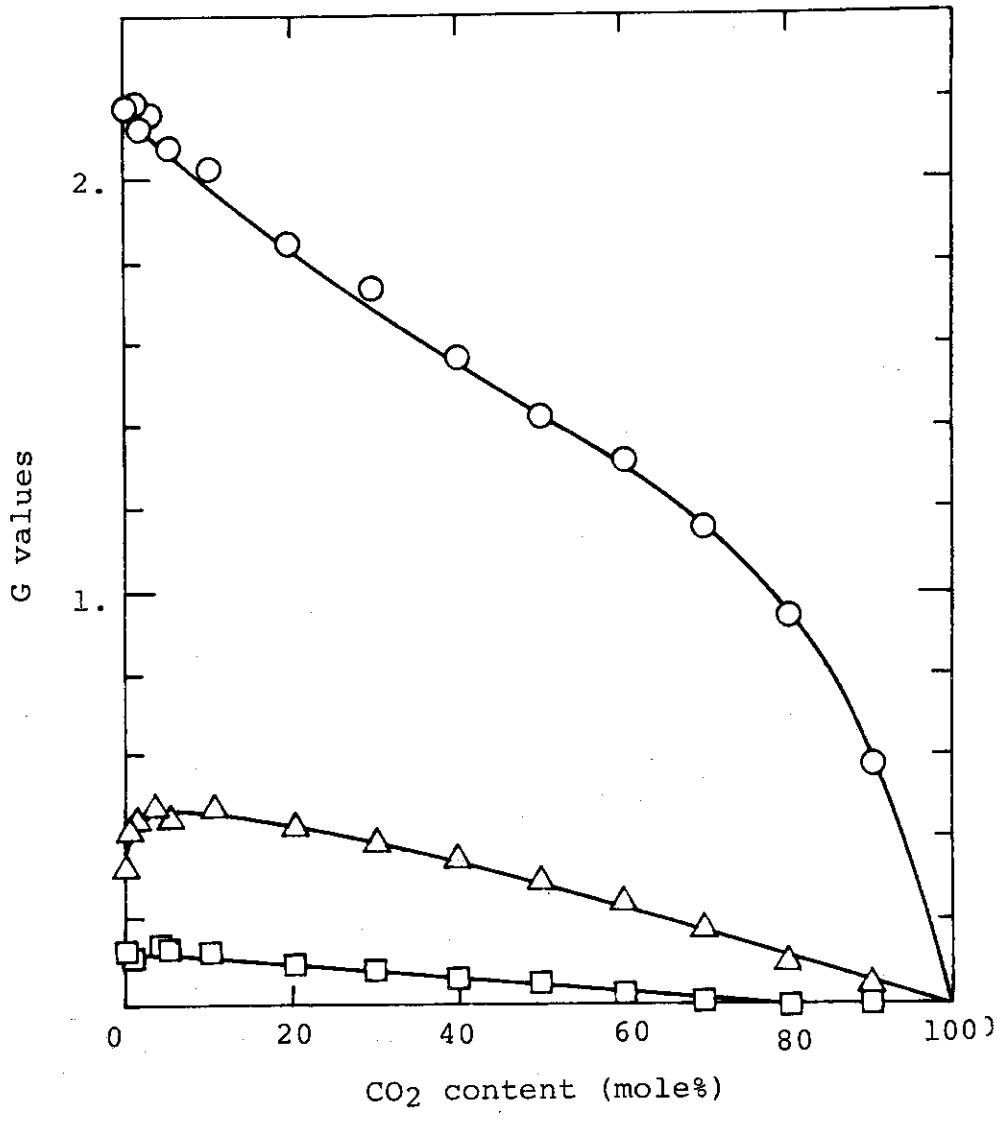

Fig. 1A. G values of saturated hydrocarbons as a function of CO_2 content: (○) ethane, (△) propane, (□) n-butane; beam current, 2mA; dose for 1:1 (by vol) mixture, 1.85×10^{22} eV·g^{-1} (24.6 Mrad); flow rate, 100/min; residence time, 0.12 min.

and concentration of CO_2 in the feed gas was altered. The dose absorbed by gas mixture was a value between 23 and 30 Mrads depending on the composition.

The G values of the products are shown as a function of carbon dioxide content in Fig. 1, 2, 3, 4, and 5, for saturated

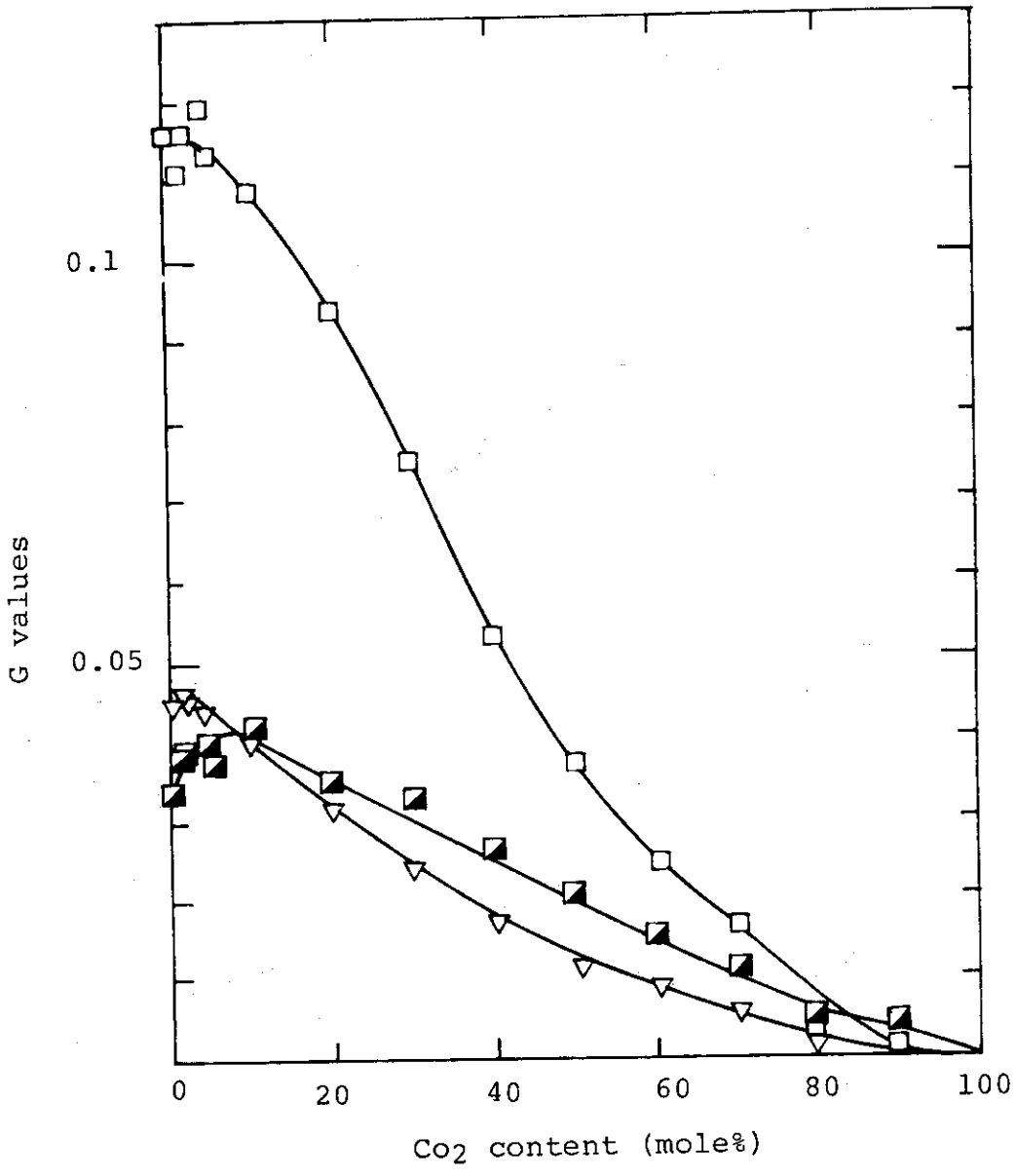

Fig. 1B. G values of saturated hydrocarbons as a function of CO_2 content: (□) n-butane, (◪) i-butane, (▽) i-pentane. The reaction conditions are given in the caption of Fig. 1A.

hydrocarbons, unsaturated hydrocarbons, aldehydes and alcohols, organic acids, and inorganic products, respectively. In Fig. 1, it is noted that the G values of ethane and n-butane decrease monotonously with increasing CO_2 content, while those of propane and i-butane were increased by addition of CO_2 and then decrease with increasing CO_2 content.

The G values of unsaturated hydrocarbons seem to decrease with increasing CO_2 content as shown in Fig. 2, and no enhancement of olefin yields was observed by CO_2 addition. Instead, various oxygen containing compounds were found to be formed as

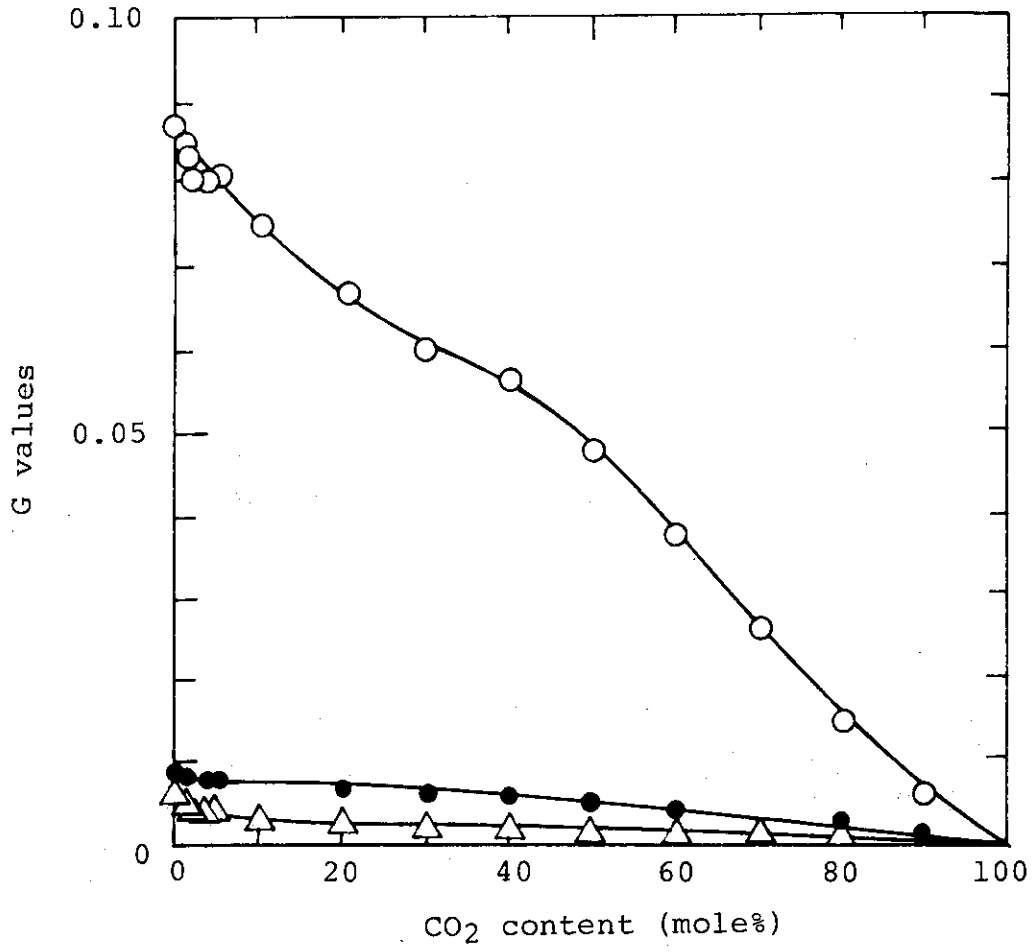

Fig. 2. G values of unsaturated hydrocarbons as a function of CO_2 content: (○) ethylene, (●) acetylene, and (△) propylene. The reaction conditions are given in the caption of Fig. 1A.

shown in Figs. 3 and 4.

In Fig. 3, the G values of alcohols and aldehydes are plotted against CO_2 content. Alcohol and aldehyde having one carbon atom have maximum G values at higher concentration at about 80 mole% CO_2 content than those having two carbon atoms (ethanol and acetaldehyde) which gave the maximum G values at 40 and 60%, respectively.

Figure 4 shows the G values of organic acids as a function of CO_2 content in the gas mixture. The G values of formic acid and acetic acid become maximum values of 3.8 and 2.8,

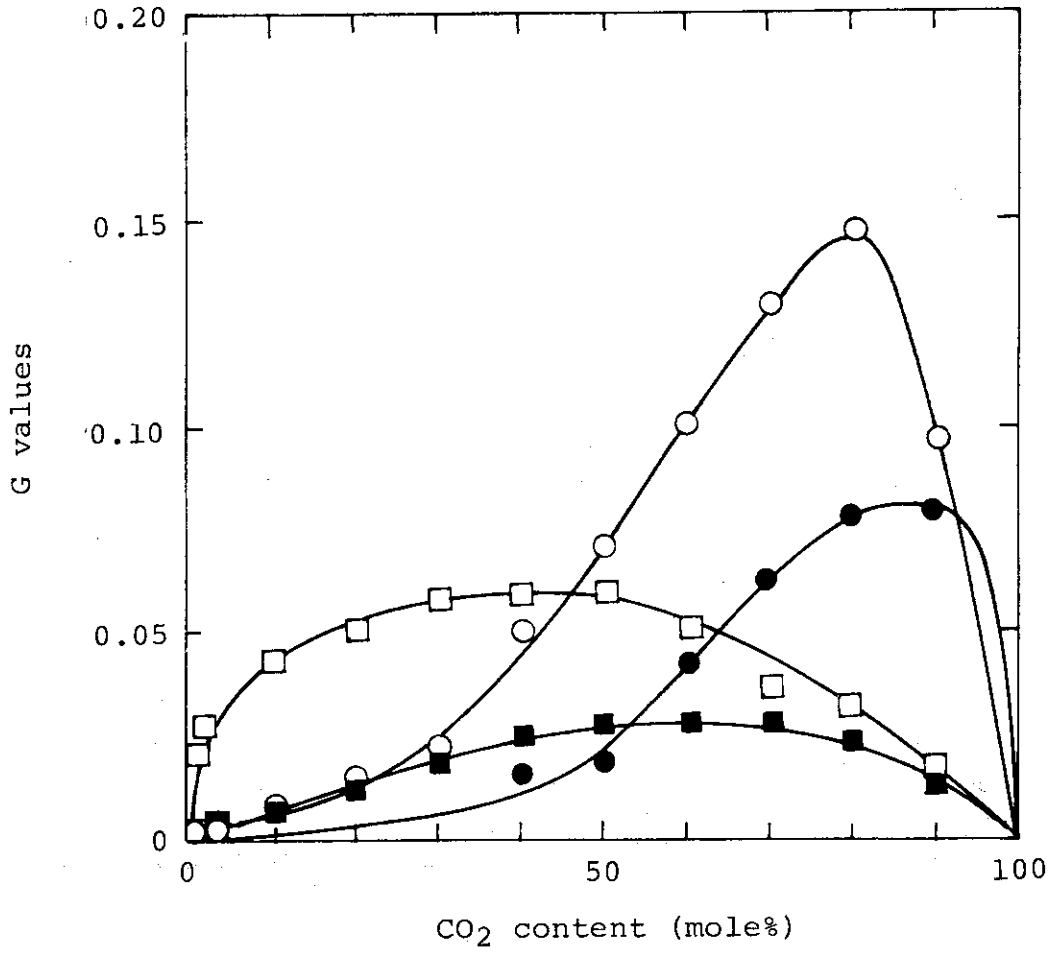

Fig. 3. G values of alcohols and aldehydes as a function of CO_2 content: (○) methanol, (□) ethanol, (●) formaldehyde, and (■) acetaldehyde. The reaction conditions are given in the caption of Fig. 1A.

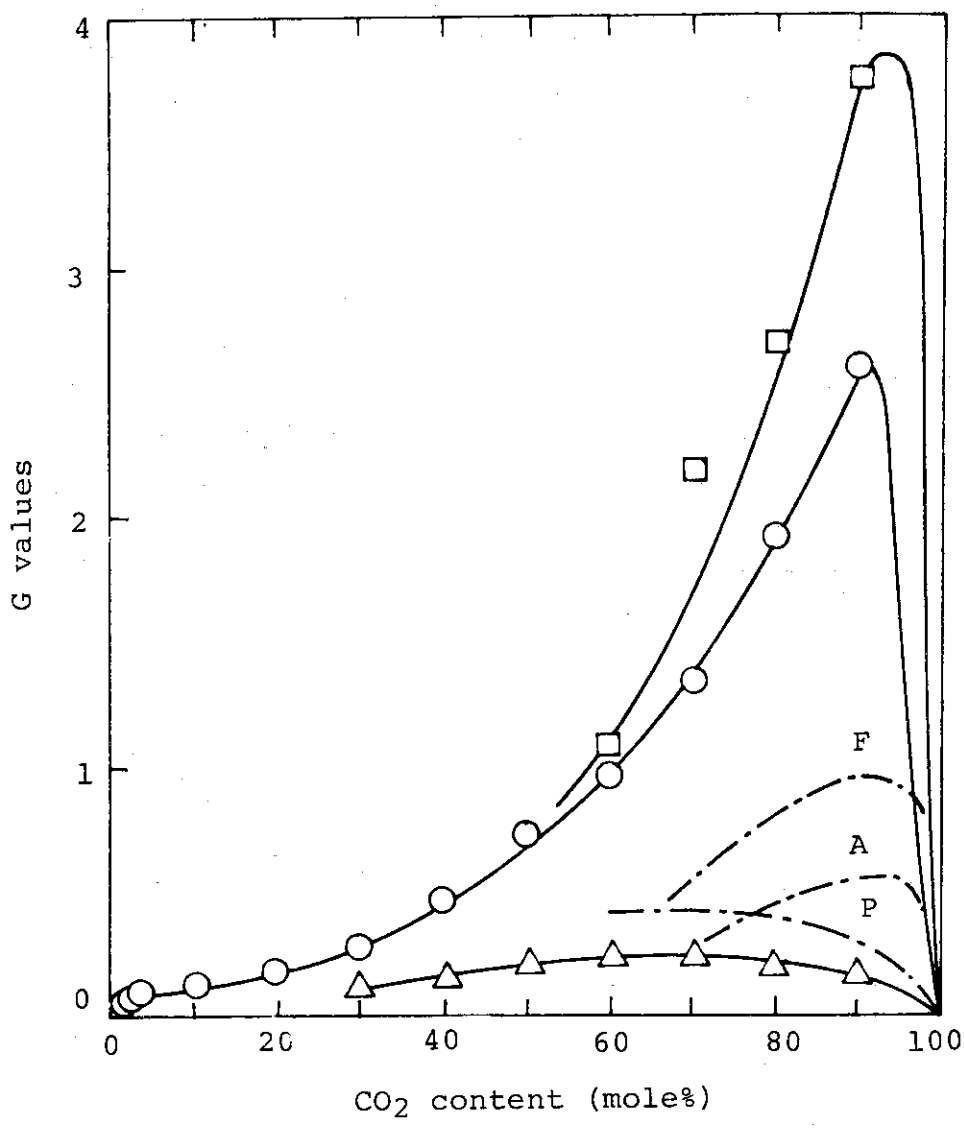

Fig. 4. G values of oraganic acids as a function of CO_2 content: (□) formic acid, (○) acetic acid, (△) propionic acid. The reaction conditions are given in the caption of Fig. 1A. Chain lines are taken from reference 1; (F) formic acid, (A) acetic acid and (P) propionic acid.

respectively, at CO_2 content of 90 mole%. The G value of propionic acid, which has more abundant hydrogen in a molecule than the former two, shows maximum at 65 mole%. Similar results were reported by Kuklin, et al.[1], but their G values are lower than ours. The amount of these organic acids produced by 1 kWh energy absorption are given in Table 1 for rough indication of energy balance which is quite reasonable for our purpose.

The G values of inorganic products are plotted against CO_2 content in Fig. 5. It is noted that G value of carbon monoxide formation from CO_2 is also increased considerably by addition of 10% methane. The G value of hydrogen also is decreased by the addition of carbon dioxide, but the decrease

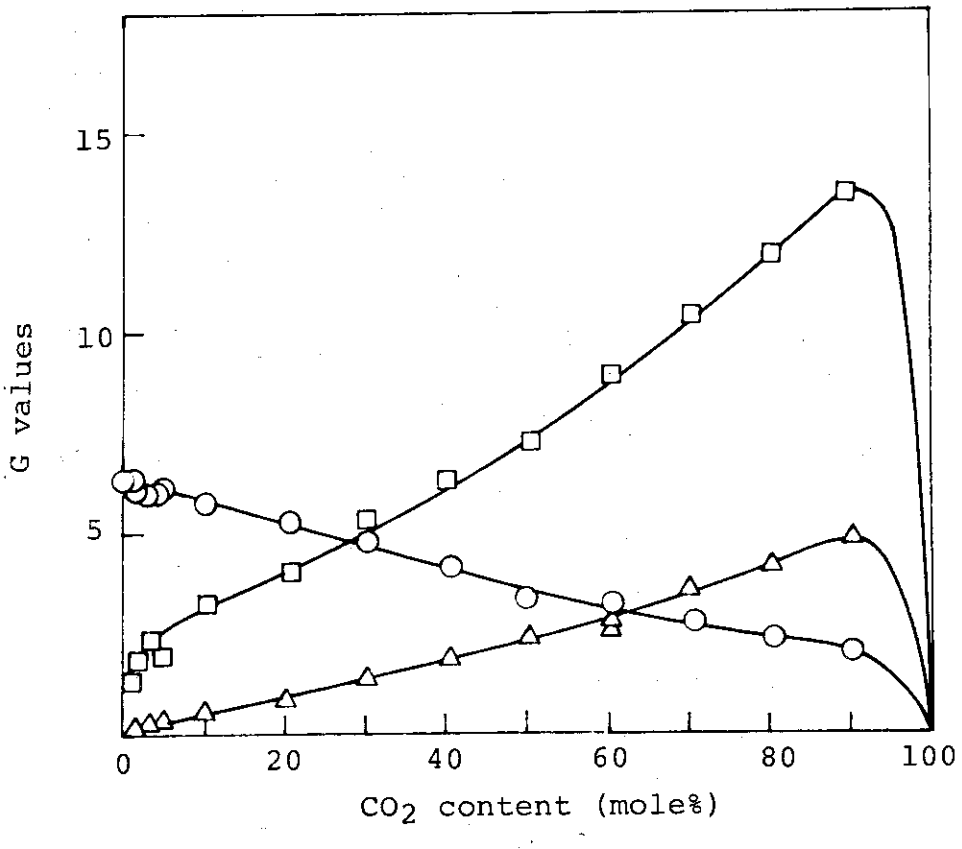

Fig. 5. G values of inorganic products as a function of CO_2 content: (○) hydrogen, (△) carbon monoxide, and (□) water. The reaction conditions are given in the caption of Fig. 1A.

Table 1. The Yields of Products per One kWh Absorbed Energy

CO_2 content (mole%)	40	90
Products	Yields (g)	
Methanol	0.6	1.2
Ethanol	2.6	0.3
Formaldehyde	0.2	0.9
Acetaldehyde	0.4	0.3
Formic Acid	0.	63.1
Acetic Acid	9.9	57.9
Propionic Acid	4.3	4.3
Carbon Monoxide	18.1	48.9

of $G(H_2)$ value is not larger than that expected from simple dilution of methane as hydrogen source. This finding means that carbon dioxide is not reactive with hydrogen to scavenge, and does not contradict with the fact that no enhancement of olefin formation was observed by addition of carbon dioxide.

(H. Arai, S. Nagai, K. Matsuda, M. Hatada)

1) Kuklin, et al., Khimiya Vysokikh Energii, 10, 286-9 (1976).

[2] Polymerization of Vinyl Monomers by High Dose Rate Electron Beams

1. Radiation-Induced Radical Polymerization of Styrene in Carbontetrachloride and Ethylene Dichloride

It was shown in the last annual report[1] that styrene (moderately dried) produced by irradiation not only in bulk but also in carbontetrachloride (CTC) and ethylene dichloride (EDC) three kinds of polymers, which can be fractionated and detected easily by GPC curves. They are oligomer, radical and cationic polymers.

Figure 1 shows, by an example carried out at room temperature with a dose rate of 6.3×10^4 rad/sec, rates of the total, radical and ionic polymerization in dependence on the styrene content (vol%) for styrene/CTC. It may be seen from the curves that the rates of both the radical and ionic polymerization become several times greater by an addition of 20 vol% CTC; after passing a maximum the rates decrease rather gradually. Even at a very low content of styrene, such as 20%, the rates are nearly so high as styrene in bulk. EDC shows similar effect as CTC, however, it is less remarkable than the latter. It is seen clearly that CTC and EDC are not simple diluents for the polymerization.

Some details of the feature of the experiments and a short discussion of the analysis of the results have already been given in the last annual report, where some unusual way of expression of the experimental results was adopted; this is revised and the present paper deals with kinetic analysis of polymerization of styrene in styrene/CTC and styrene/EDC by radical mechanism.

In the case of radiation induced reaction of a binary mixture, there is some difficulty to carry out a series of experiments of different styrene/halogenated hydrocarbon mixtures at the same dose rate of the absorption energy of radiation. Therefore, for convenience, the irradiation of a

series of mixtures was carried out at a constant dose rate which corresponds to a certain value of the absorbed energy for pure styrene, and the value is simply designated as the dose rate.

Important experimental aspect for the analysis is that the rate of radical polymerization (R) is proportional to the square root of the dose rate (I) at any styrene content as shown, for the case of styrene/CTC, in Fig. 2 ∿ Fig. 4. The

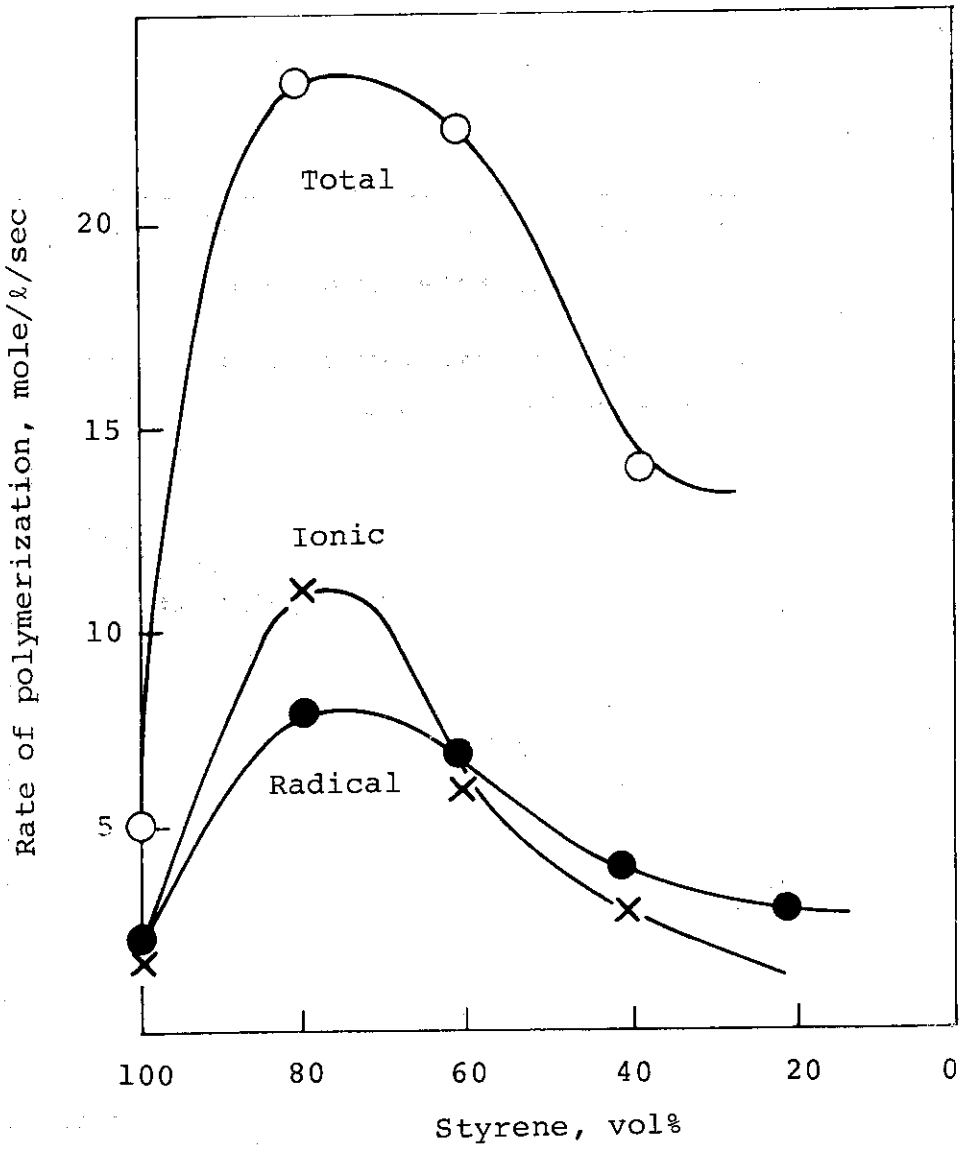

Fig. 1. Rates of total, radical and ionic polymerization of styrene in dependence of styrene cont. of styrene/CTC. Dose rate, 6.3×10^4 rad/sec.

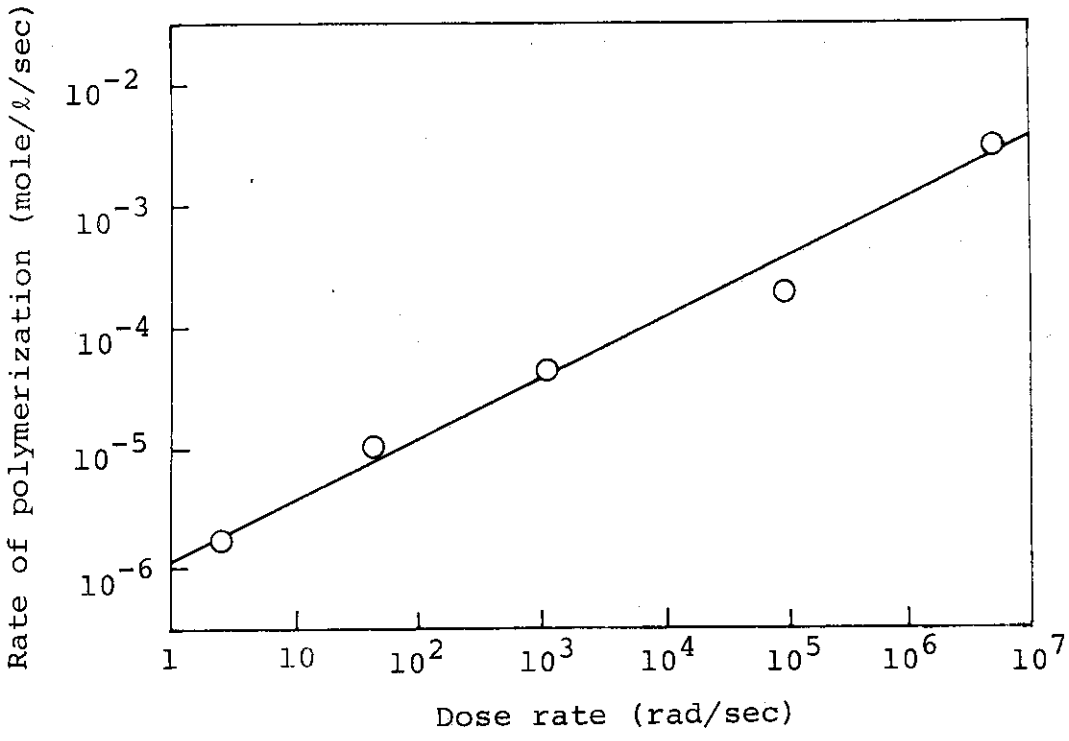

Fig. 2. Rate of radical polymerization of pure styrene in dependence on the dose rate.

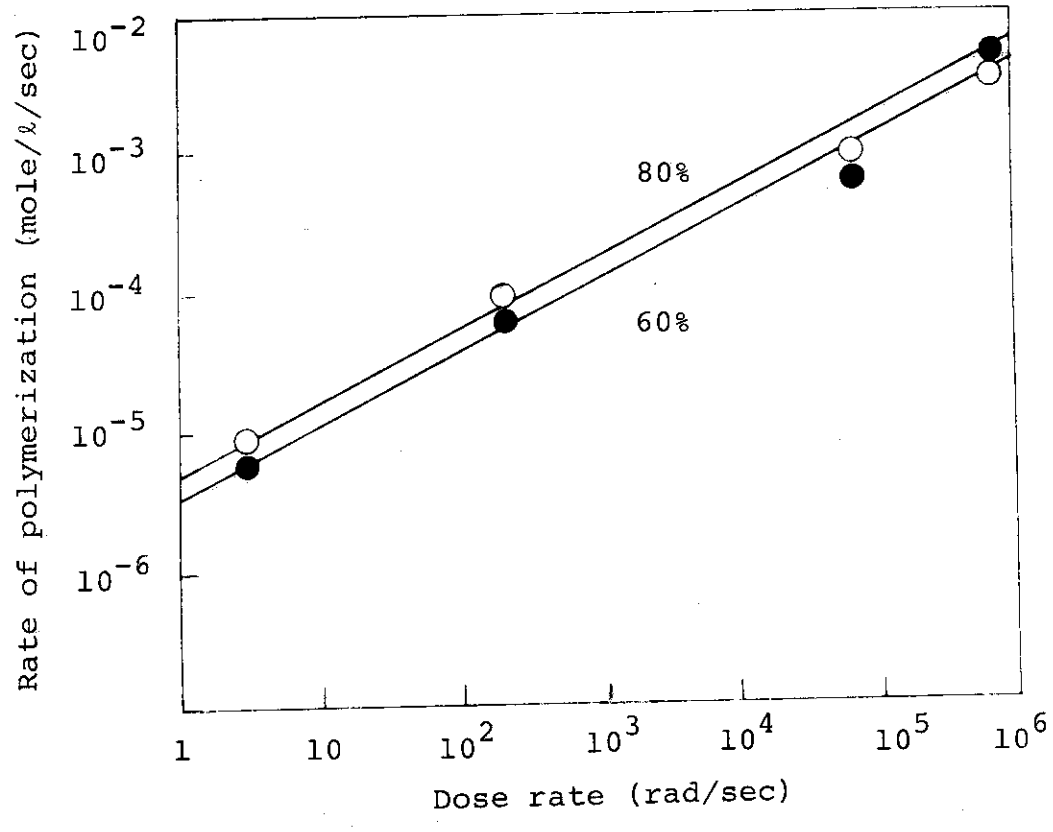

Fig. 3. Dose rate dependence of radical polymerization of styrene for 80 and 60 vol% styrene in styrene/CTC.

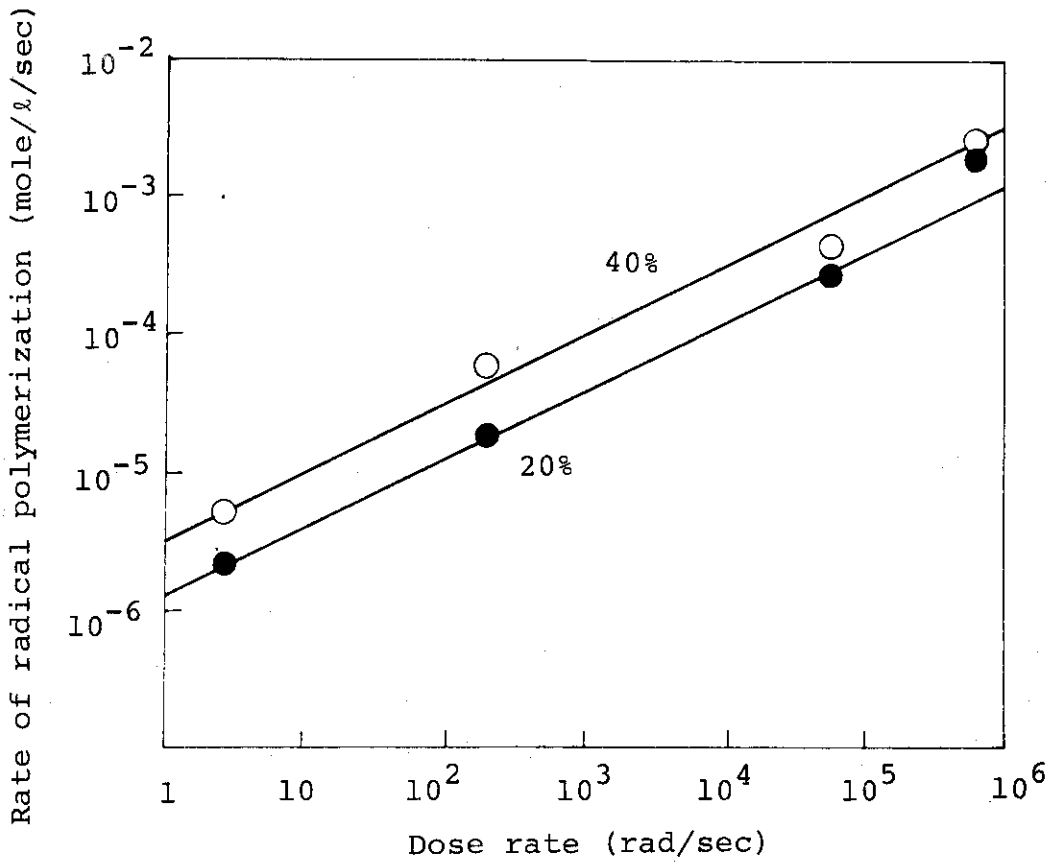

Fig. 4. Dose rate dependence of radical polymerization of styrene for 40 and 20 vol% styrene in styrene/CTC.

experiments cover a dose rate range from 2.5 rad/sec to 6 x 10^6 rad/sec and styrene content from 100 to 20 vol percent. The system of styrene/EDC gives similar results.

The scheme of the radical polymerization may be expressed by the following equations, where M, M·, S and S· mean styrene molecule, styrene radical, solvent molecule and solvent radical, respectively.

Initiating radical formation:

$$M \rightsquigarrow M\cdot \qquad (1)$$

$$S \rightsquigarrow S\cdot \qquad (2)$$

Growth

$$M\cdot + M \longrightarrow M_2\cdot \qquad (3)$$

$$S\cdot + M \longrightarrow SM\cdot \qquad (4)$$

If we neglect the possible difference of the reactivities of M· and S· and denote both the radicals with a common notation Q, then we can express termination as follows:

Termination

$$Q\cdot + Q\cdot \longrightarrow Q - Q \tag{5}$$

In the case of catalytic radical polymerization it is well known that termination is predominantly a coupling of two growing radicals. In the present case also equation (5) was used for the termination.

Concerning chain transfer reaction it was pointed out that CTC was a very strong transfer agent for the catalytic polymerization of styrene. In the mechanism of radiation polymerization it is quite natural to take similar transfer into account.

Transfer

$$Q\cdot + S = Q + S\cdot \tag{6}$$

Kinetic equations may be expressed as follows, and the equation for the rate of polymerization derived under assumption of a stationary state.

Rate of initiating radical formation:

$$\frac{d[Q\cdot]}{dt} = (\Phi_m[M] + \Phi_s[S])\ I \tag{7}$$

where [Q·], [M] and [S] are concentrations in mole per liter of Q, M and S respectively, Φ_m and Φ_s are the rate constants of free radical production of the monomer and solvent, respectively per unit dose, and I is the dose rate in rad/sec.

Rate of polymerization:

$$R = -\frac{d[M]}{dt} = k_p[Q\cdot][M] \tag{8}$$

Rate of termination:

$$-\frac{d[Q\cdot]}{dt} = k_t[Q\cdot]^2 \tag{9}$$

The stationary state is (7) + (9) = 0, and the concentration of the free radicals is found to be

$$[Q]^2 = \frac{I}{k_t}(\Phi_m[M] + \Phi_s[S]) \tag{10}$$

Putting (10) into (8) we obtain:

$$R = k_p[M](I/k_t)^{1/2}\ (\Phi_m[M] + \Phi_s[S])^{1/2} \tag{11}$$

The equation shows that R is proportional to $I^{1/2}$, which agrees with experimental results shown in Fig. 2, 3 and 4.

The rate of bulk polymerization R_0 is obtained by putting [S] = 0 in the above equation.

$$R_0 = k_p[M]_0^{3/2}(\Phi_m I/k_t)^{1/2} \tag{12}$$

where $[M]_0$ is styrene content in mole/ℓ of bulk styrene.

From equations (11) and (12), the following relation is obtained, which enables us to find the numerical value of Φ_s/Φ_m graphically.

$$(\frac{R}{R_0})^2(\frac{[M]_0}{[M]})^3 - 1 = \frac{\Phi_s}{\Phi_m}\ \frac{[S]}{[M]} \tag{13}$$

Figure 5 shows the plot of $(R/R_0)^2([M]_0/[M])^3 - 1$ against [S]/[M] for styrene/CTC.

According to the equation the plots are expected to give a straight line, whose inclination corresponds to Φ_s/Φ_m. Though the scattering of the points is somewhat large, it may be regarded to be due to experimental error. The experiments were carried out at three different dose rates, that is at 2.5, 2.2×10^2 and 6.3×10^4 rad/sec; Φ_s/Φ_m is found to be 43 independent of the dose rate. It means that CTC produces 43 times larger number of initiating radicals than styrene by a

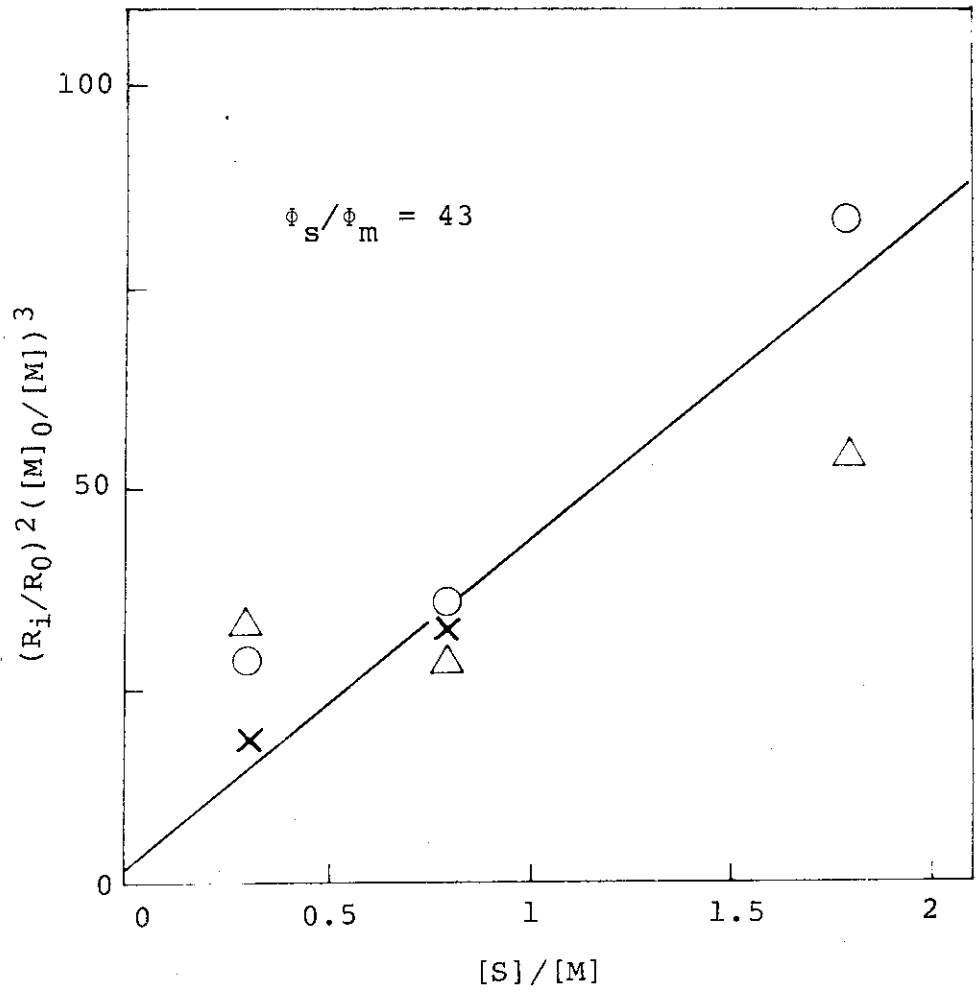

Fig. 5. Dependence of $(R_i/R_0)^2([M]_0/[M])^3$ on [S]/[M] in styrene/CTC. Dose rate: (o) 2.5, (×) 2.2 x 10^2, and (Δ) 6.3 x 10^4 rad/sec.

unit dose.

Similar plot for styrene/EDC at a dose rate of 2.5 rad/sec is shown in Fig. 6. Scattering of the points is much less in this case and Φ_s/Φ_m is found to be 10.

For the discussion of chain transfer, it is necessary to know the degree of polymerization. Though chain transfer has no effect on the rate of polymerization, it has essentially a great effect on the degree of polymerization.

Stable polymer molecules are formed not only by termination but also by transfer. The rate of stable polymer

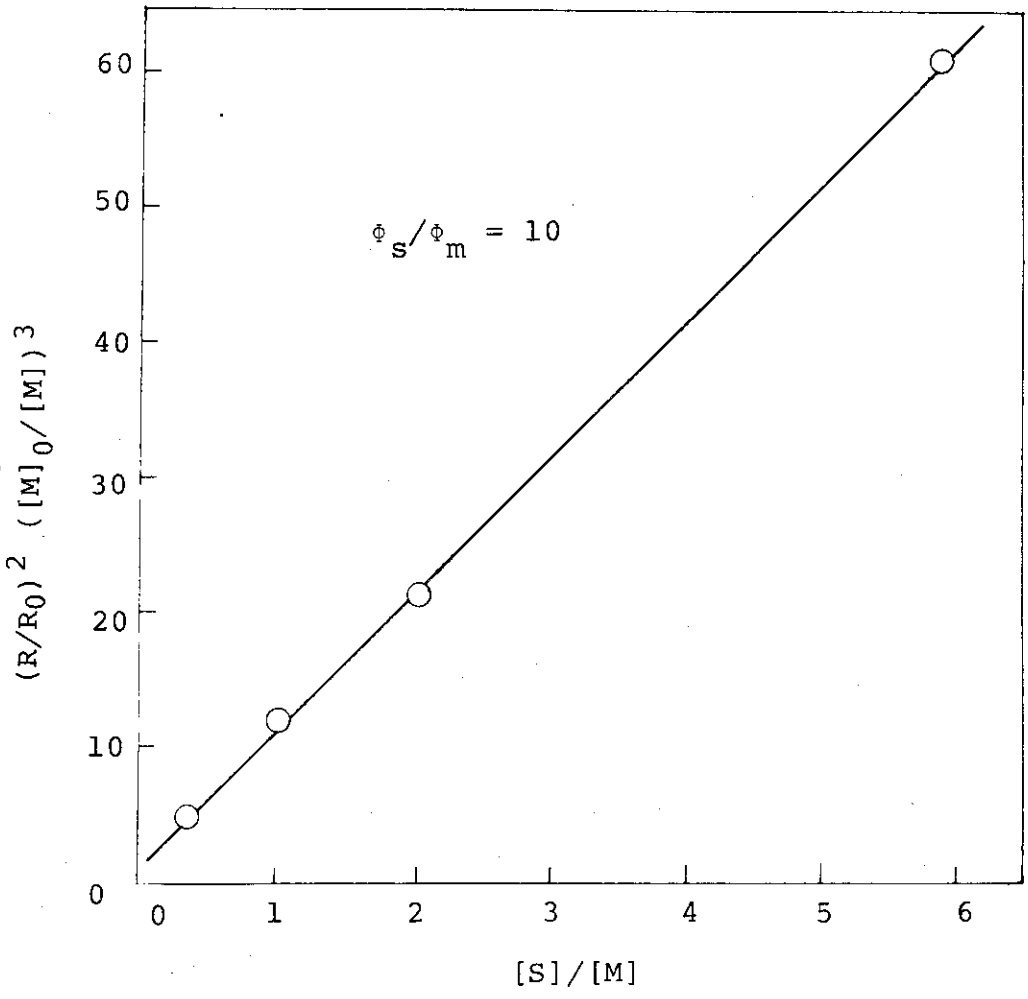

Fig. 6. Dependence of $(R/R_0)^2([M]_0/[M])^3$ on [S]/[M] in styrene/EDC for the radical polymerization. Dose rate: 2.5 rad/sec.

formation may be expressed as follows:

$$\text{Rate of stable polymer formation (mole/}\ell\text{/sec)} = k_{tr}[Q\cdot][S] + (k_t/2)[Q\cdot]^2 \quad (14)$$

Degree of polymerization P is obtained by dividing the rate of polymerization R with the rate of stable polymer formation as follows:

$$\frac{1}{P} = \frac{k_{tr}[S]}{k_p[M]} + \frac{k_t^{1/2}}{2k_p}\frac{I^{1/2}}{[M]^{1/2}}\Phi_m^{1/2}\left(1+\frac{\Phi_s}{\Phi_m}\frac{[S]}{[M]}\right)^{1/2} \quad (15)$$

In the case of the bulk polymerization equation (15) is reduced to

$$\frac{1}{P_0} = \frac{k_t^{1/2}}{2k_p} \frac{I^{1/2}}{[M]_0^{1/2}} \Phi_m^{1/2} \tag{16}$$

From equations (15) and (16) we obtain,

$$\frac{P_0}{P} = \frac{k_{tr}}{k_p} \frac{[S]}{[M]} P_0 + \left(\frac{[M]_0}{[M]}\right)^{1/2} \left(1 + \frac{\Phi_s}{\Phi_m} \frac{[S]}{[M]}\right)^{1/2} \tag{17}$$

P_0/P is the ratio of the degrees of polymerization of the bulk to solution polymers, in other words it is the ratio of the numbers of polymer molecules per unit volume of the solution to bulk polymers. The first and the second terms of the right hand side of equation (17) correspond to the numbers of polymer molecules produced by the transfer and termination, respectively.

All values in the equation except k_{tr}/k_p are known either by experimental conditions or as experimental results. As a trial we have calculated the value of the second term and compared it with the experimental value of P_0/P for styrene/CTC at a dose rate of 2.2×10^2 rad/sec. The results are as follows:

Styrene cont. vol%	80	60	40	20
Value of 2nd term	4.2	7.6	13.9	3.2
P_0/P	3.7	6.2	14.5	(24.6)

As may be seen, the calculated numerical values are, with one exception, nearly the same as to the observed values of P_0/P; it means that the term of transfer is too small to be detected because termination by mutual reaction of growing chains far exceeds the former.

If we neglect, therefore, the first term of equation (17), it is simplified to,

$$\left(\frac{P_0}{P}\right)^2 \left(\frac{[M]}{[M]_0}\right) = 1 + \frac{\Phi_s}{\Phi_m} \frac{[S]}{[M]} \tag{18}$$

By plotting $(P_0/P)^2([M]/[M]_0)$ against [S]/[M] straight lines are obtained both for the case of styrene/CTC and styrene/EDC as shown in Fig. 7 and 8. And further, the values of Φ_s/Φ_m were found from the inclination of the curves to be 47 and 8 for styrene/CTC and styrene/EDC, respectively. The agreement of these values calculated from the degrees of polymerization with the values of 43 and 10 obtained from the rates of polymerization may be regarded to be satisfactory.

The most important feature of the radiation induced solution polymerization of styrene in CTC and EDC is that about 50 and 10 times greater number of initiating radicals

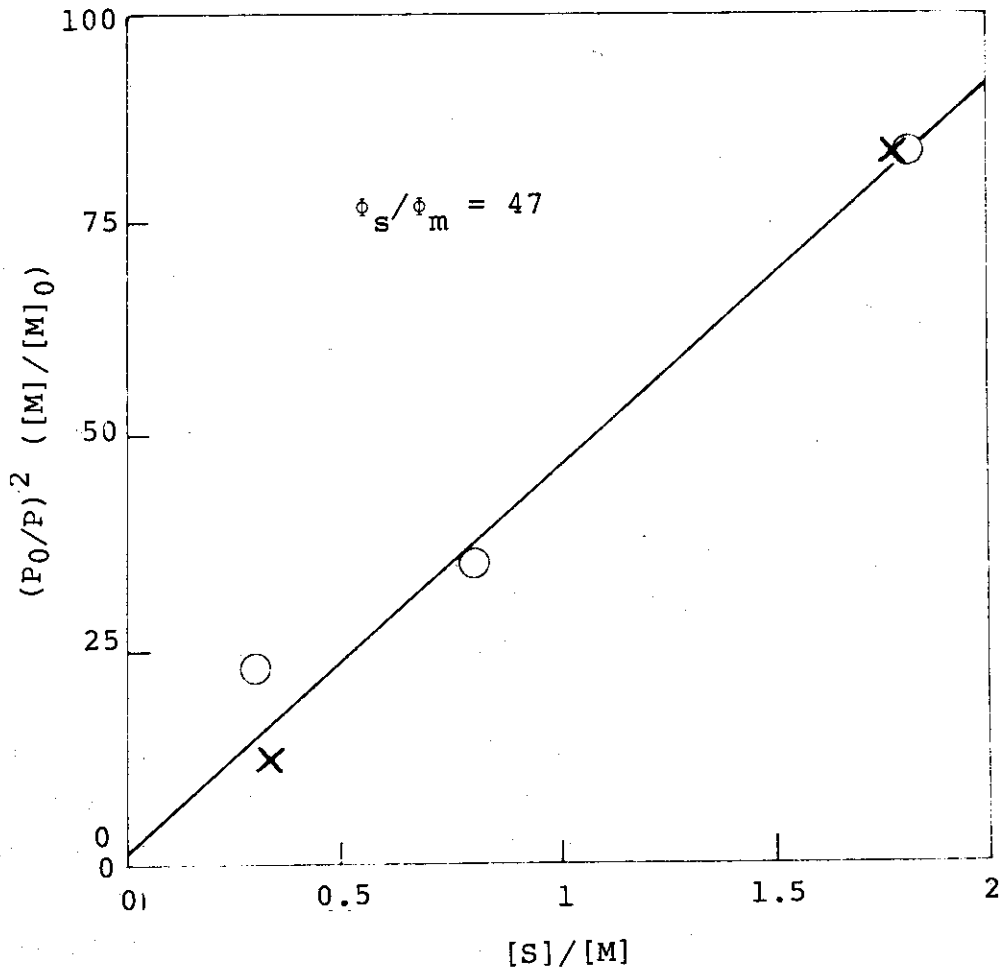

Fig. 7. $(P_0/P)^2([M]/[M]_0)$ in dependence on ([S]/[M]) for the radical polymerication of styrene in styrene/CTC. Dose rate: (o) 2.5 and (×) 2.2 x 10^2 rad/sec.

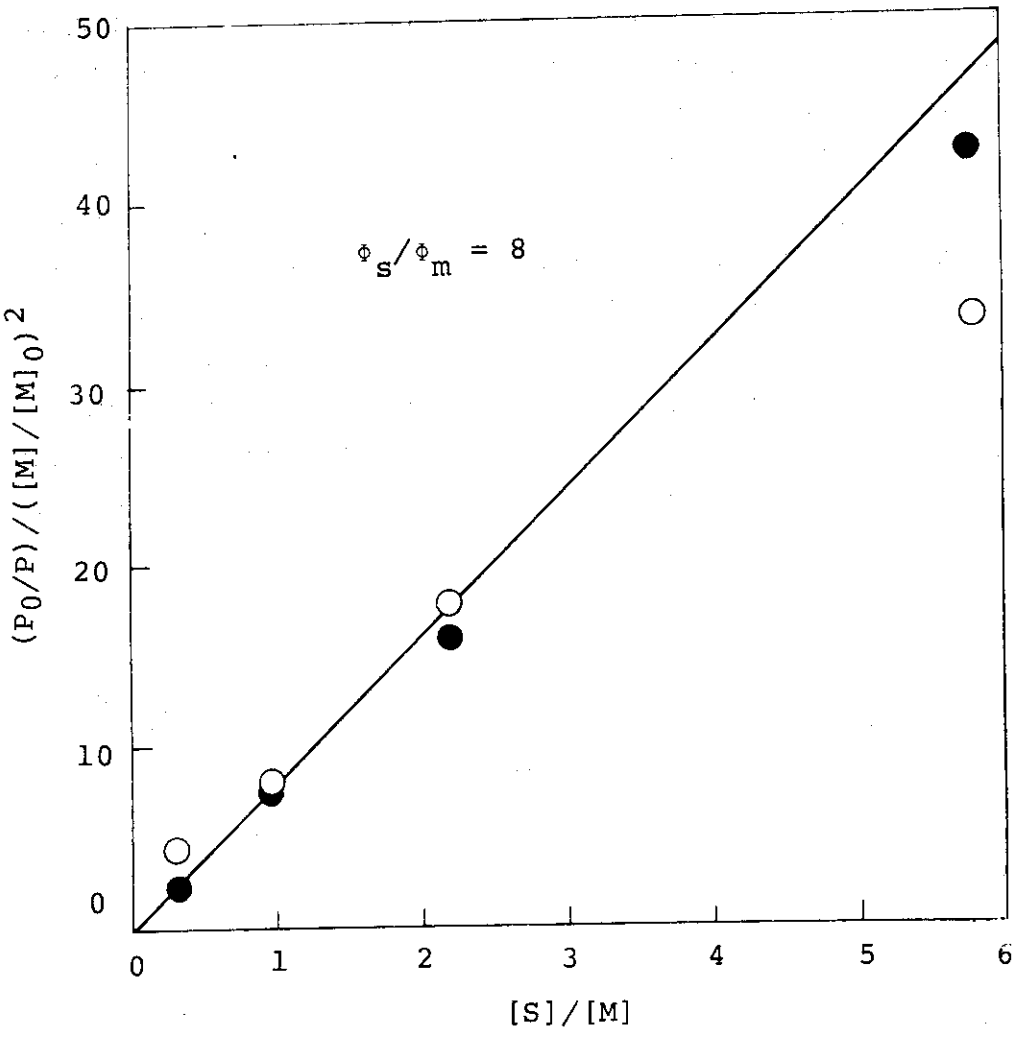

Fig. 8. Dependence of $(P_0/P)/([M]/[M]_0)^2$ on [S]/[M] in styrene/EDC for the radical polymerization. Dose rate: (o) 2.5 and (●) 4.3 rad/sec.

are formed by irradiation from CTC and EDC than from styrene. Initiating radicals grow and the termination by mutual interaction of the growing radicals occurs so frequently that the transfer to solvent molecules, which is important in the catalytic polymerization can not be detected. The feature is not changed in a wide range of dose rate i.e. from 2.5 rad/sec to 6×10^6 rad/sec and styrene content from 100 to 20 vol%.

(I. Sakurada, J. Takezaki, T. Okada)

1) I. Sakurada, J. Takezaki, T. Okada, JAERI-M 7949, 38, 52 (1978).

2. Radiation-Induced Cationic Polymerization of Styrene in Carbontetrachloride and Ethylene Dichloride

In the preceeding report experimental results and discussion of radical polymerization of styrene in CTC and EDC were described. In the above experiments cationic polymerization also takes place simultaneously; the higher the dose rate, the larger the amount of cationic polymers. The present paper deals with the kinetics of cationic polymerization of styrene in CTC and EDC.

Only a little is known about the kinetics of radiation induced ionic polymerization of vinyl monomers in solution [1]. Essential problem of the solution polymerization is the contribution of solvent molecules to each step in the

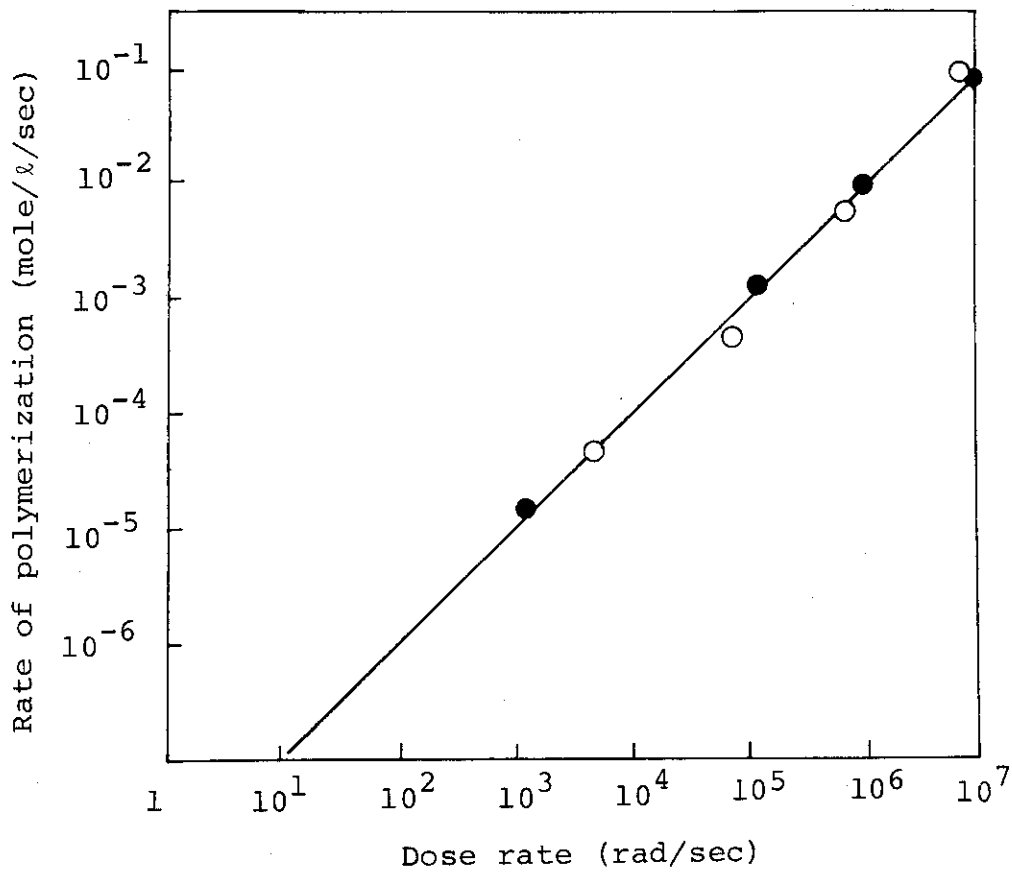

Fig. 1. Dose rate dependence of ionic polymerization of pure styrene: (o) styrene/CTC and (●) styrene/EDC.

polymerization i.e. initiating ion formation, growth (propagation), termination and transfer.

To give general aspects of ionic solution polymerization, dose rate (I) dependence of the rates of polymerization (R) for styrene/CTC of various styrene contents, i.e. from 100 to 20 vol% are shown in Fig. 1, 2 and 3.

It may be seen from the figures, that in all cases the plots of R against I are straight lines, which show direct proportionality of R to I. The results suggest that mechanism of the solution polymerization is essentially the same as that of the bulk polymerization so long as it is concerned with the rate of polymerization. Therefore the steps of the polymerization may be described as follows.

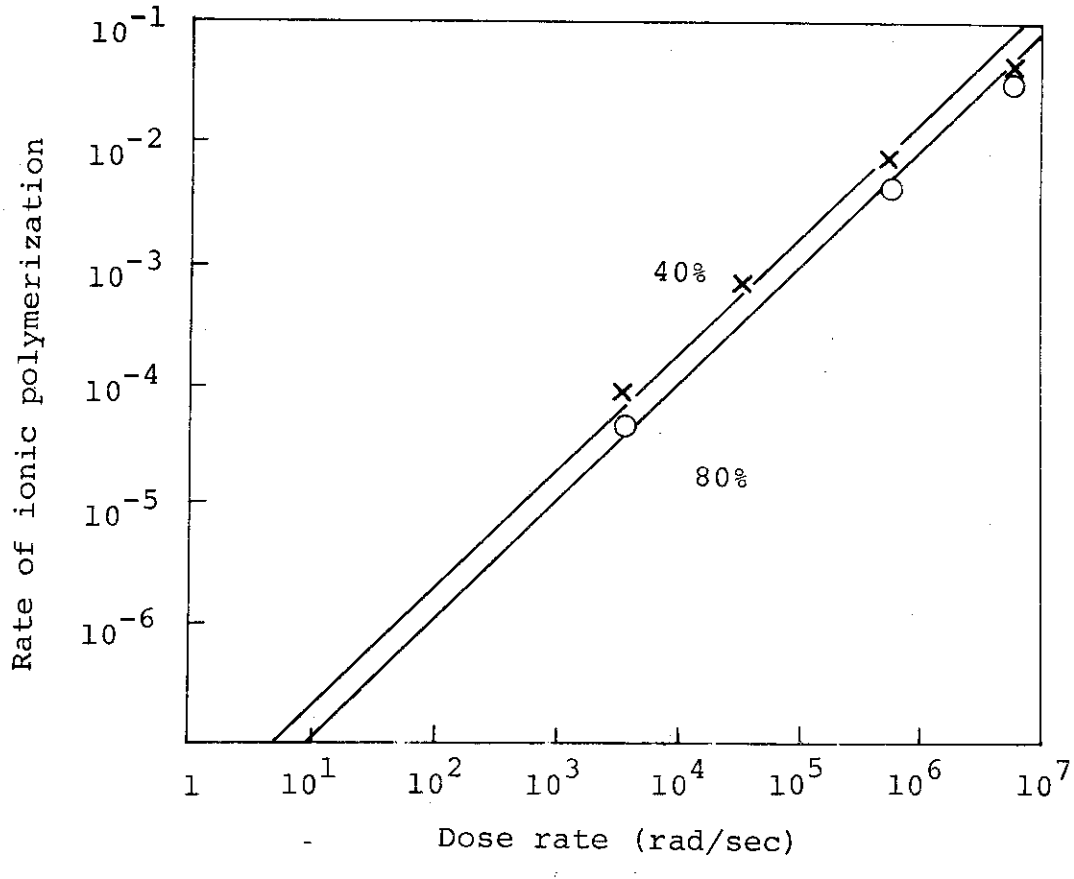

Fig. 2. Dose rate dependence of ionic polymerization rate of styrene for 80 and 40% styrene content in styrene/CTC.

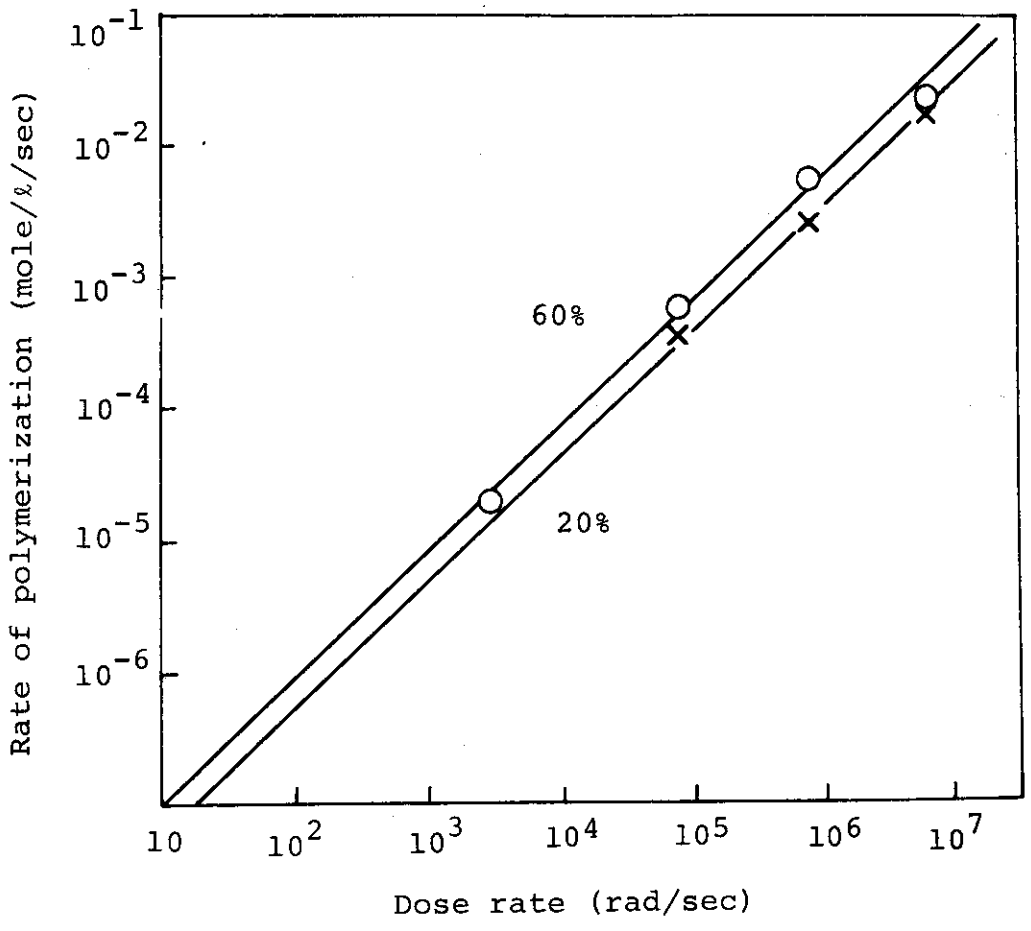

Fig. 3. Dose rate dependence of ionic polymerization rate of styrene for 60 and 20 vol% styrene in styrene/CTC.

Initiating ion formation:

$$M \sim\sim\sim\longrightarrow M^+ \qquad (1)$$
$$S \sim\sim\sim\longrightarrow S^+$$

where M, M^+, S and S^+ are monomer, monomer ion, solvent and solvent ion, respectively.

Both M^+ and S^+ participate in the growth.

Growth

$$M^+ + M \longrightarrow M_2^+ \qquad (2)$$

$$S^+ + M \longrightarrow SM^+ \qquad (3)$$

In the bulk polymerization of styrene, water contained as impurity in styrene plays a dominant role in the chain termination. In the solution polymerization water contained in solvent also has to be taken into account.

$$\text{Ion} + H_2O \longrightarrow M_n + \text{fragment} \qquad (4)$$

where Ion means M^+ or S^+, however the concentration of S^+ may be regarded to be far lower than that of M_n^+. In the case of solution polymerization termination with a solvent molecule may occur.

Solvent termination

$$\text{Ion} + S \longrightarrow M_n + S' \qquad (5)$$

It is well known in the case of bulk polymerization, that monomer transfer is important.

Monomer transfer

$$M_n^+ + M \longrightarrow M_n + M^+ \qquad (6)$$

Further it may be eventually possible that solvent transfer also occurs.

Solvent transfer

$$M_n^+ + S \longrightarrow M_n + S^+ \qquad (7)$$

Though transfer has a great effect on the degree of polymerization (P), it does not change the rate of polymerization because the concentration of growing ions is not changed by transfer.

Kinetic equations for the polymerization are derived from the above reactions.

Initiating ion formation

$$\frac{d[\text{Ion}]}{dt} = (\Phi_m[M] + \Phi_s[S])\ I \qquad (8)$$

where symbols with brackets are concentrations in mole/ℓ of the respective substances, Φ_m and Φ_s are the rate constants of ion formation of the monomer and solvent respectively per unit dose, and I is the dose rate in rad/sec.

Rate of growth (polymerization)

$$R = -\frac{d[M]}{dt} = k_p[Ion][M] \tag{9}$$

Rate of termination

$$-\frac{d[Ion]}{dt} = k_{tx}[Ion][H_2O] + k_{ts}[Ion][S] \tag{10}$$

where k_{tx} and k_{ts} are rate constants of water and solvent termination, respectively. Water comes from monomer and solvent.

$$[H_2O] = w[M] + u[S] \tag{11}$$

where w and u are water content in mole per one mole monomer and solvent, respectively.

Stationary state of ion concentration is obtained by equating (8) and (10)

$$[Ion] = \frac{\Phi_m[M] + \Phi_s[S]}{k_{tx}w[M] + (k_{tx}u + k_{ts})[S]} I \tag{12}$$

The rate of polymerization is expressed as follows.

$$R = \frac{k_p(\Phi_m[M] + \Phi_s[S])}{k_{tx}w[M] + (k_{tx}u + k_{ts})[S]} I[M] \tag{13}$$

The equation indicates that R is directly proportional to I when the polymerization is carried out at constant solvent content of the solution. This is in good agreement with the experimental results shown in Fig. 1, 2 and 3. However, it is difficult to find values of Φ_s/Φ_m and k_{ts} from equation (13).

To obtain further information from experiments, degrees of polymerization can be utilized. Theoretically degree of polymerization is calculated by dividing the rate of

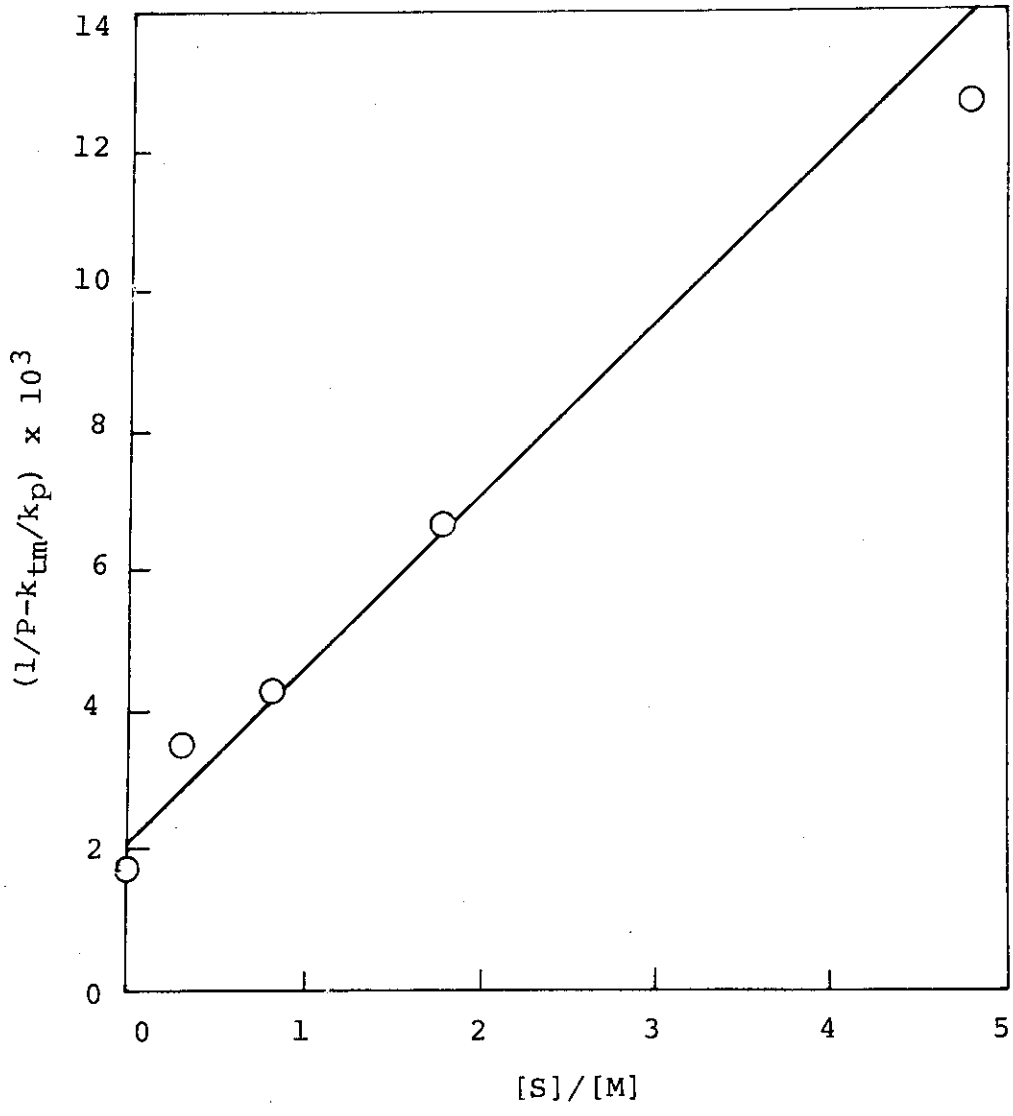

Fig. 4. Dependence of $(1/P - k_{tm}/k_p)$ on [S]/[M] for the ionic polymerization of styrene/CTC: dose rate, 6.0×10^5 rad/sec.

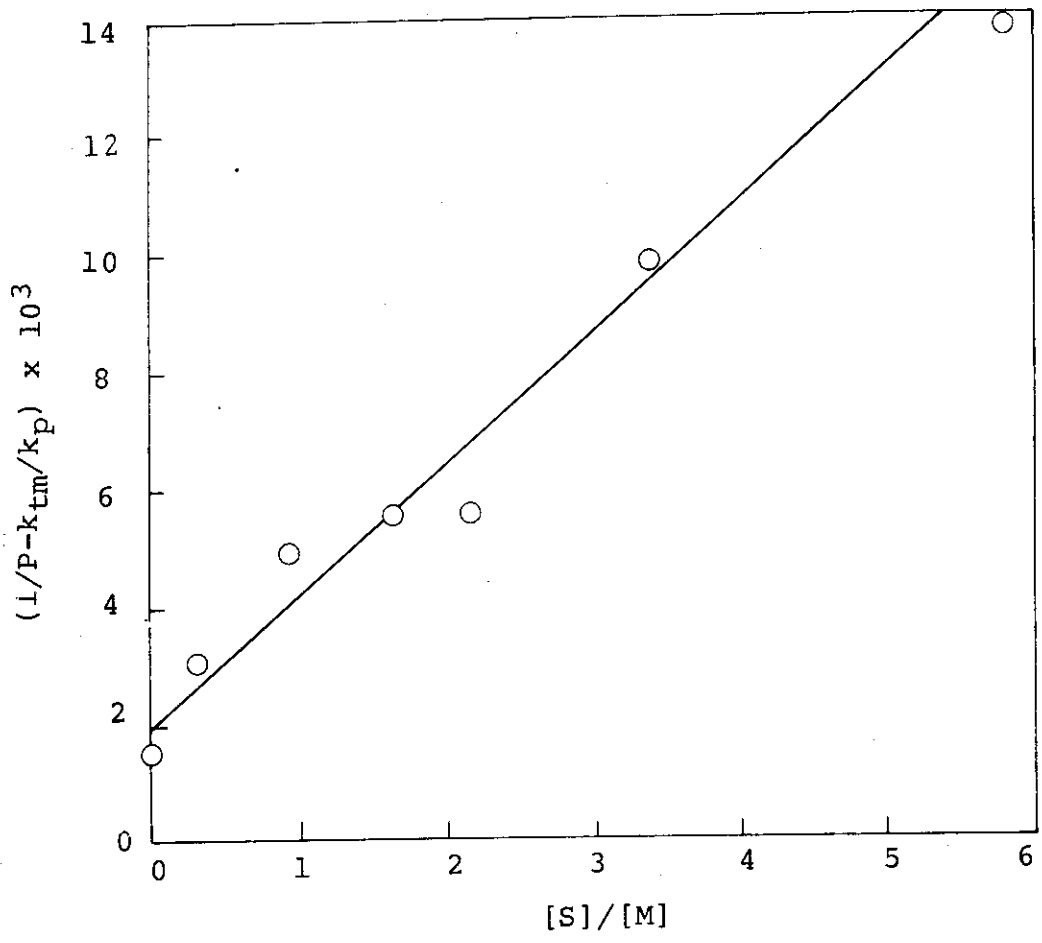

Fig. 5. Dependence of $(1/P - k_{tm}/k_p)$ on [S]/[M] for the ionic polymerization of styrene/EDC: dose rate, 6.0×10^6 rad/sec.

polymerization with the rate of stable polymer formation. Stable polymers are formed by reactions shown in equations (4), (5), (6) and (7). The final equation obtained as 1/P is

$$\frac{1}{P} = \frac{k_{tm}}{k_p} + \frac{k_{tx}}{k_p} w + \frac{1}{k_p}(k_{tx}u + k_{ts} + k_{trs}) \frac{[S]}{[M]} \qquad (14)$$

where k_{trs} is the rate constant of solvent transfer. The above equation means that the plot of $1/P - k_{tm}/k_p$ against [S]/[M] is a straight line. The value of k_{tm}/k_p is known from our earlier experiments [2] to be 1.70×10^{-3}, so that the plots may be easily drawn. Two examples, one for styrene/CTC and the other for styrene/EDC, are shown in Fig. 4 and 5. It may

be seen that the experimental values agree satisfactorily with the theoretical equation.

The values of $(k_{tm}/k_p)w$ are found from the figures in both the cases to be ca. 2×10^{-3}; k_{tx}/k_p is 1.37 from our earlier experiment. And w i.e. mole water contained per mole styrene is found to be 1.46×10^{-3}; this is reasonable as a conventionally dried styrene.

Discussion concerning the third term of eq. (14) is difficult but trial calculations show that $(k_{ts} + k_{trs})$ can not be neglected to $k_{tx}u$ in the case of styrene/CTC. When we do a simplification, that only termination is effective to the

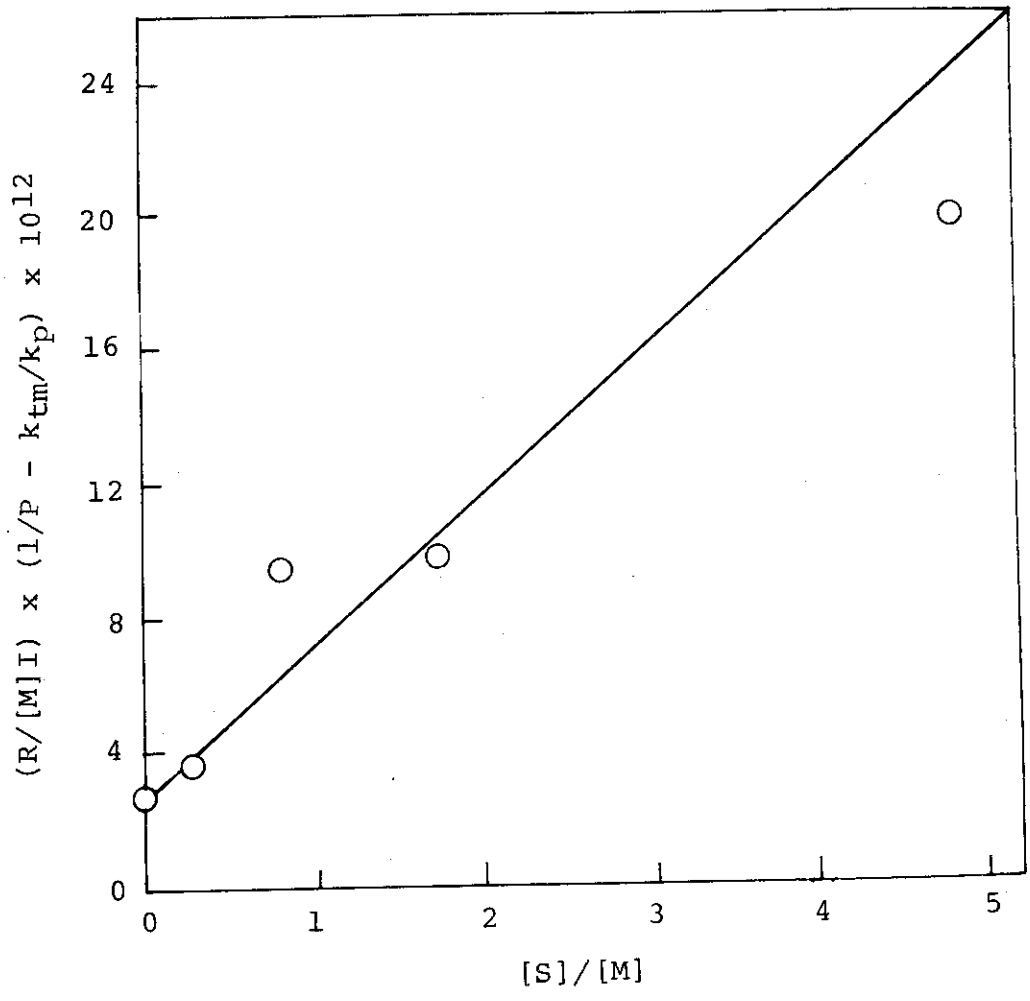

Fig. 6. Dependence of $(R/[M]I)(1/P - k_{tm}/k_p)$ on [S]/[M] in styrene/CTC for the ionic polymerization at a dose rate of 6.0×10^5 rad/sec.

reaction and neglect k_{trs} in the third term, then we can combine eq. (14) with (13), and arrive at the following relation.

$$\frac{R}{I[M]}\left(\frac{1}{P} - \frac{k_{tm}}{k_p}\right) = \Phi_m + \Phi_s \frac{[S]}{[M]} \qquad (15)$$

Now it is able to plot the left hand side of the equation against [S]/[M] to find Φ_s. Figure 6 shows the plot; Φ_m, Φ_s and Φ_s/Φ_m are 1.8×10^{-12}, 7.2×10^{-12} and 4, respectively. It is noteworthy that Φ_s/Φ_m for initiating ion formation is much smaller than that for initiating radical formation.

In the case of EDC, it can or probably contain more water than CTC and $k_{tx}u$ is solely responsible for the slope of the curve in Fig. 5. In this case also eq. (15) may be used and the values found from the curve shown in Fig. 7 are $\Phi_m = 1.8 \times$

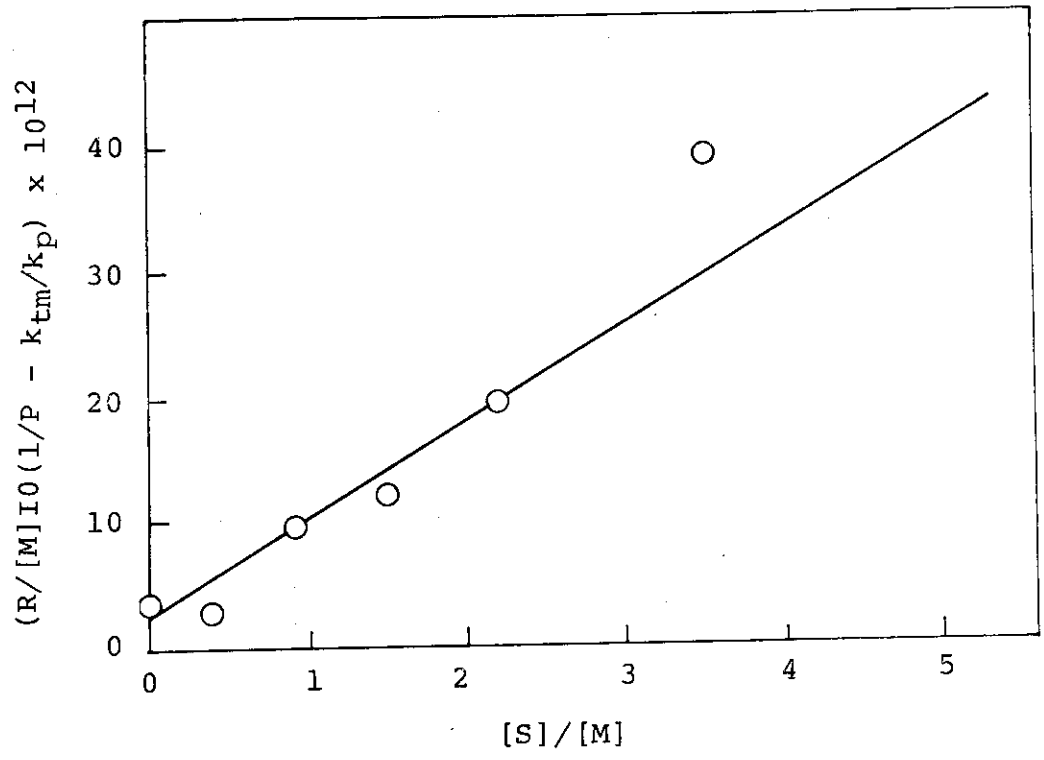

Fig. 7. Dependence of $(R/[M]I)(1/P - k_{tm}/k_p)$ on [S]/[M] in styrene/EDC for the ionic polymerization at a dose rate of 6.0×10^6 rad/sec.

10^{-12}, $\Phi_s = 14 \times 10^{-12}$ and $\Phi_s/\Phi_m = 8$.

It is necessary to carry out further experiments to elucidate the kinetics of the radiation-induced polymerization in detail, the general feature may be however summarized as follows. By radiation CTC and EDC produce more initiating ions than styrene. When $(\Phi_s/\Phi_m)_{ion}$ is compared with $(\Phi_s/\Phi_m)_{radical}$ the ratios are almost the same in the case of styrene/EDC; the ratio for the ionic initiation is however much smaller than that for the radical initiation in the case of styrene/CTC. The initiating ions grow to form polymers. Reaction with water which is contained in monomer and solvent as an impurity is important for termination. Monomer transfer of styrene plays also an important role. It is also probable that chain transfer by solvent has an effect in the case of CTC, though it could not be detected in the case of EDC.

(I. Sakurada, J. Takezaki, T. Okada)

1) I. Sakurada, J. Takezaki and T. Okada, JAERI-M 7949, 38, 52 (1978)
2) J. Takezaki, T. Okada and I. Sakurada, J. Appl. Polymer Sci., 21, 2683 (1977); 22, 3311 (1978).

3. Radiation-Induced Solution Polymerization of Styrene in n-Butylamine

In the course of the experiments on the radiation-induced polymerization of styrene in carbontetrachloride (CTC)[1], small amount of n-butylamine (BA), an inhibitor to cationic polymerization, was added to the polymerization mixture. Strange to say, the rate of polymerization was not decreased but increased by the addition of n-butylamine.

Figure 1 shows the comparison of the rate of polymerization of styrene in styrene/CTC in the presence and absence of BA. The polymerization mixture contained 20 vol% styrene, the amount of added BA is 1 mole/ℓ, and the polymerization carried out at a very wide range of dose rate at room temperature.

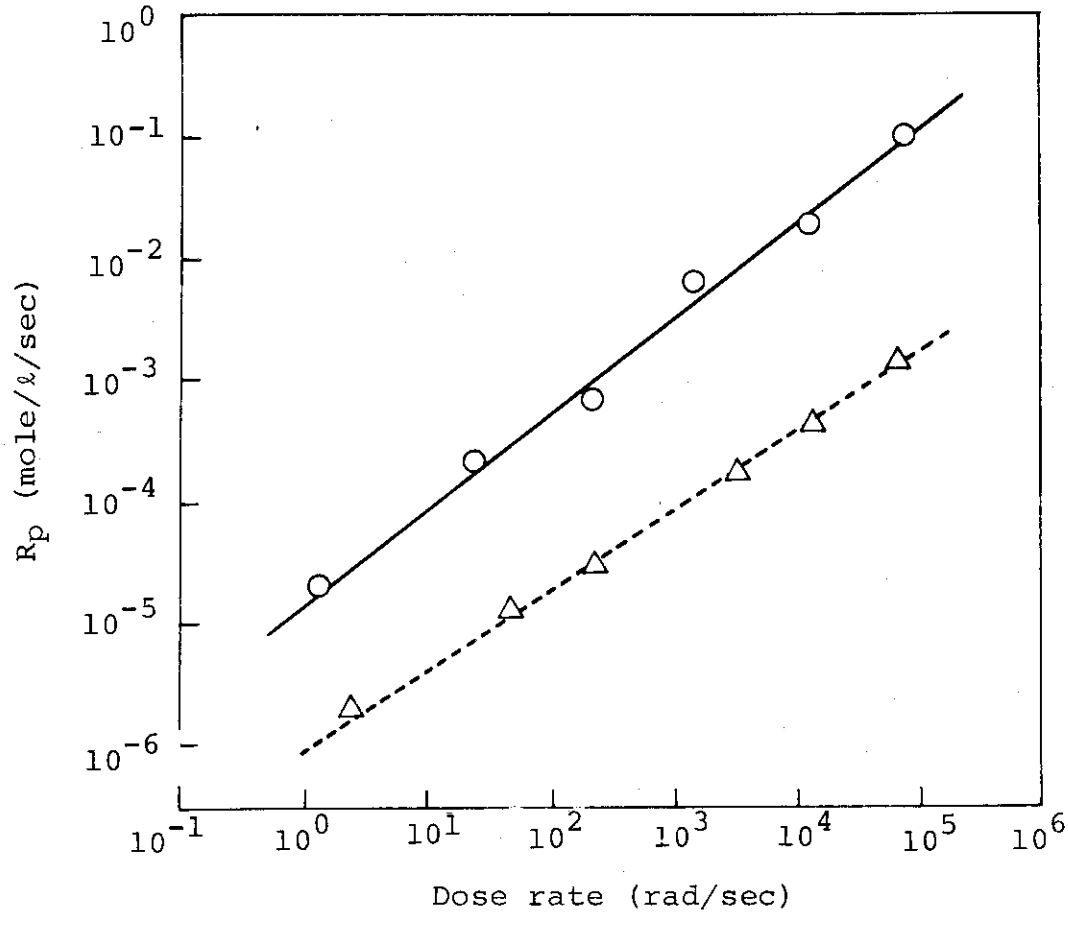

Fig. 1. The rate of polymerization of styrene-CCl_4 mixture as a function of dose rate: styrene content, 20 vol%; (△) no additive, (○) n-butylamine (1 mole/ℓ).

It is clearly seen that the polymerization rate with BA is 15 ∿ 30 times and 60 ∿ 70 times greater than that without BA at lower and higher dose rates, respectively.

Though it was clear that CTC played an important role in the reaction, fundamental studies on the solution polymerization of styrene in BA was taken up first.

Polymerization of styrene in binary mixtures of styrene/BA of different styrene content i.e. from 100 to 20 vol% was carried out at a dose rate between 0.75 rad/sec and 6.0×10^6 rad/sec. The rates of polymerization, R_p as a function of the composition of the mixtures are shown in Fig. 2 for various dose rates of irradiation.

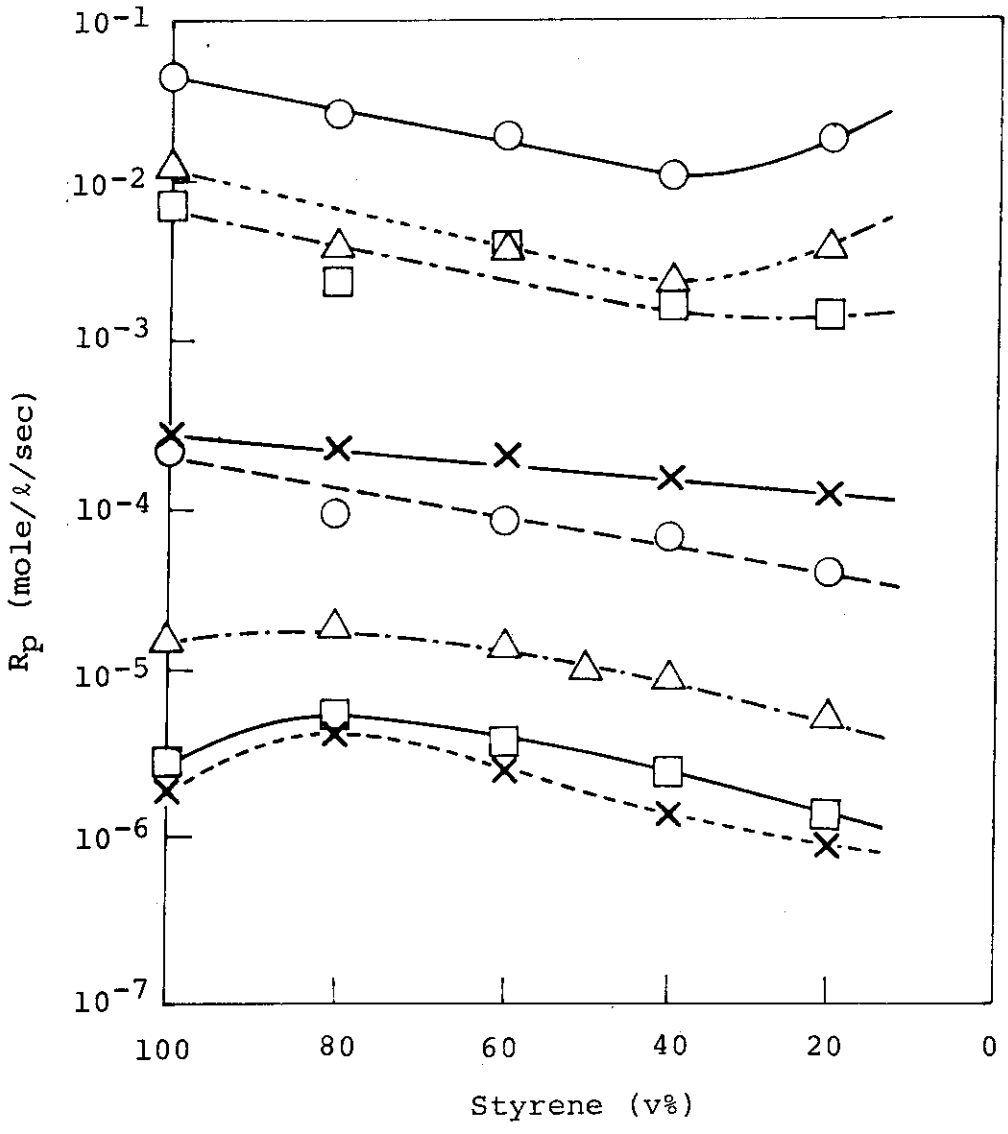

Fig. 2. The rate of polymerization of styrene/BA as a function of styrene content at different dose rates: dose rate (rad/sec), (—○—) 6.0×10^6; (----△----) 6.0×10^5; (—·-□-·—) 1.2×10^5; (——×——) 1.2×10^4; (----○----) 1.2×10^3; (—·-△-·—) 2.4×10; (——□——) 2.5; (----×----) 7.5×10^{-1}.

It may be seen from the figure that R_p's decrease with decreasing content of styrene in the polymerization above 1.2 x 10^3 rad/sec, though some increase at 20 vol% is observed in the case of polymerization at a very high dose rate such as 6.0 x 10^5 rad/sec and 6.0 x 10^6 rad/sec. When the dose rate is low, R_p's increase a little when styrene content drops from 100 vol% to 80 vol%. It may be said that the curves show no dramatic feature such as observed in the case of an addition of BA to styrene/CCl_4, where R_p increased about one or two orders of magnitude by the addition of BA.

GPC analysis of molecular weight distribution of the products obtained in the experiments in Fig. 2 is carried out. Fig. 3 shows GPC curves of polymers obtained by irradiation at a dose rate of 1.2 x 10^4 rad/sec for 250 sec at room temperature. It is known from our previous investigations [1] of polymerization of styrene in bulk approximately the same amounts of radical and cationic polymers are formed. The uppermost curve is that for 100 vol% styrene; the fractions shown by dotted lines are from the left to the right oligomer, radical polymer and cationic polymer, respectively. In all mixtures which contain BA, fraction of cationic polymer almost completely disappears; new peaks which appear at higher molecular weight will be discussed later.

Another example of GPC curves is shown in Fig. 4; the irradiation was carried out at a dose rate of 2.4 x 10^2 rad/sec for 2100 seconds. Cationic polymer is not detected at such a low dose rate, and as expected oligomer and radical polymer are formed as main products. However, it is noteworthy that distinct peaks appear at molecular weight about a million. Such a peak in GPC curve was first observed in the polymerization of water saturated styrene at dose rates greater than 10^5 rad/sec; the fraction was called for convenience super polymer. The super polymer is formed not only by water contained as an impurity in styrene but also by many other impurities such as methanol, acetic acid, ethylene glycol, nitrobenzene, chlorobenzene, benzene and DPPH etc. In all these cases it was necessary to employ irradiation of higher dose rates. It is,

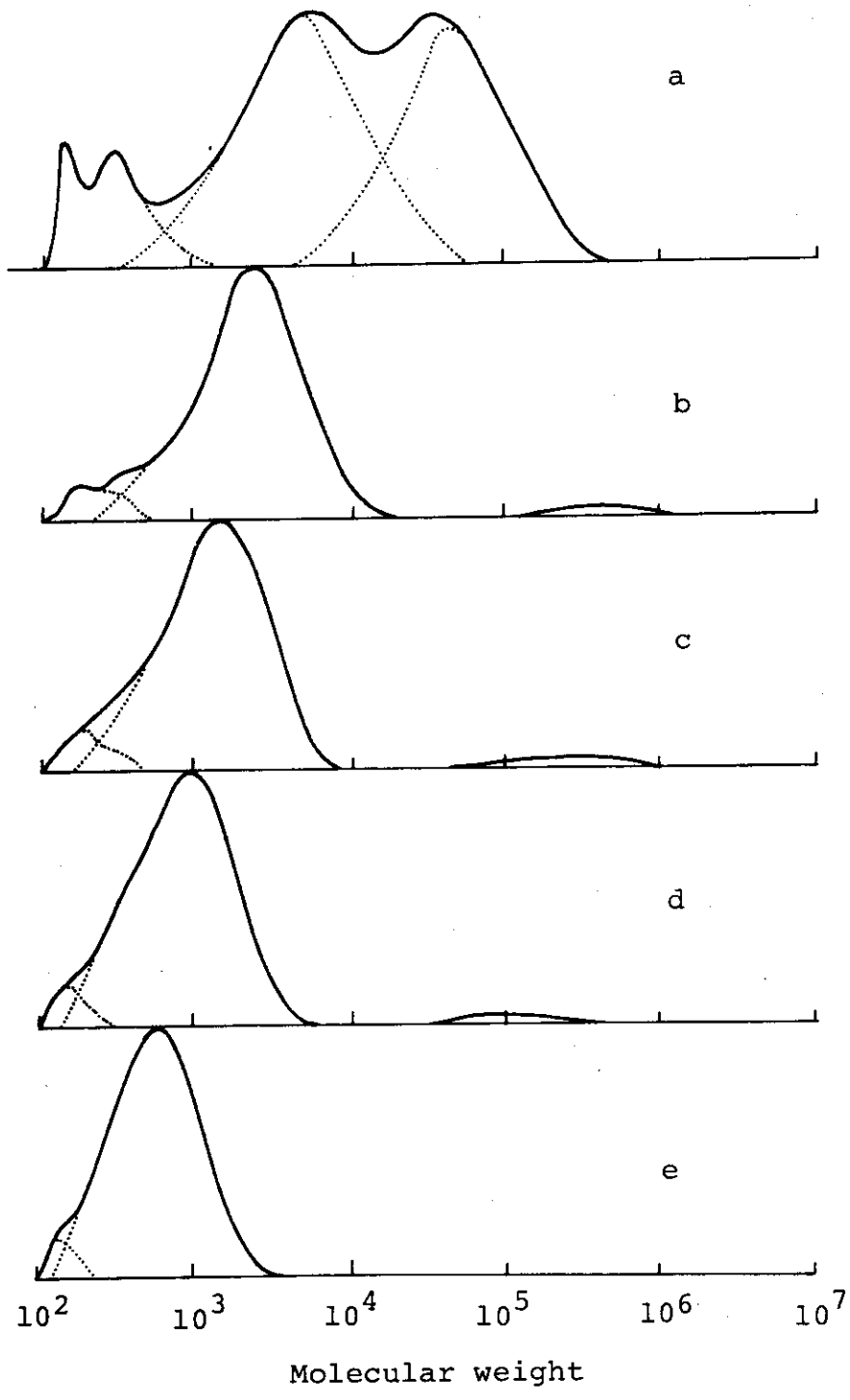

Fig. 3. GPC curves of polymers obtained from styrene/BA mixture at different styrene contents in vol%: (a) 100, (b) 80, (c) 60, (d) 40 and (e) 20; dose rates, 1.2×10^4 rad/sec; irradiation time, 250 sec.

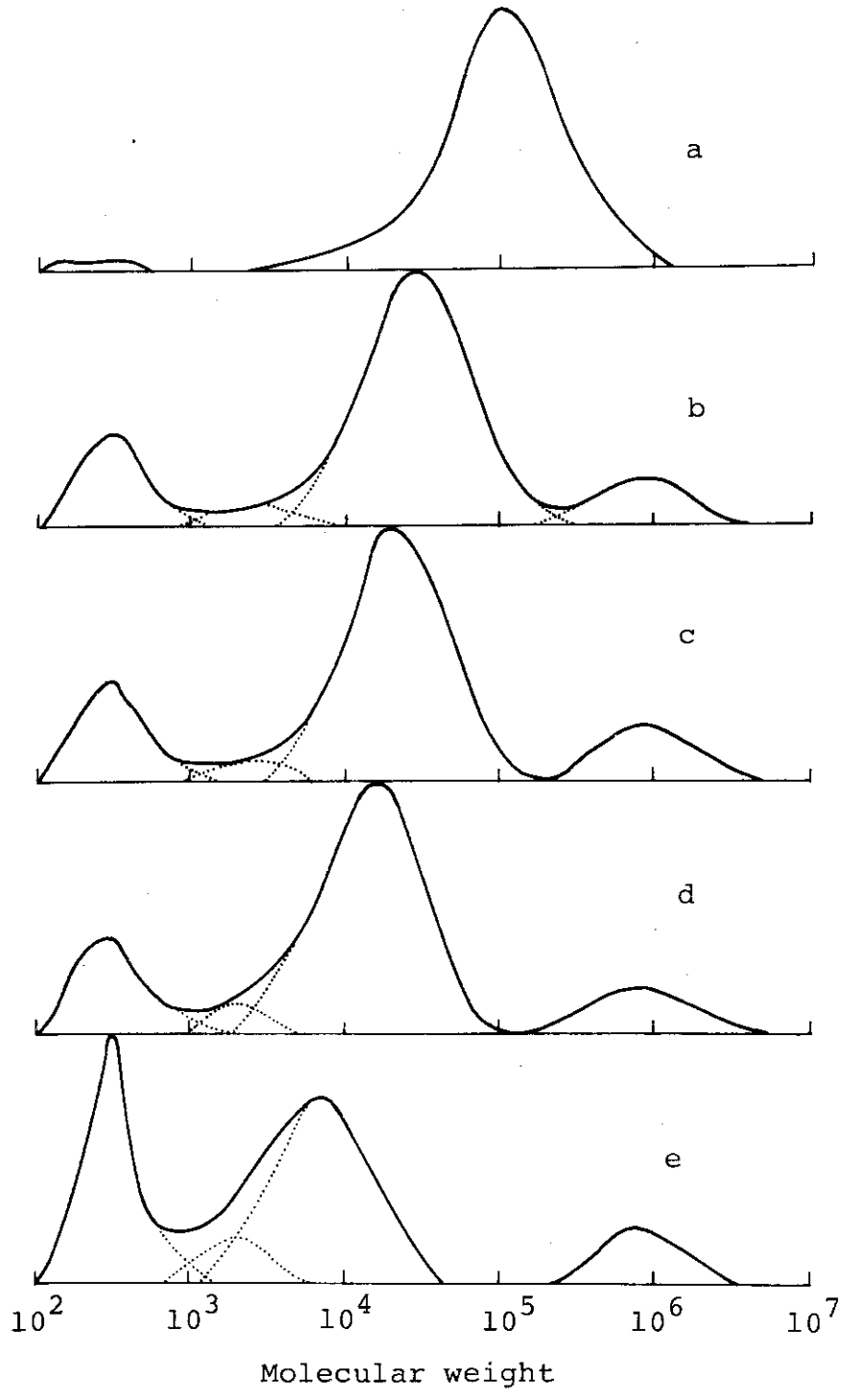

Fig. 4. GPC curves of polymers obtained from styrene/BA mixture by irradiation at different styrene contents in vol%: (a) 100, (b) 80, (c) 60, (d) 40 and (e) 20; dose rate, 2.4 x 10^2 rad/sec; dose, 0.5 Mrad.

therefore, very important that styrene produces super polymer in the presence of a large amount of BA by irradiation at such a low dose rate as 2.4×10^2 rad/sec. The formation of the super polymer is observed even at a dose rate as low as 0.75 rad/sec, when the mixtures contain BA in an amount above 40 vol%.

It is further interesting that there is an indication in GPC curves of Fig. 4, as shown by dotted lines, that a new peak appears between peaks for oligomer and radical polymer. The indication becomes more prominent when the polymerization is carried out at still lower dose rate.

Figure 5 shows the aspects and nature of the new peak of GPC curve more clearly. The polymerization was carried out at a dose rate of 0.75 rad/sec for 3×10^5 sec. As is seen from the uppermost curve, 100 vol% styrene shows only oligomer and radical polymer. When styrene/BA of 80 vol% styrene content is used, the new peak appears between oligomer and radical polymer clearly. By an addition of a small amount of a radical scavenger, 2.5×10^{-2} mole/ℓ of DPPH, to the above mixture both the peak of radical polymer and new peak disappear. Therefore, it is very probable, that the new peak is due to radical polymerization. If this conclusion is right, we have to differentiate between two types of growing radicals.

The lowest BA content in the above polymerization was 20 vol% (2.03 mole/ℓ); experiments were, therefore, undertaken to know the effect of very small amounts of BA to the polymerization of styrene. The concentration of BA in the mixture was varied between 1.00×10^{-4} mole/ℓ and 2.03 mole/ℓ. The dose rate was 2.1×10^5 rad/sec, the irradiation was carried out for 100 sec. Though the details of the experimental result are not given in this paper, it was found that the GPC curves below BA concentration of 2.28×10^{-3} mole/ℓ were consisted of three parts that is oligomer, radical and ionic polymers; the amount of oligomer increased with increasing concentration of BA. Above 2.54×10^{-3} mole/ℓ the amount of cationic polymer decreased to a greater extent and a new peak whose existence was already indicated in Fig. 3 appeared distinctly. The peak

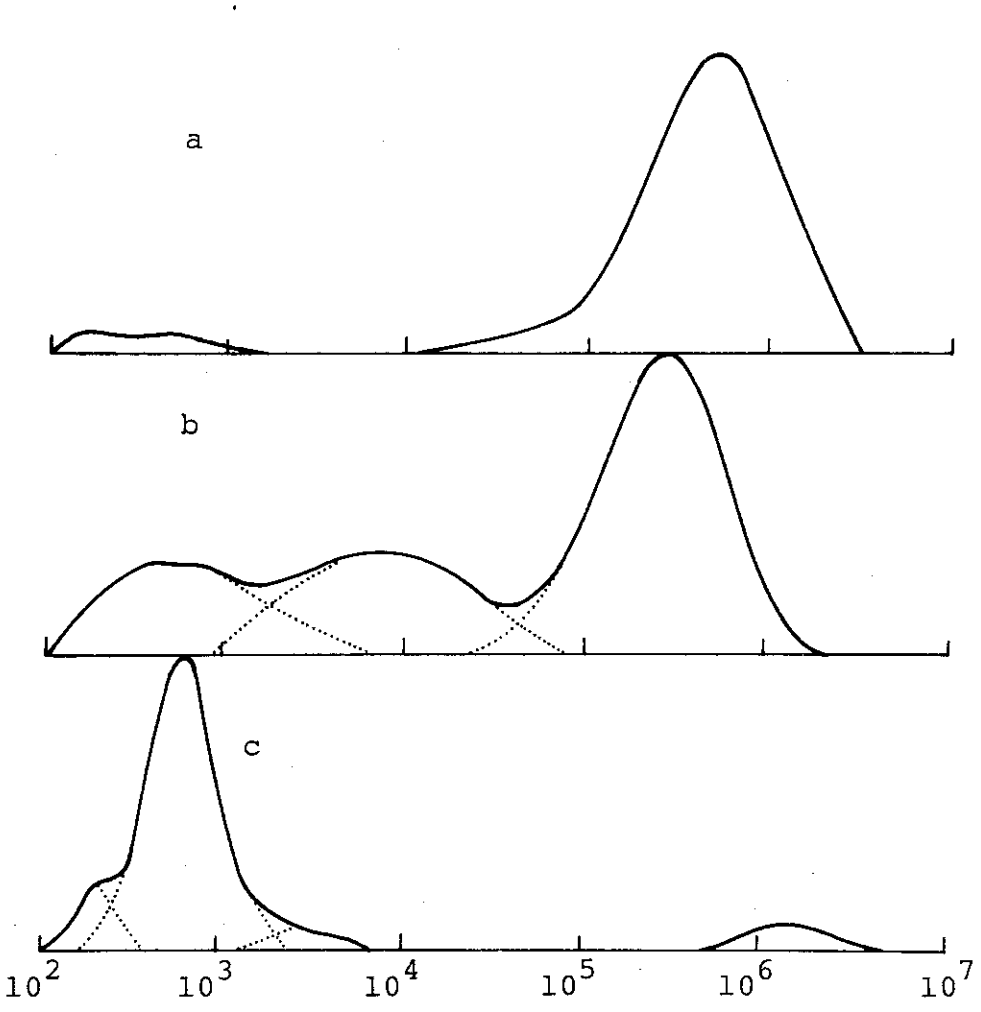

Fig. 5. GPC curves of polymers obtained from styrene/BA mixture by irradiation with or without the presence of additive: (a) styrene content, 100 vol%, no additive; conversion, 6.70%; (b) styrene content, 80 vol%; conversion, 19.8%; (c) styrene content, 80 vol%; 2.5×10^{-2} mole/ℓ DPPH; conversion, 0.906%; dose rate, 7.5×10^{-1} rad/sec; dose, 0.23 Mrad.

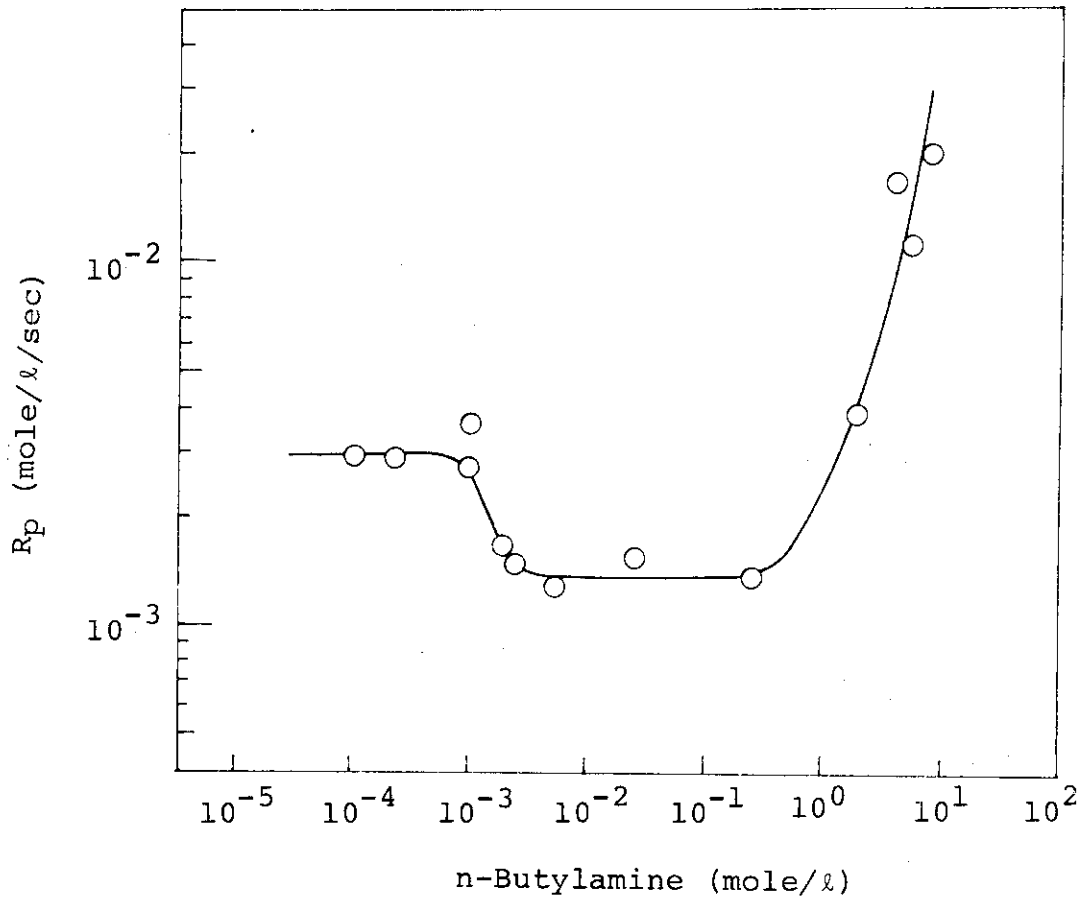

Fig. 6. The rate of polymerization of styrene as a function of BA content (mole/ℓ): dose rate, 2.1 x 10^5 rad/sec.

is located at a molecular weight about 10^5, and it is considered, for the present, to be different from the peak of the super polymer which is located at a molecular weight of 10^6. When styrene with 2.54 x 10^{-1} mole/ℓ BA is irradiated after an addition of 2.5 mole/ℓ DPPH all peaks except that of oligomer disappear.

Dependence of the rate of polymerization of styrene on the content of BA is shown in a log-log scale in Fig. 6 for a very wide range of BA content i.e. between 10^4 mole/ℓ and 10 mole/ℓ. Polymerization rate is almost constant between 10^{-4} and 10^{-3} mole/ℓ, where oligomer, radical and cationic polymers are formed; the rate drops between 1 x 10^{-3} and 2.54 x 10^{-3}

mole/ℓ due to the inhibition of cationic polymerization. Between 3 x 10^{-3} mole/ℓ and 2.54 x 10^{-1} mole/ℓ radical polymerization and oligomer formation take place and the rate is almost constant. At higher concentration of BA larger amount of oligomer is formed while the amount of radical polymer remains almost unchanged. (J. Takezaki, T. Okada)

1) I. Sakurada, J. Takezaki, and T. Okada, JAERI-M 7949, 38 (1978).

4. Effect of Additives on the Polymerization of Styrene

Attempts to promote the rate of polymerization of styrene with cationic mechanism are made by two different ways, additions of emulsifiers and electron acceptors.

It seems likely that an addition of emulsifier to monomer forms water-in-oil type micells resulting a decrease of the concentration of dispersed water in the polymerization system. With all of four emulsifiers used, it has been well known the formations of micells in non-polar solvents and we actually confirmed that they all can solubilize water in styrene.

Emulgen-910 (Kao-Atlas Co.): polyoxyethylene nonylphenylether (n=10)

Emulgen-913 (Kao-Atlas Co.): the same as above (n=13)

Neocol-P (Dai-ichi Kogyo Seiyaku Co.): di(2-ethylhexyl)-sodium sulfosuccinate + methanol-water

Neocol-SWC (Dai-ichi Kogyo Seiyaku Co.): the same as above + isopropanol-water

All of these emulsifiers are heated in vacuum to eliminate water and alcohol as possible. Styrene is purified by ordinary method and dried by CaH_2.

In Table 1, polymer yields in the presence of emulsifiers

Table 1. Polymer Yield (%) in the Presence of Emulsifiers

	Irrad. time (sec)	[Emulsifier] (mole/ℓ)		
		0	1.0×10^{-2}	1.0×10^{-3}
Emulgen-910	1,000	31.8	4.5	7.3
-913	400	5.1	4.8	2.7
Neocol-P	400	5.1	3.1	2.9
-SWC	400	6.1	3.4	3.7

Dose rate, 8.8×10^4 rad/sec; temperature, 25°C.

are given. Since maximum water content in styrene is ca. 0.03 mole/ℓ, emulsifier of $10^{-2} \sim 10^{-3}$ mole/ℓ is presumably enough to form micells in styrene. In no case, however, increase of the polymer yield by the additives was found. This is probably because that water concentration in the monomer is too low to form micells and these emulsifiers themselves act as inhibitor for the cationic reaction as well as water molecules still included in these additives.

It was recently reported that the rate of cationic polymerization was increased by the addition of electron scavengers as pyromellitic dianhydride (PDAH)[1] and p-benzoquinone (BQ)[2]. However, the promotion effect of R_p seems to be limited in low monomer concentration in polar solvent at low temperature. In this work, therefore, effects of additives are studied at two monomer concentration, 0.6 and 2.0 mole/ℓ in methylene dichloride solution at -78 and 0°C. For the ease of experiments, γ-irradiation is used at the dose rate of 31 rad/sec.

PDAH, BQ and chloranil (C) are used after sublimation in vacuo. In Table 2, polymer yields at -78 and 0°C are shown. To avoid irreproducibility in R_p, all the polymer yields in the presence of additive are compared to its corresponding blank values, which are obtained at the same time as the samples containing the particular additive. The figures in parenthesis are somewhat unusual values compared with other

Table 2. Polymerization of Styrene in the Presence of Electron Acceptors in CH_2Cl_2 Solution [Acceptor]=0.022 mole/ℓ

Additive	Temp. (°C)	[St] (mole/ℓ)	Polymer yield(%)		R_p ratio	Change in MWD
			Blank	additive		
PDAH	-78	0.6	2.0	26.2	13.1	0
BQ	-78	0.6	1.8	15.0	8.3	0
C	-78	0.6	(14.6)	14.5	(1.0)	X
PDAH	-78	2.0	16.8	34.3	2.0	0
BQ	-78	2.0	21.2	9.9	0.5	X
C	-78	2.0	(5.5)	13.7	(2.5)	0
PDAH	0	0.6	3.0	4.2	1.4	0
BQ	0	0.6	4.5	7.1	1.6	0
C	0	0.6	3.8	4.4	1.2	
PDAH	0	2.0	1.8	2.6	1.4	0
BQ	0	2.0	(5.0)	4.1	(0.8)	X
C	0	2.0	1.7	2.5	1.5	

Dose rate, 31 rad/sec; Irrad. time, 4 hrs.

two blank values. At -78°C and [St] = 0.6 mole/ℓ, additions of PDAH and BQ enhance the polymer yield greatly. MW's of the products are ca. 300 in the absence of additives and it exceeds 10^5 in the presence of PDAH and BQ. When [St] is increased to 2.0 mole/ℓ, increase of the polymer yield is found by PDAH addition but MW of the product, ca. 2×10^5 remained unchanged. With other two additives, the polymer yields are much less than that with PDAH. At 0°C, in most of all cases, the polymer yield is enhanced slightly by the additives though the yields are much reduced that at -78°C. The MW distributions of the products are generally bimodal having peaks at the MW of ca. 600 and 2×10^4. With the increase of the yield, the relative amount of the high MW fraction is increased.

From these results, it is found that the promotion of the polymer yield is notable only at low temperature and low

monomer concentration. Therefore, for the practical purpose to increase the space-time yield of the product, this is of no use. (K. Hayashi, S. Okamura)

1) Y. Yamamoto, A. Morioka, M. Irie, and Ko. Hayashi, Macromol., 10, 266 (1977).
2) A. V. Ragimov, A. Yu. Nagiev, R. A. Kurbanova, and B. I. Rigonsky, Paper presented to 26th IUPAC Symposium, E09, (Sept. 1977, Tokyo).

[3] Radiation-Induced Polymerization of Dienes

1. Polymerization of Butadiene

For these years studies on the polymerization of several vinyl and diene compounds in bulk have been carried out in a wide dose rate range, $5 \sim 2 \times 10^5$ rad/sec [1~6]. Two major features were found concerned with the high dose rate polymerization as a potential means of polymer manufacturing process. The first is, of course, high rate of the reaction. The second is that it is suitable for the formation of oligomeric product, which is available for paints, adhesives, plasticizers etc.

Taking account of the fact that most of commercial oligomers at present are products of α-olefins and dienes, studied on the polymerization of dienes have been carried out since last year. Results of isoprene and chloroprene were briefly described in the last issue of this report.

In this year the polymerization of bulk butadiene is studied in some detail. As shown in Fig. 1, the rate of polymerization is proportional to the 0.9th power of the dose rate in the entire dose rate range studied. This seems to indicate that the polymerization proceeds with a single mechanism with which the rate of polymerization is, in kinetic equation, proportional to dose rate. The molecular weight distributions of the products obtained at different dose rates are very similar one another as shown in Fig. 2. The distributions are seemingly bimodal arisen from the non-linear relationship between log MW and elution count in the column set used. $\overline{M}_n$ value determined by vapor-pressure osmometry is 2,300 approximately for the product polymerized at 2.2×10^5 rad/sec. These relationships of R_p and MW with dose rate indicate cationic mechanism throughout the dose rate range studied.

The structure of the product is studied by IR and ^{1}H-NMR methods. As is shown in Table 1, the values by two methods

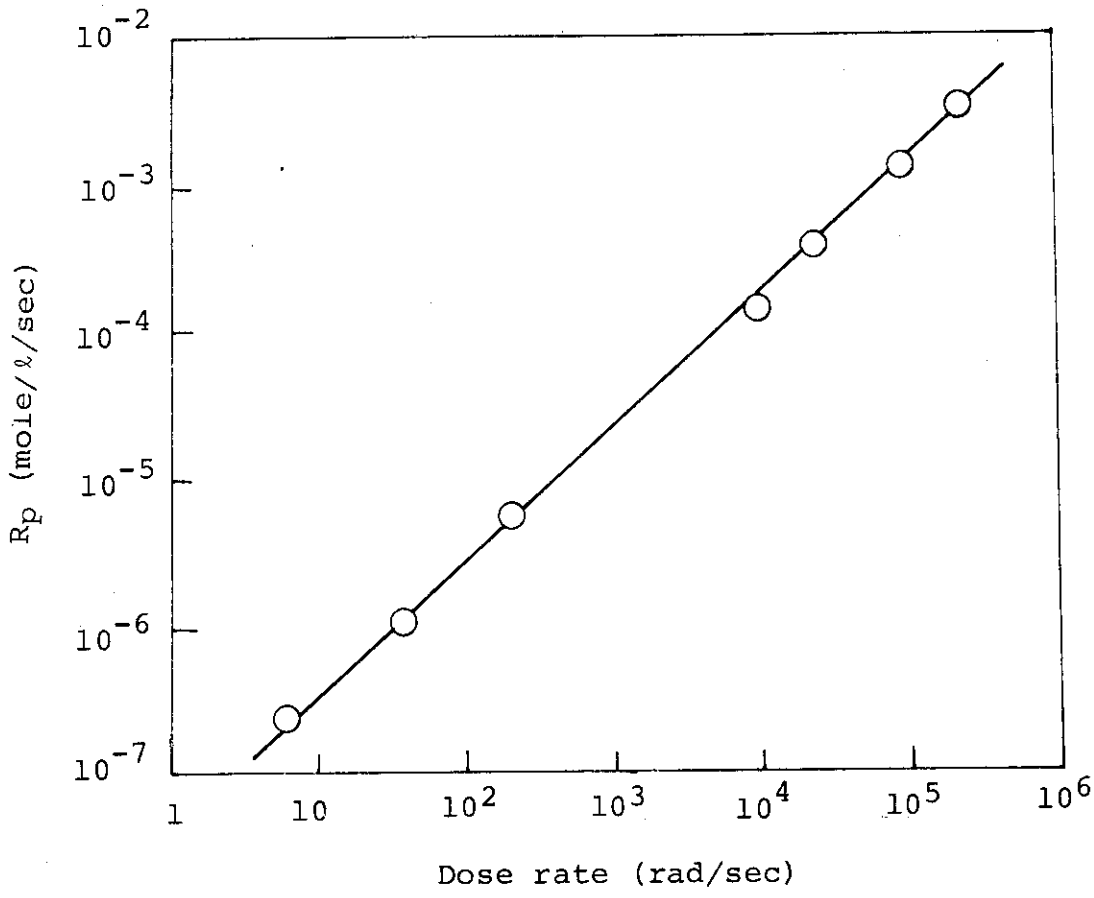

Fig. 1. Dose rate dependence of R_p of butadiene at -10°C.

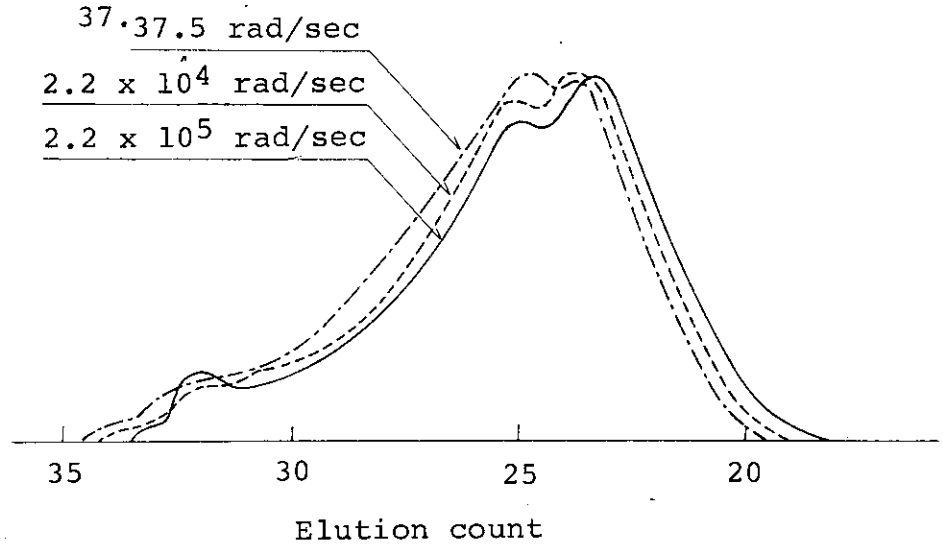

Fig. 2. MW distributions of polybutadienes obtained at different dose rates.

Table 1. Microstructure of Polybutadienes

Dose rate (rad/sec)		2.2×10^5	8.8×10^3	200	37.5
Conversion (%)		8.0	6.7	7.3	6.7
Residual double bond (%)	IR	80.2	81.7	-	83.5
	^{1}H-NMR	84.3	78.9	83.4	83.4
Vinyl (%)	IR	25.2	24.9	-	25.4
	^{1}H-NMR	23.3	23.9	21.1	24.5

agree fairly well. It is noted that structures of these products polymerized at different dose rate are essentially identical. It is found that approximately 80% double bond remained in the polymer. Their microstructures are mainly of trans-1,4 unit with ca. 25% of vinyl unit. Sucha structural features, especially partial loss of double bond probably because of cyclization reaction and absence of cis unit are commonly observed in the polymer formed by cationic initiators.

All of the above described results indicate that the polymerization of butadiene proceeds solely with cationic mechanism in a very wide dose rate range. In other words, no radical polymerization takes place in bulk butadiene somehow.

(K. Hayashi, S. Okamura)

1) J. Takezaki, T. Okada, and I. Sakurada, J. Appl. Polym. Sci., 21, 2683 (1977).
2) J. Takezaki, T. Okada, and I. Sakurada, J. Appl. Polym. Sci., 22, 3311 (1978).
3) K. Hayashi, J. Polym. Sci. Polym. Chem. Ed., in press.
4) K. Hayashi and N. Kotani, J. Polym. Sci. Polym. Chem. Ed., in press.
5) K. Hayashi, T. Okada, and S. Okamura, JAERI-M 7949, 60 (1978).
6) K. Hayashi, T. Osaka, and S. Okamura, JAERI-M 7949, 64 (1978).

2. Copolymerization of Butadiene with Styrene and Vinyl Chloride

Bulk copolymerizations of butadiene with styrene and vinyl chloride are carried out to study the possibility of modifying the butadiene oligomer.

Copolymerization with styrene is made at two different dose rates. At 2.2×10^5 rad/sec, the addition of styrene reduces the polymerization rate approximately to the half of that of homopolymerization of butadiene and the molecular weight of the copolymer is much lower than that of polybutadiene obtained at the same reaction conditions. The obtained copolymer is fractionated into two parts by centrifugation of its methanol solution. Copolymer analysis is made by ^{1}H-NMR method using absorptions of olefinic protons of butadiene unit and ring protons of styrene unit.

As shown in Fig. 1, compositions of low molecular weight fractions, recovered from THF-methanol solution after centrifugation, lie on a smooth line though the results for high molecular weight fraction scatter considerably. Result by γ-ray copolymerization is also included in Fig. 1. It agrees very well with the consequence of high dose rate copolymerization. The copolymerization parameters, r_1 and r_2 (M_1=styrene) are found to be 2.5 and 0.45, respectively. These values disagree with those for radical copolymerization in emulsion system, for instance, $r_1 = 0.78$ and $r_2 = 1.3$. This indicates that copolymerization reaction also proceeds with cationic mechanism as well as in homopolymerization of butadiene.

Copolymerization with vinyl chloride is carried out at the dose rate of 2.2×10^5 rad/sec as shown in Fig. 2. The copolymer composition is also determined by ^{1}H-NMR method. Although the points are scattered considerably, the copolymerization parameters (M_1=vinyl chloride) are evaluated to be $r_1 = 0.02$ and $r_2 = 10$, approximately. In this system, the decrease of reaction rate compared with homopolymerization rate of butadiene is slight but molecular weight of copolymer is substantially lower than that of polybutadiene. The incorporation

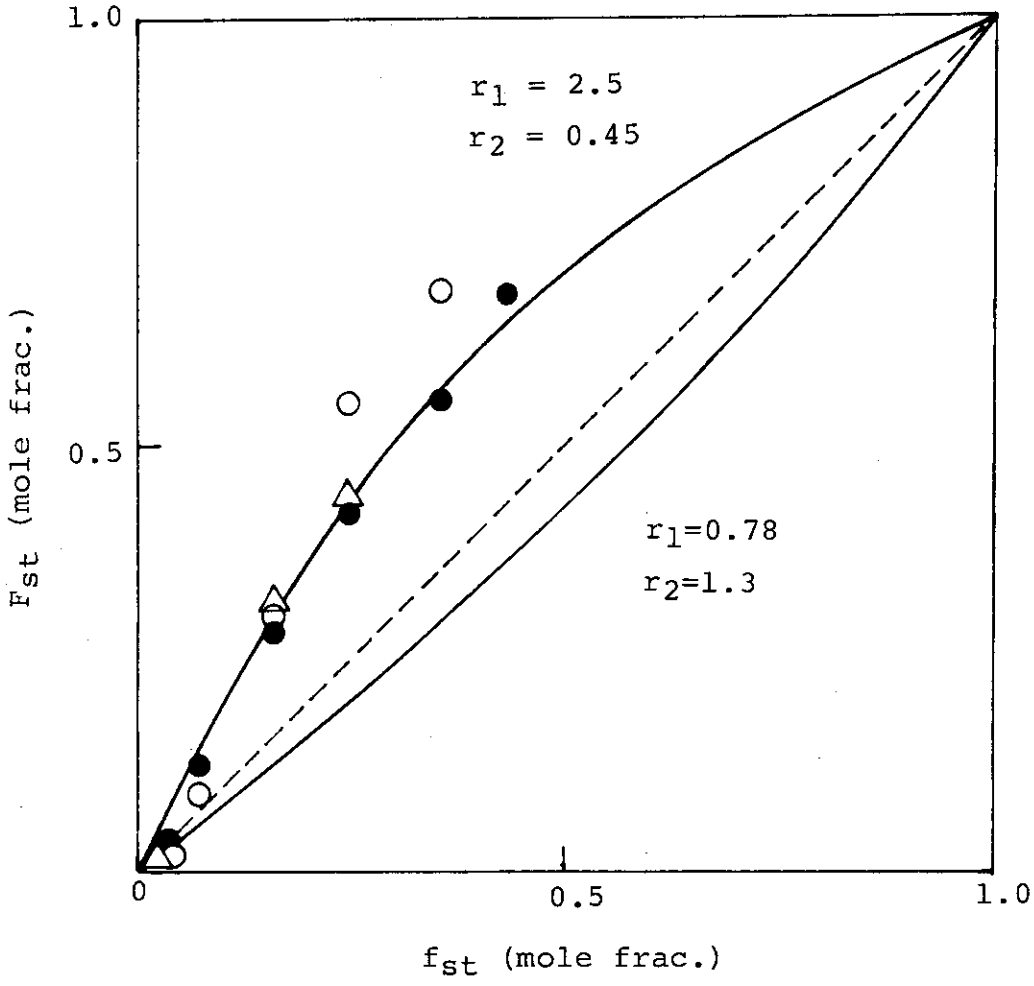

Fig. 1. Compositions of butadiene-styrene copolymers as a function of monomer compositions. Dose rate, 2.2×10^5 rad/sec; low MW fraction (●) and high MW fraction (○); 37.5 rad/sec, total product (△).

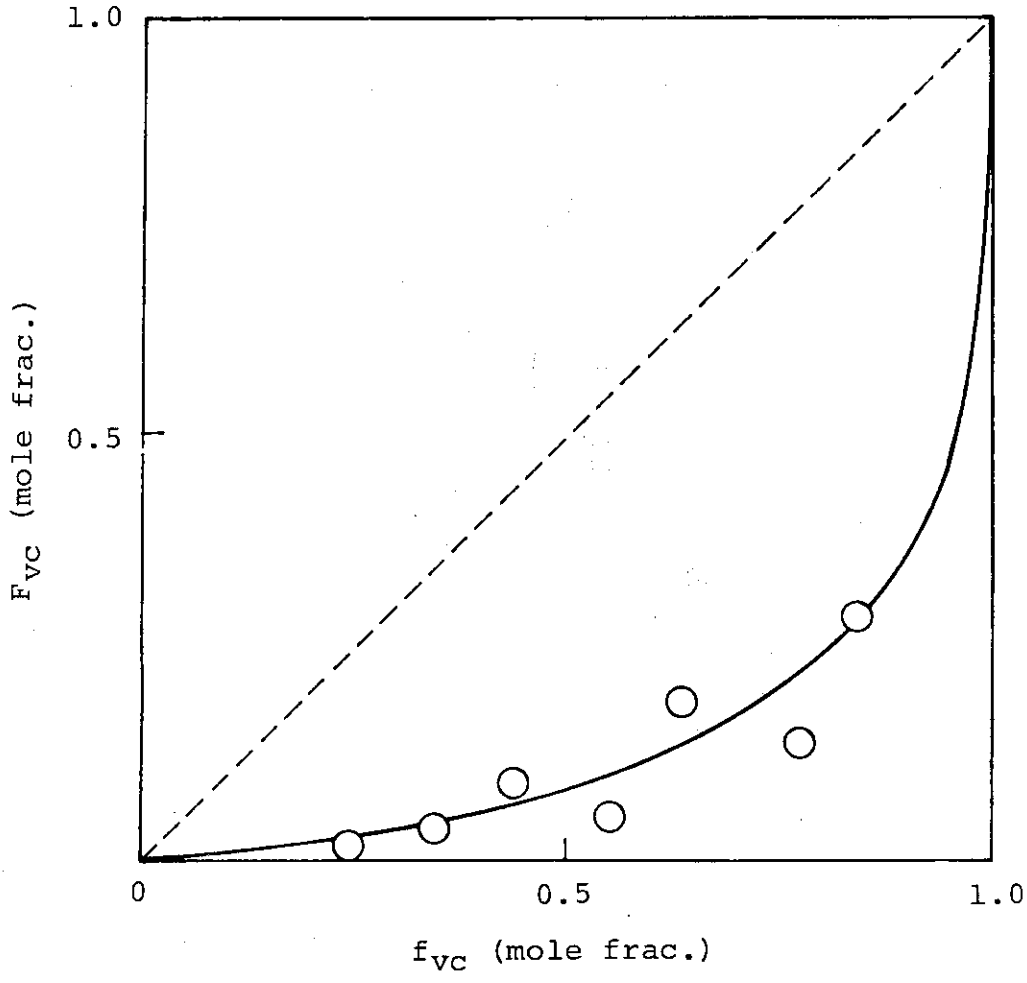

Fig. 2. Compositions of butadiene-vinyl chloride copolymer as a function of monomer composition. Dose rate, 2.2×10^5 rad/sec.

of vinyl chloride unit in the copolymer is demonstrated by ^{13}C-NMR method. This seems the first instance of obtaining random copolymer of butadiene-vinyl chloride except the γ-ray copolymerization in urea canal complex.

(K. Hayashi, S. Okamura)

3. Cyclization and Crosslinking in the Polymerization Process of Butadiene

In the bulk polymerization of butadiene by electron beams, partly crosslinked polymer is formed when the polymer conversion exceeds ca. 10%. On the other hand, it is found that approximately 20% of double bond in the polymer is missing somehow. This means that two subsidiary reactions, crosslinking and consumption of polymer double bond, are taking place in the course of polymerization.

Fraction of residual unsaturation is determined by ^{1}H-NMR method for polybutadiene of different time of irradiation. Fraction of pendant vinyl unit, which is supposed to be much more reactive than a double bond in the main chain, to the theoretical amount of total double bond in the polymer is also included in Fig. 1. The results at the irradiation times of 700 and 1,400 second are for samples from which gel is removed by solvent extraction. It is clear that fractions of residual double bond and pendant vinyl unit remain constant in the course of the polymerization. Such a trend is also observed at much lower dose rate, 37.5 rad/sec by γ-rays. These results indicate that the rate of the reaction to consume the double bond is always in a fixed proportion to the rate of polymerization.

To study the mechanism of the formation of crosslinks and loss of double bonds, a model study is carried out using a commercial liquid polybutadiene, Hycar-CTB4000 (Goodrich) which has relatively similar microstructure and molecular weight as the polybutadiene obtained by radiation. In Fig. 2, gel formation in n-hexane solution is studied at the same

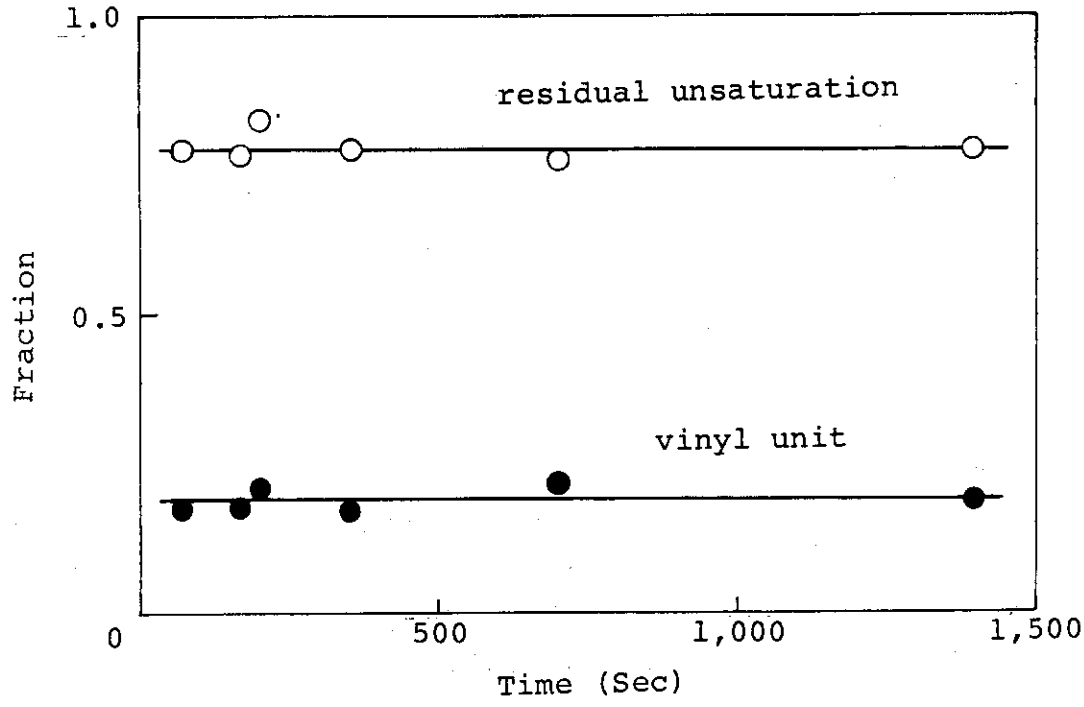

Fig. 1. Structure of polybutadiene polymerized by electron beam irradiation at -10°C. Dose rate, 2.2×10^5 rad/sec.

reaction conditions as in the polymerization studies. The fact that gel formation is retarded by the addition of triethylamine (TEA) indicates a cationic mechanism of cross-linking. In addition, fraction of residual unsaturation is determined for soluble part of these polymer irradiated. The initial G values for the consumption of double bond are in the decreasing order of no additive, 0.1 mole/ℓ TEA and 1.0 mole/ℓ TEA. This also means that the cationic mechanism is responsible to the loss of double bond in the polymer.

It has been already pointed out that cyclization of main and side chain double bond occurred with Lewis acid. This is a chain reaction making fused condensed rings of saturated chains at the expense of double bond and eventually terminates by proton elimination reaction leaving a trisubstituted double bond. Actually, the relatively broad peak at 1.5 ppm in ^{1}H-NMR spectra of the polybutadiene by radiation can be assigned to

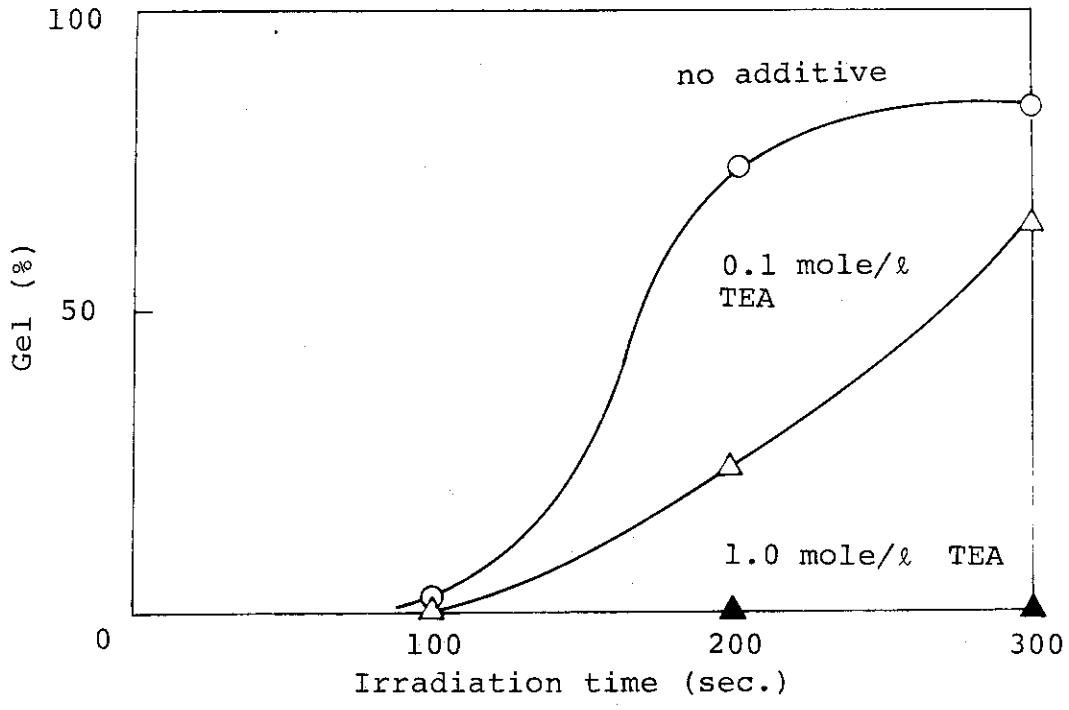

Fig. 2. Gelation of polybutadiene (Hycar CTB4000) in n-hexane solution at -10°C. Concentration, 160 g/ℓ; dose rate, 2.2×10^5 rad/sec.

the absorptions of CH_2 and CH protons in the saturated rings and a weak absorption at 846 cm^{-1} in the IR spectra indicates the presence of trisubstituted double bond.

From these results, we can conclude that cyclization and crosslinking reactions of the polymer are taking place mainly by cationic mechanism and that in the polymerization system, these two reactions as well as the propagation reaction occurs concurrently through proton transfer reaction. In other words, a cationic species once undergoes propagation, then makes cyclization attacking double bond of the polymer for a while and sometimes attacks neighboring polymer chain to form a crosslink in a life of the species. (K. Hayashi, S. Okamura)

[4] Modification of Polymers

1. Radiation-Induced Grafting of Acrylic Acid onto Polyethylene Filaments

Polyethylene has excellent properties such as lightness, high tensile strength, low-temperature toughness and high chemical resistance when it is used in the form of filaments as industrial materials. However its usage or application is rather limited because of a disadvantage that the softening temperature is low.

We have studied radiation induced grafting of acrylic acid onto high density polyethylene filament in order to raise the softening temperature and improve hydrophilic properties.

The purpose of this study is to make excellent man-made fibers for general use. Polyethylene filament was employed in the present experiment only because it is easily available. The diameter of the filament is about 220 μm.

The grafting of acrylic acid was carried out in a mixture of acrylic acid - water - ethylene dichloride. It was also necessary to add Mohr's salt to the monomer mixture to prevent homopolymerization of acrylic acid outside the filament. The direct irradiation method was employed for the grafting using γ-rays from a ^{60}Co source.

The rate of grafting for the filament was much lower than that for high density polyethylene film (20 μm and 100 μm thick) and only 2% graft was obtained at room temperature even after irradiating for 8 hours at a dose rate of 1.8×10^4 rad/h. Grafting was, therefore, carried out at higher temperatures to obtain higher percent graft.

Fig. 1 shows the plots of percent graft against irradiation time at a dose rate of 1.8×10^4 rad/h at various temperatures. The initial rate of grafting increases with increasing irradiation temperature. The overall activation energy for the initial rate of grafting was found to be 15 kcal/mol at 20 to 60°C and 10 kcal/mol at 60 to 80°C.

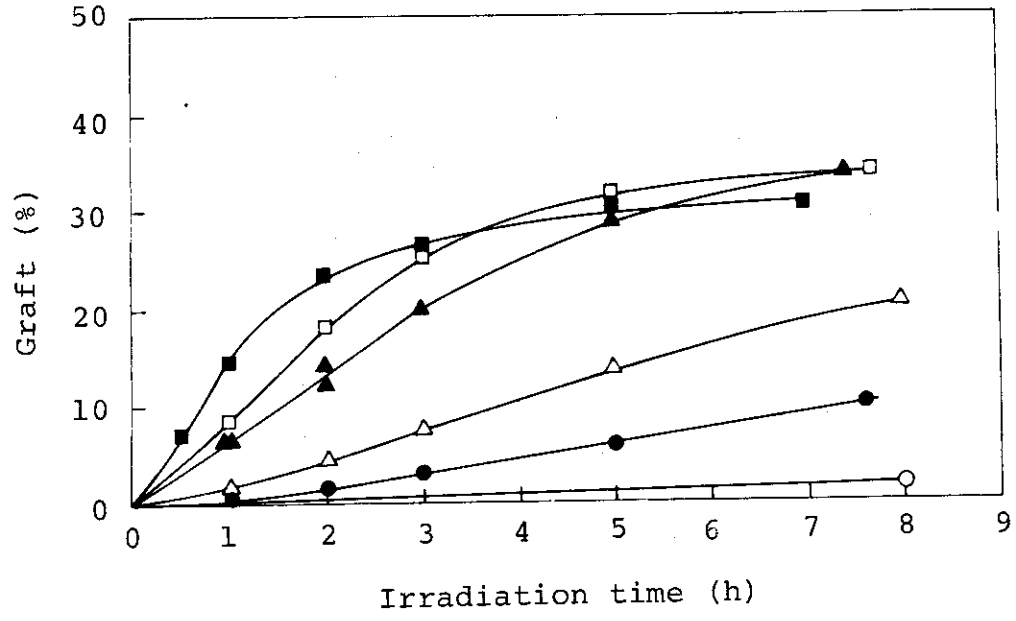

Fig. 1. Grafting of acrylic acid onto polyethylene filament at 1.8 x 10^4 R/h at different temperatures. Monomer mixture: AA : H_2O : $(CH_2Cl)_2$ = 50 : 25 : 25 (containing Mohr's salt of 4 x 10^{-3} mole/ℓ); irradiation temperature: (○) room temperature, (●) 40°C, (△) 50°C, (▲) 60°C, (□) 70°C, and (■) 80°C.

Acrylic acid graft polyethylene filaments could be dyed clearly with cationic dyes at 1 graft percent. The cross-section of graft polyethylene filaments dyed with a cationic dye (Sevron Brill. Red B) was observed with microscope and distributions of acrylic acid in the graft filaments were examined. The depth of the colored part from the surface is mainly determined by graft percent of acrylic acid.

The heat-resistance of acrylic acid graft polyethylene was studied from the measurement of heat-shrinkage. Heat-shrinkage curves are shown in Fig. 2. The original polyethylene filament begins to shrink at 60°C and reaches a maximum shrinkage of 50% at 130°C. After that it breaks off at 136°C. Thirty four percent graft filament heat-treated at 180°C for

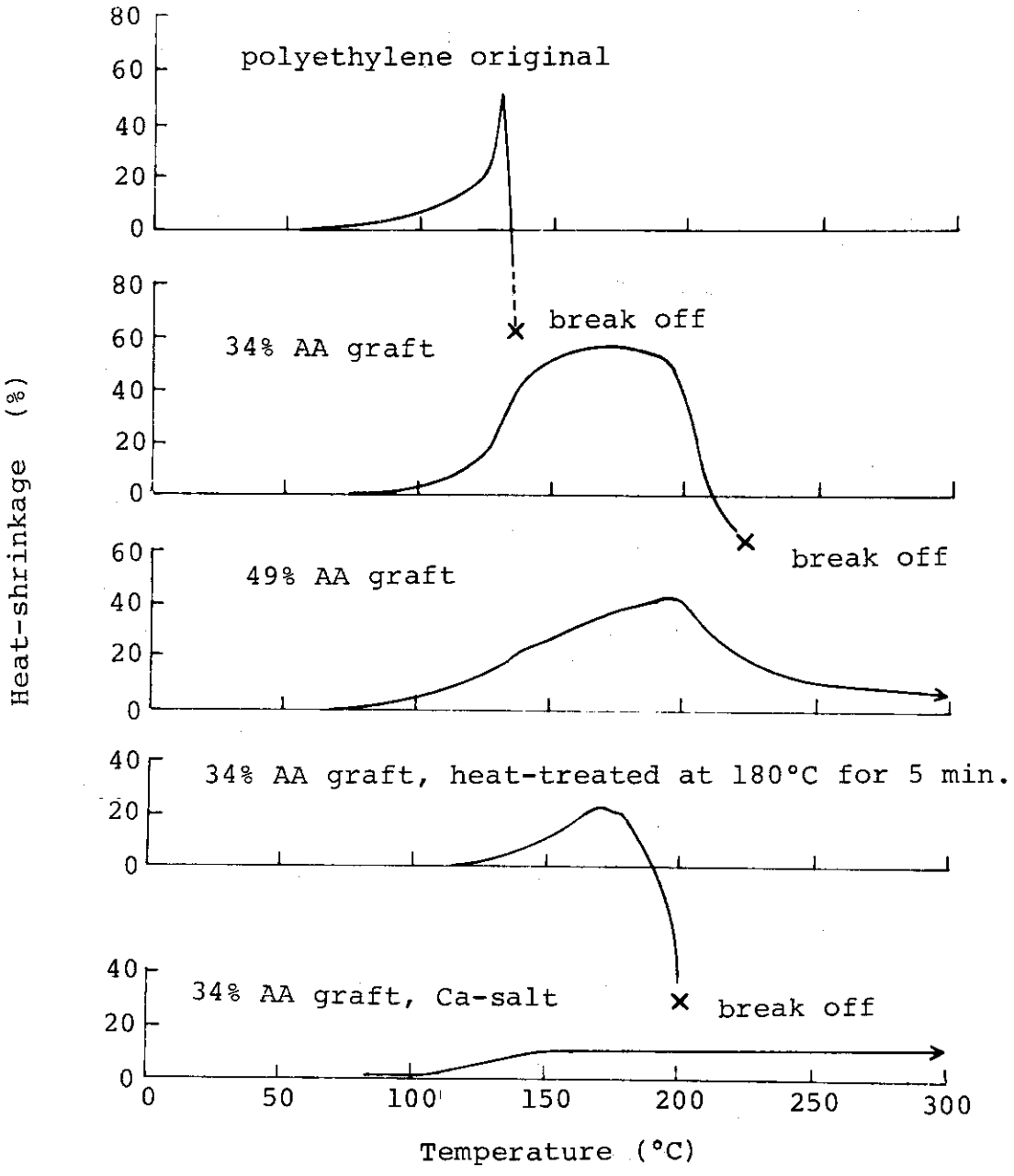

Fig. 2. Heat-shrinkage of acrylic acid graft polyethylene filaments.

5 minutes shows a maximum shrinkage of 20% and breaks off at 200°C. When acrylic acid graft polyethylene was converted to the calcium salt, the graft filament retained its filament form even at 300°C and gave a maximum shrinkage of 12 ∿ 13%.

The tensile strength and elongation were not decreased neither by grafting nor by converting the graft fiber to the Ca-salt. (T. Okada, K. Kaji)

2. Radiation-Induced Graft Polymerization of Acrylic Acid onto Poly(vinylchloride)

--- Adsorption of Metal Ions by Graft Polymer ---

The purpose of the present study is to prepare polymers in powder form having hydrophilic and hydrophobic parts, and to study the structure of the polymer powder through studies on the properties of the powder. In the last annual report, we described radiation-induced graft polymerization of acrylic acid (AA) onto polyvinylchloride (PVC) powder and some properties of powder of the graft polymer such as adhesion ability to metal surface, adsorption of metal ions, and electric conductivity. Among these properties, the adsorption behavior of cupric ion by the powder seems to be most closely related to the structure of the powder of graft polymers which were prepared from ethylene dichloride (EDC) solution of different compositions using PVC of $\overline{DP}$ = 500.

In this year, adsorbability of cupric ion to the powder of graft polymer has been studied in order to know the structure of the powder of graft polymer obtained from PVC of different degrees of polymerization under different reaction conditions. The polymers of three different degrees of polymerization (500, 970, and 1800) were used in the present study. The methods of grafting and evaluating the adsorbability were the same as those described in the previous report [1].

Figure 1 A-C shows the rate of graft polymerization obtained under various ethylene dichloride (EDC) contents for

the above three kinds of PVC powders. In the case of the low molecular weight PVC ($\overline{DP}$ = 500), EDC content in the system greatly affects the rate of graft polymerization throughout the reaction period studied. This fact confirms the conclusion of the previous study [1] that EDC is effective as a swelling agent to the low molecular weight polymer and promotes greatly monomer diffusion into the PVC particles.

In the case of the medium molecular weight polymer ($\overline{DP}$ = 970) the rate of grafting was independent of the EDC concentration except at the highest EDC concentration studied, where the rate of grafting was significantly enhanced by EDC (curve IV ($AA/H_2O/EDC = 50/15/35$) in Fig. 1B), especially, at later stage of the polymerization. This means that for the polymer of $\overline{DP}$ = 970, EDC was not apparently an effective swelling agent, but the enhancement of the rate of the grafting found at the later stage might be resulted from that the graft polymerization in the early stage with the presence of EDC may result in losening the polymer structure thus causing monomer to diffuse more and more into the particle.

Induction period was observed for the polymer of the highest molecular weight ($\overline{DP}$ = 1800) when the EDC content is low (Fig. 1C, curves I (40/54/6) and II (50/40/10)). The reason of this is not clear at present. But grafting rates were almost the same one another for all systems when the grafting was once initiated. Thus, the grafting seems to be independent of the EDC content. The EDC in this system acts as a solvent which dissolves the monomer to prevent the monomer from homopolymerization or to prevent cross-linking between the grafted side chains. The latter produced three dimensional network which sometimes in our experiment keeps the functional groups inside of the particles and away from access of cupric ions.

The adsorption of the cupric ion was examined for the graft polymers of similar degrees of grafting around 15%. Graft polymer containing twice the molar quantity of the carboxyl groups to the cupric ion was added to 20 ml of the cupric sulfate solution in 100 ppm concentration as cupric ion.

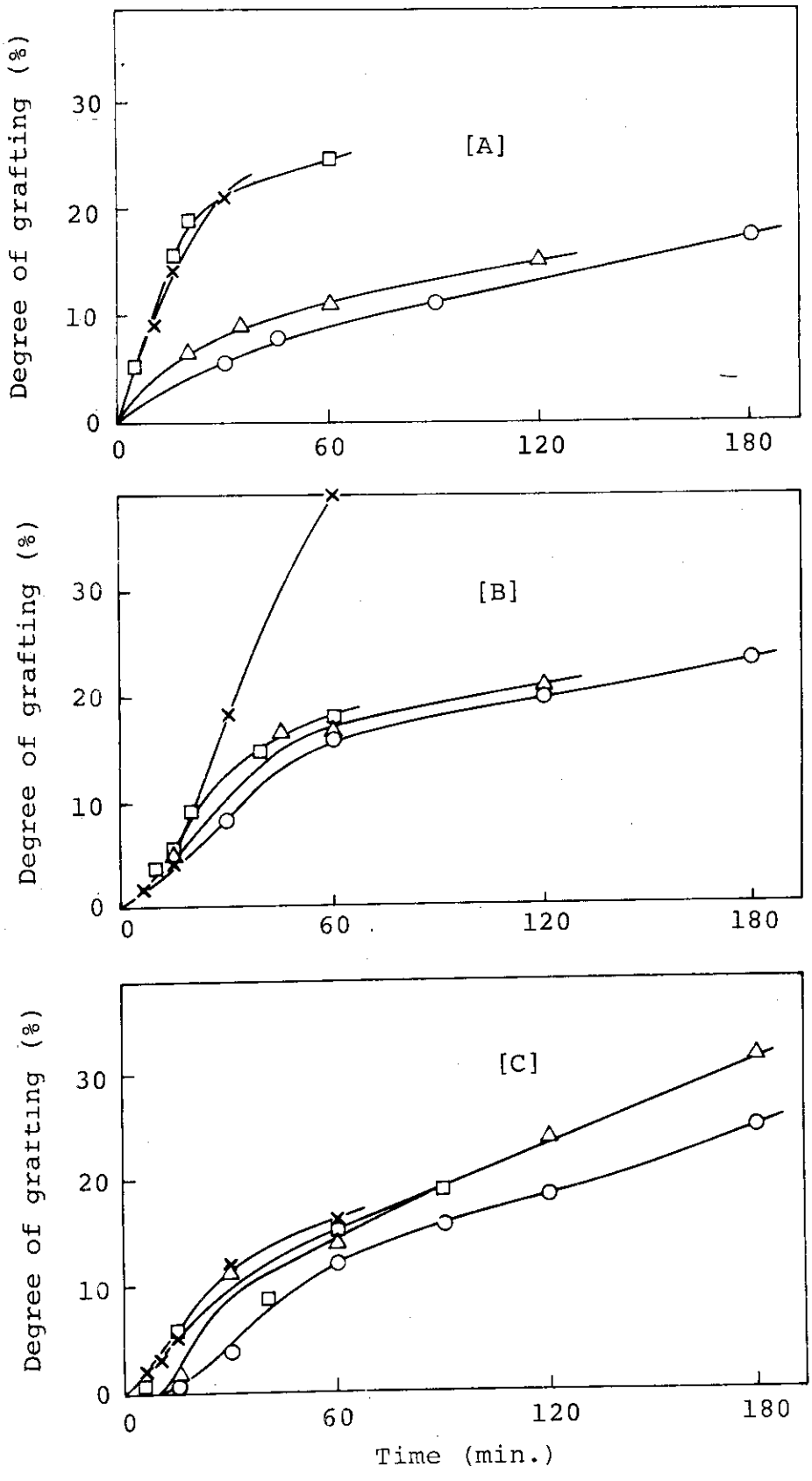
Degree of grafting (%)
[A]
[B]
[C]
0
10
20
30
60
120
180
Time (min.)

Other experimental conditions were the same as in the previous report [1]. Figure 2 A ∿ C shows the adsorption of cupric ion by the graft powder as a function of time. In Fig. 2 A, the graft powders obtained from PVC ($\overline{DP}$ = 500) by the systems I (40/54/6) and II (50/40/10) in which the EDC content is comparatively low, show good adsorbability. It is noted that the graft powder obtained by similar time conversion curves, for example, curves I (40/54/6) and II (50/40/10) in Fig. 1A give quite similar adsorption behavior each other as shown by the corresponding curves I (40/54/6) and II (50/40/10) in Fig. 2 A. For the graft powder obtained from PVC ($\overline{DP}$ = 1800) at four different monomer concentrations, which give the time conversion curves of similar shape (Fig. 1 C), the adsorption rate curves of the four graft polymers are similar to one another (Fig. 2 C). Similar relationship between the time conversion curves by which the graft powders were obtained and the adsorption rate curves of the graft powder is observed for the graft polymer of PVC ($\overline{DP}$ = 970), although the correlation is not so good as the former two.

The close correlation observed between the time conversion curves by which the graft powder was obtained and the adsorption rate curves of the graft polymer may come from the circumstance that the graft powder obtained by different time conversion curves have corresponding distribution of the graft side chain, which may in some way relate to the adsorption of cupric ion.

Optical microscopic observation of the cross section on the graft polymer particle was examined, that is, grafted

Fig. 1. Time conversion curves of graft polymerization obtained under the various ethylene dichloride contents in the systems. $\overline{DP}$ of PVC: [A] 500, [B] 970, and [C] 1800; composition of the monomer mixtures: (○), I AA/H_2O/EDC = 40/54/6; (△), II (50/40/10); (□), III (50/25/25); (×), IV (50/15/35). Irradiation temperature, room temperature; radiation source, Co^{60} γ-ray source; dose rate, 6 x 10^4 R/hr. Systems I, II, III, and IV correspond to systems a, e, s, and d in the previous report[1], respectively.

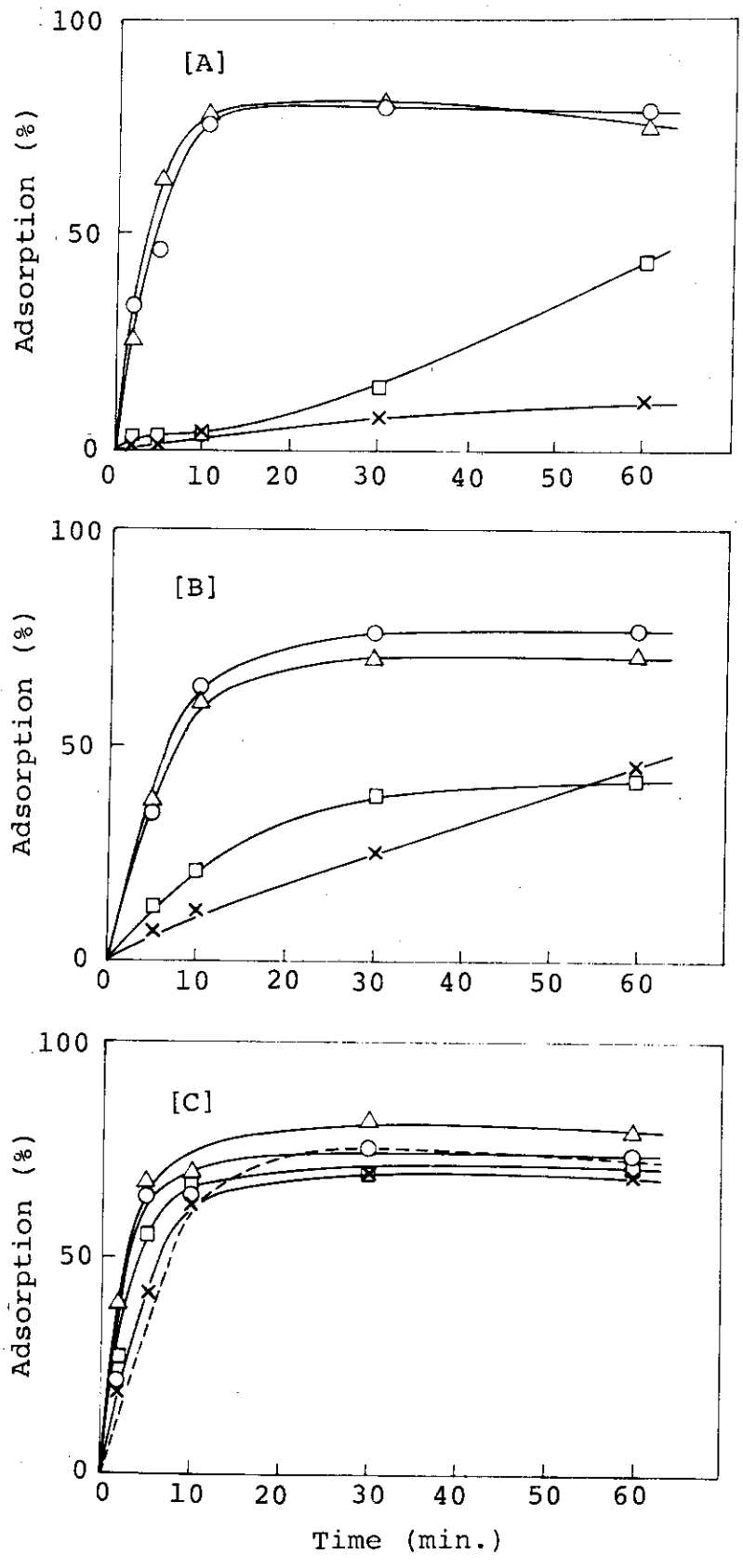
[A]
[B]
[C]
Adsorption (%)
100
50
0
0
10
20
30
40
50
60
Time (min.)

samples were immersed in paraffin and cut into thin flakes which were dyed with a cationic dye. The graft powder has a diameter ranging from 20 μm to 100 μm. The dyed cross section of the grafted sample for the low molecular weight PVC ($\overline{DP}$ = 500) obtained under the water rich system I (40/54/6) (in Fig. 1 A) shows surface grafting. On the other hand, the graft polymer particles obtained in the EDC rich system IV (50/15/35), non grafting area was observed near the surface of the particle, showing "core grafting". This may indicate that the monomer distributes uniformly throughout the particle by the rapid diffusion of the monomer into the particle due to the swelling with EDC, while the distribution of Mohr's salt is limited near the surface region of the particle to inhibit the grafting in this region.

For the particles grafted onto the polymers of medium molecular weight ($\overline{DP}$ = 970) at different EDC contents, patterns of the cross section of the particle are similar to one another and almost independent of EDC content. In this case the grafting seems to proceed uniformly in the particle.

For the polymers of the highest molecular weight studied ($\overline{DP}$ = 1800), the grafting proceeded completely uniformly in water rich system I (40/54/6) and gave graft polymers whose cross section is similar in appearance to that obtained in the EDC rich systems III (50/25/25) and IV (50/15/35). In these cases,

Fig. 2. Adsorption of cupric ion by the graft polymer particles obtained under different reaction conditions. $\overline{DP}$ of PVC: [A] 500, [B] 970, and [C] 1800; types of the monomer mixtures, with which the grafting was carried out, and graft percents (given in the parentheses);
[A]: (○) I (17.2%), (△) II (15.1%), (□) III (15.6%), (×) IV (17.1%);
[B]: (○) I (19.8%), (△) II (15.7%), (□) III (14.3%), (×) IV (18.6%);
[C]: (○) I (15.4%), (△) II (14.0%), (□) III (15.0%), (×) IV (16.2%).
EDC contents of the mixtures I, II, III, and IV are given in the caption of Fig. 1. The dotted line in [C] indicates the adsorption rate curve obtained for Amberite CG 50.

Table 1. Ion Exchange Ability of the Graft Polymer

			500		970		1800		
	Sample No.		II-54	II-55	II-93	II-95	II-188	II-184	CG-50(I)
	Degree of Grafting	(%)	15.1	24.4	16.8	20.4	14.0	21.0	-
	Total Capacity	(meq/g)	1.71	2.36	1.61	2.16	1.60	2.26	9.7
	(Calculated)	(meq/g)	1.83	2.81	2.00	2.38	1.70	2.73	10
(II)	Equilibrium Adsorption	(%)	93.4	84.0	80.5	90.8	94.1	82.8	97
	Wet Volume	(ml/g)	2.0	2.2	2.7	2.8	2.0	2.2	4.8
	Degree of Swelling (%)	[$Na^+ \rightarrow H^+$]	≃0	≃0	3.8	7.7	-9.1	≃0	-33
	Capacity (Wet)	(meq/ml)	0.86	1.07	0.60	0.77	0.80	1.03	2.08(3.0)
	Sample No.		IV-52	IV-53	IV-98	IV-95	IV-185	IV-187	IR120B
	Degree of Grafting	(%)	13.9	21.3	6.4	18.6	12.3	16.2	-
	Total Capacity	(meq/g)	0.40	1.20	0.25	1.31	1.26	1.46	4.4
	(Calcualted)	(meq/g)	1.69	2.44	0.83	2.18	1.52	1.94	-
(IV)	Equilibrium Adsorption	(%)	23.7	49.2	30.4	60.1	82.9	75.3	-
	Wet Volume	(ml/g)	2.2	2.6	2.6	2.8	2.7	2.8	2.3
	Degree of Swelling (%)	[$Na^+ \rightarrow H^+$]	10	8.3	9.0	5.6	8.3	7.6	5 ∿ 10
	Capacity (Wet)	(meq/ml)	0.18	0.46	0.10	0.47	0.47	0.52	1.9

many hair cracks appeared in the particle.

The microscopic observations mentioned above would be related to the adsorption behavior (rate and equilibrium adsorption), because the adsorption of metal ions by the graft powder is greatly affected by its hetero structure, that is distribution of the grafted chains in the polymer particle. Since the distribution of the grafted chain can be controlled easily by the reaction conditions and by selecting trunk polymer of appropriate $\overline{DP}$, it is possible to obtain the graft polymer of appropriate properties by the grafting method.

In the present study, it was revealed that the close correlation among the reactivity, structure and adsorbability to cupric ion was obtained for the polymer having hydrophobic and hydrophilic parts prepared by grafting of acrylic acid onto PVC. The properties of the grafted PVC powder as a cation exchange resin [2] are listed in Table 1 along with those of a commercial one, Amberite CG50, and the adsorption rate curves of the commercial one in Fig. 2 C for comparison. The graft powder shows excellent rate of adsorption and dimensional stability. The total capacity is, however, lower than that of the commercial one. (Y. Kusama, T. Yagi)

1) Y. Kusama, T. Yagi, and T. Okada, JAERI-M 7949, 74 (1977).
2) A. Kambara and S. Fujiwara, "Hand Book of Polymer Analysis", Asakura Publishing Co., Tokyo, 901 (1965).

3. Mechanical Properties of WPC from Caprinus Tschonoskii

Caprinus Tschonoskii was obtained from Miyawaki Kogyo Co. and was cut to pieces of 10 mm x 10 mm x 190 mm. Resin solutions for impregnation were mixture (A) consisting of epoxy acrylate prepolymer (RE-2), vinyl acetate (VAc) and hydroxyethyl acrylate (HEA) in weight ratio of 60 : 30 : 10, and mixture (B) consisting of Blenmer GP, butyl acrylate (BA) by weight ratio of 90 : 10, and 0.5 benzoyl peroxide.

A piece of wood specimen was placed in a 3 ℓ desiccator and was deaerated at 1 Torr for 3 hours. The resin solution was introduced into the desiccator, so that the specimen is completely covered by the solution, and then nitrogen was introduced to atmospheric pressure to force the solution into the specimen. Some of the specimens were further compressed in a metal cylinder at 300 kg/cm^2.

The impregnated samples with or without further compression were packed with aluminium foil and then irradiated by electron beams (1.5 MeV, 100 μA; 0.35 Mrad/sec) from a Van de Graaf accelerator on a conveyor which carries the specimens. The irradiation was carried out repeatedly under the irradiation window back and forth until a required dose is irradiated.

Polymer loading, and bending strength of the irradiated specimen for mixture (A) are plotted as a function of specific gravity before irradiation in Fig. 1 A and B. The bending strength of the original wood is also given for comparison. Both sides of the specimen were irradiated and the dose was 7 Mrads on one side. As shown in Fig. 1 A, the bending strength of the original wood increases with increasing specific gravtiy and the bending strength of WPC is higher than the original wood. The specimen treated with the mechanical compression before irradiation shows higher strength than WPC prepared without mechanical compression, but the polymer loading of the compressed WPC was lower than the WPC and independent of specific gravity of the original wood. This means that the bending strength depends on that of the original wood and is independent of polymer loading.

Plots for WPC obtained using resin mixture (B) are shown in Fig. 2 A and B. Similar tendency as those of Fig. 1 A and B is observed. The dose received on one side was 3.5 Mrads in this case. The same improvement of the bending strength of the original wood was obtained by the WPC procedure despite of the poor bending strength of cured resin mixture (B) (see Table 1).

The results obtained in this study indicate that the WPC of excellent mechanical properties can be obtained by

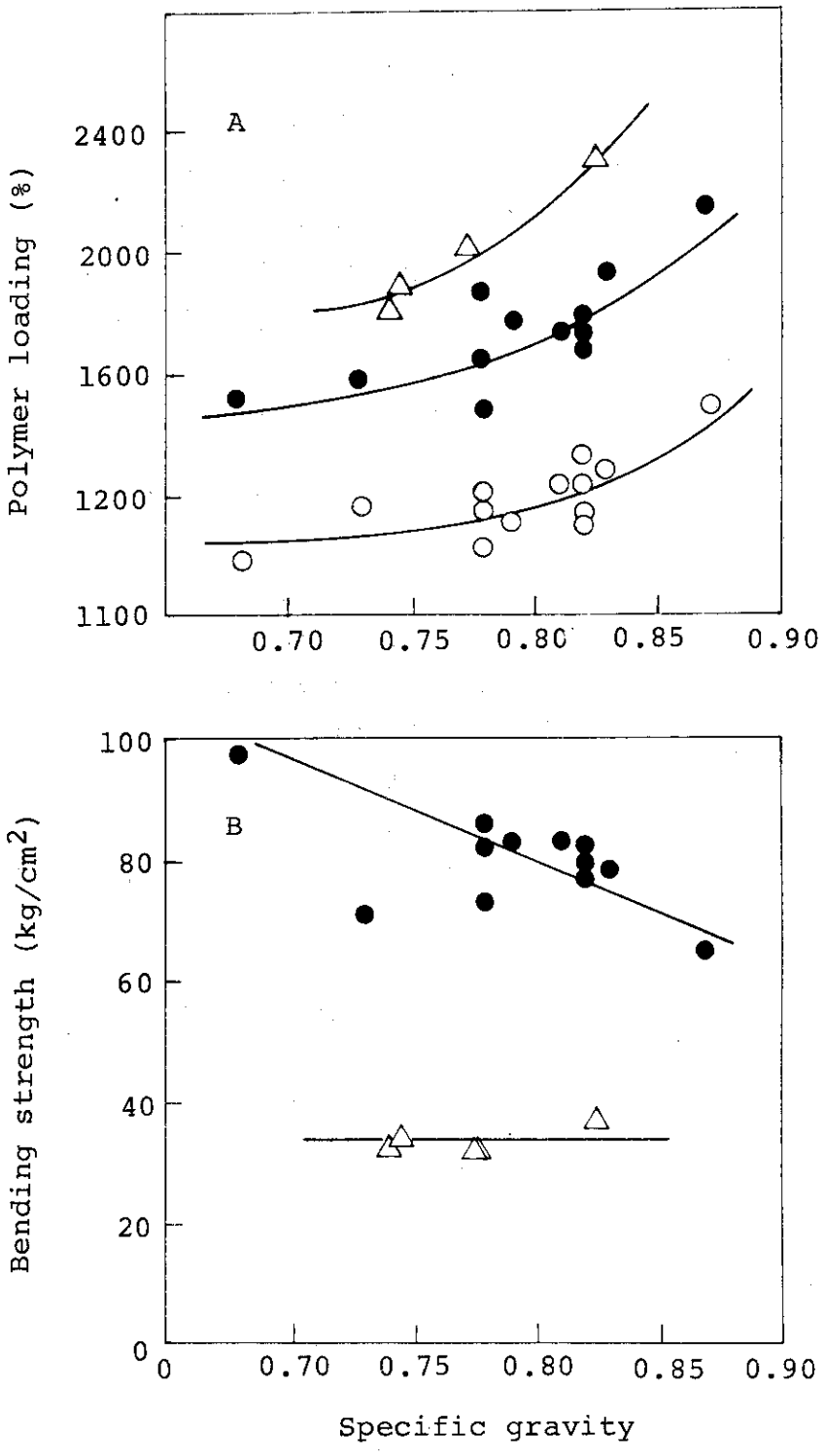

Fig. 1. Effect of specific gravity of the wood on the bending strength of WPC (A) and polymer loading (B): (○) original wood, (●) WPC, and (△) compressed WPC. Resin mixture: epoxy acrylate (RE-2)/vinyl acetate/ hydroxyethyl acrylate (60/30/10).

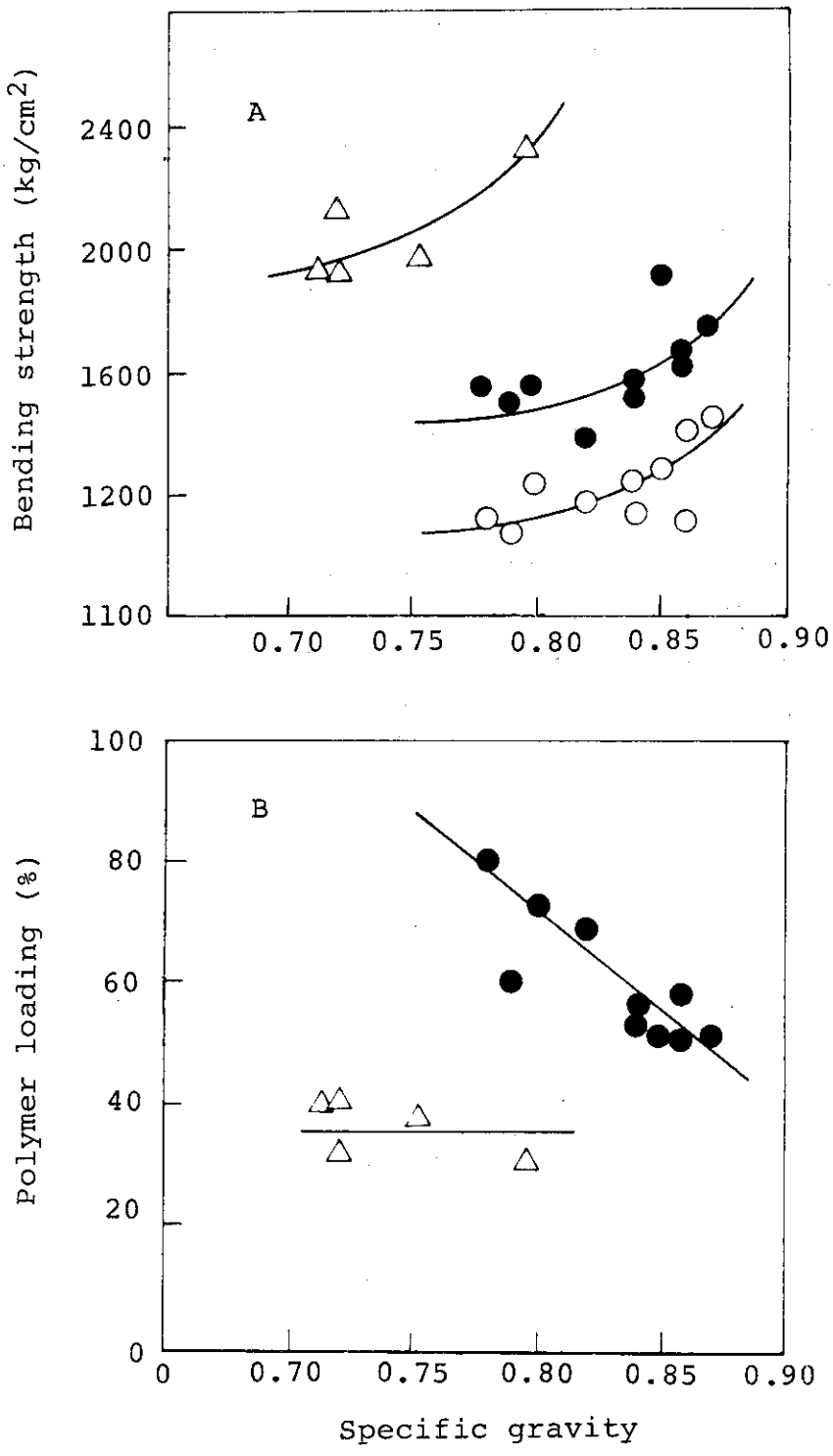

Fig. 2. Effect of specific gravity of the wood on the bending strength of WPC (A) and polymer loading (B): (○) original wood, (●) WPC, and (△) compressed WPC. Resin mixture: Blenmer GP/butyl acrylate/benzoyl peroxide (90/10/0.1).

Table 1. The Bending Strength of the Cured Resins*

Resins	Specific Gravity	Bending Strength (kg/cm^2)
A	1.4	1801
B	1.2	364

* The curing was carried out with Co^{60} γ-rays at a dose rate of 2×10^5 R/hr.

impregnation with a small amount of polymer which fills the mechanically weak amorphous part of the wood, and the compression procedure before irradiation is effective for this purpose. (T. Yagi, M. Gotoda)

[5] Studies on Radiation Dosimetry

1. W Values of Argon-Ethane Mixtures with Electron Beams under Elevated Pressures

Ion pairs are produced when atoms or molecules interact with charged particles. The energy necessary to produce an ion pair, W value, is defined as the total amount of charged particle energy dissipated divided by the total number of ion pairs formed. We measured W values of gas mixtures of argon and ethane (coargon) when the gas mixtures are irradiated with electron beams under elevated pressures up to 7 atm, in order to examine whether the results well fit to the model derived by Hurst, et al.[1] based on their experimental data on alpha-particle ionization of binary gas mixture of argon and ethane.

An ionization chamber of parallel plate electrode type was used. The gas mixture was introduced in the cell which had been evacuated up to 10^{-4} Torr in advance. The electron beam (600 keV, 10 μA) penetrated into the chamber through a 30 μm titanium window. Ionization current was measured using a microammeter.

Absolute determination of absorbed energy can be made for alpha-particle ionization, but not for electron beams from an accelerator, because the range of electron beam is longer than that of alpha-particles and thus it is difficult to assume that whole energy of electron is absorbed in the gas. We, therefore, calculate relative W value of gas mixture using stopping power of each gas and W value of argon which is well established to be 26.30 [eV·ip^{-1}] for β-ray ionization.

The W value for gas mixture, W_m [eV·ip^{-1}], can be calculated by

$$W_m = \frac{P_{Ar} \cdot S_{Ar} + P_E \cdot S_E}{K \cdot I_i} \qquad (1)$$

where P_{Ar} and P_E are gas pressure of argon and ethane in atm., whose stopping powers are S_{Ar} and S_E [eV·molec^{-1}], respectively,

I_i is ionization current [μA], and K is a constant [atm·ip·molec^{-1}·μA^{-1}].

According to Hurst et al.[1], alpha particle ionization in gas mixture of argon and ethane can be explained by the following mechanism. Two excited states, ε_1 (11.6 eV) and ε_2 (ca. 14 eV), of argon are known to be formed when argon interacts with ionizing radiation. These states contribute to ionization of ethane through following three competing processes: (i) spontaneous radiative deactivation of Ar^*, (ii) radiative or radiationless transfer of energy between Ar and Ar^*, and (iii) collision energy transfer with ethane designated as X, where * indicates electronic excitation. The number of energy transfers to X by (iii), $N_i(X^*)$, can be calculated by

$$N_i = \frac{\bar{v}_X \sigma_{ix} f_X}{\bar{v}_X \cdot \sigma_{ix} \cdot f_X + \bar{v}_{Ar} \cdot \sigma_{iAr} f_{Ar} + (\lambda/N_0 P)} \beta_i E_0 \qquad (2)$$

where the subscript i refers to the two energy levels of argon, ε_1 and ε_2; f, v, and σ are mole fraction, average relative velocity with Ar, and cross section for energy transfer from Ar* to the component indicated by subscript. The λ is the decay constant for process (i), N_0 is the number of gas atoms per cubic centimeter and $\beta_i E_0$ is the number of excitation of argon to ε_i state.

The W_m value can be expressed by

$$W_m^{-1} = [(W_X^{-1} - W_{Ar}^{-1}) Z + W_{Ar}^{-1}] + \sum_i \frac{\alpha_i f_X (1 - Z)}{f_X + C_i \cdot f_{Ar} + (\frac{\lambda \bar{v}_X \sigma_{iX}}{N_0 P})} \qquad (3)$$

where $\alpha_i = \eta_i \beta_i$, $C_i = (\bar{v}_{Ar} \sigma_{iAr})/(\bar{v}_X \sigma_{iX})$ and $Z = f_X/(f_X + a f_{Ar})$. The parameters a included in Z is an empirical parameter depending on coargon, and η_i is the fraction of X^* leading to ionization of X. Since the ionization potential of ethane (11.6 eV) is equal to or lower than the energy level of either excited state of argon, two terms due to the excited states of argon may be considered when the data are fitted to Eq. (3).

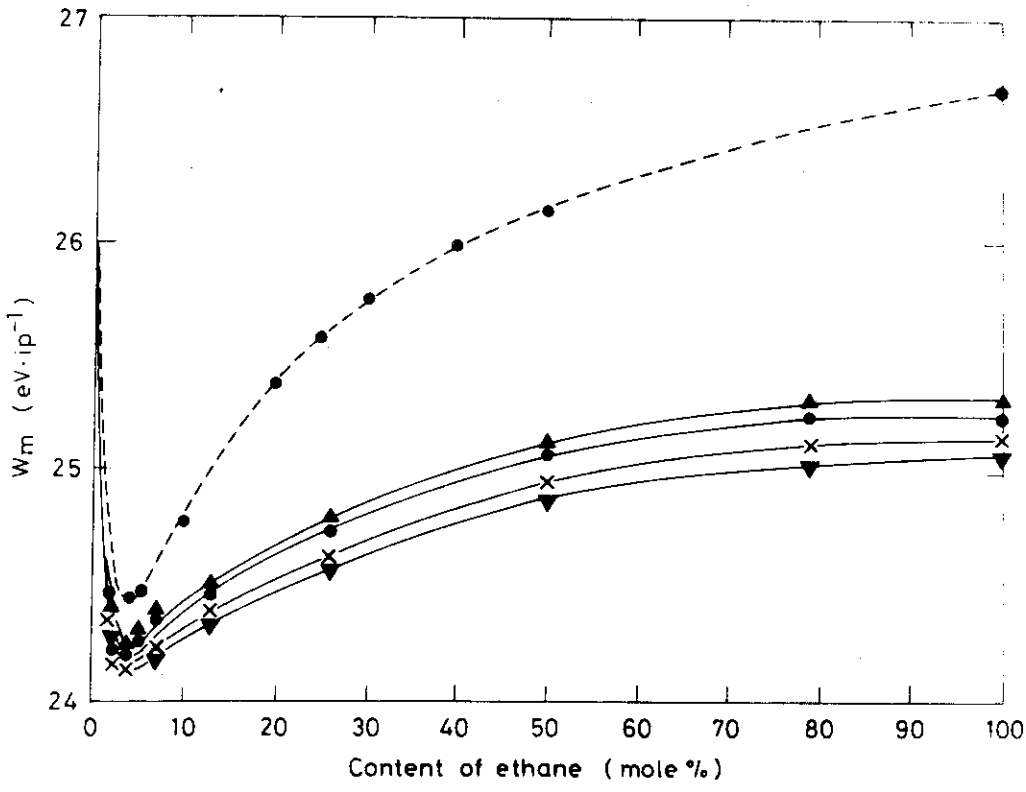

Fig. 1. W_m value of the argon-ethane gas mixture as a function of ethane content: pressure, (▲) 1 atm., (●) 3 atm., (×) 5 atm., and (▼) 7 atm. The broken line indicates the curve for alpha-particle ionization[1].

In Fig. 1, W_m values of the gas mixture obtained at four different pressures are plotted against ethane content in the gas mixture, along with the plot obtained for alpha particle ionization obtained by Hurst, et al. As shown in the figure, W_m value decreases sharply by addition of small amount of ethane, reaches the minimum value, 24.2 [eV·ip^{-1}], at 4% ethane content, and then increases gradually to W value of ethane, 25.2 [eV·ip^{-1}]. W_m value for electron ionization comes below those obtained for alpha-particle ionization in the whole gas composition range studied. This tendency seems to be reasonable from the fact that most data obtained by β-ray are smaller than those obtained for alpha-particle ionization, but the values obtained for ethane in the present study are

higher than reported values for β-ray ionization.

The W_m value decreases with increasing pressure, indicating that the ionization proceeds favorably at higher pressures.

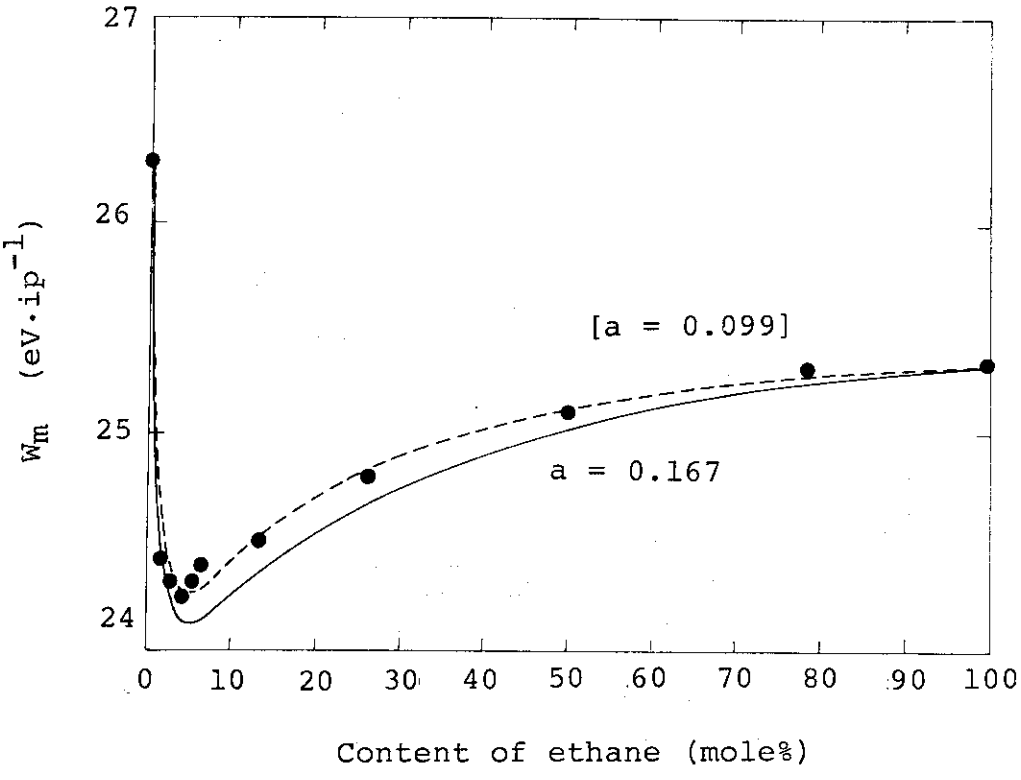

Fig. 2. Fitting of the W_m value obtained at 1 atm.
(-----) a = 0.099, (———) a = 0.167.

In Fig. 2, the W_m value obtained at 1 atm. gas pressure is replotted from Fig. 1, with the calculated values from Eq. (3). The solid line indicates the calculated curve using the parameters determined by Hurst, et al. for the alpha-particle ionization. It is evident in the figure that the data are fairly close to the fitted curve, but the agreement is not satisfactory. The reason for this small discrepancy between the calculated and the experimental points may come from that the parameter, a, determined for alpha-particle ionization is not applicable to electron ionization, since the parameter, a, is ratio of the stopping powers of the component gases, which may not be the same for electron ionization. Therefore, we

determined the parameter, a, by fitting the experimental data to Eq. (3) with least squares, other parameters being kept constant. The best fitted curve was obtained using a = 0.099 as shown by broken line in Fig. 2. Similar fitting was made for data obtained at elevated pressures and the parameters are listed in Table 1. The other parameters taken from ref. 1 and used in the fitting of the data are listed in Table 2.

Table 1. The Parameters Determined by Best Fitting of Eq. (3)

Pressure (atm)	a
1	0.099
3	0.110
5	0.133
7	0.129

Table 2. The Parameters Used in Calculating W_m values for the Gas Mixtures[1)]

Parameters	Value
α_1	0.000804
α_2	0.00401
C_1	0.000138
C_2	0.012

The fact that precise agreement between the experimental and the calculated was obtained with appropriate parameters in Eq. (3) indicates that the ionization mechanism through energy transfer from Ar^*, which is proposed for alpha-particle

ionization, is applied for ionization by electrons.

(K. Matsuda, T. Takagaki)

1) G. S. Hurst and T. E. Bortner, J. Chem., Phys., 42, 713 (1965).

2. Coloration Mechanism of the CTA Film Dosimeter

Studies have been carried out to find what species give rise to the optical density at 280 nm for the irradiated cellulose triacetate (CTA) film dosimeter. The results are described below, including those reported preliminarily last year [1].

The CTA films containing 16% triphenyl phosphate (TPP) employed in this study were those supplied by Fuji Photo Films Co. and Numelec Co., both of which gave similar results. CTA films containing no additives, referred to hereafter as pure CTA films, were prepared by evaporating methylene chloride-methanol solution of CTA. Cellulose films by Tokyo Cellophane Co. were also employed in this study. Irradiations were carried out with electron beams of 1.5 MeV and 50 μA from a Van de Graaff accelerator. Radiation effects on the CTA film dosimeter, pure CTA films and cellulose films were studied by UV and ESR spectrometers. Product analysis was carried out for irradiated TPP powder by a gaschromatograph, Shimadzu GC-7A equipped with Tenax GC columns.

When the CTA film dosimeter was irradiated in air at room temperature, the value of the optical density change at 280 nm, ΔOD (280 nm), before and after irradiation decreases rapidly by several percents until about 20 min after irradiation, followed by a gradual increase with storage time. This behavior indicates that the coloration occurs not only during irradiation (in situ coloration) but also after irradiation (post coloration), the former further consisting of unstable and stable components.

It was found that atmospheres during and after irradiation

strongly influence the ΔOD (280 nm) for the CTA film dosimeter. The ΔOD (280 nm) in vacuo slightly decreases with time after irradiation without any increase at longer storage time in contrast to the ΔOD (280 nm) in air. The ΔOD (280 nm) in O_2 decreases with time by a greater extent than in air and does not increase at longer time. The ΔOD (280 nm) in N_2 changes little with time after irradiation. These findings indicate that the unstable component of in situ coloration is related to reaction between O_2 and color centers produced in the dosimeter. The fact that the post coloration proceeds only in air and does not occur either in vacuo, N_2, or O_2, suggests that some product other than O_2 and ozone produced from air, most likely nitrogen oxides, may play a role for the coloration. In addition, since irradiated pure CTA films also exhibit post coloration when irradiation is carried out in air as described below, the post coloration in the CTA dosimeter may arise from reaction of nitrogen oxides with CTA and TPP.

In order to see if the coloration arises from radiation effects on TPP or CTA, or both, we studied the ΔOD (280 nm) of pure CTA films in vacuo and in air. The ΔOD (280 nm) in vacuo decreases gradually with time. The ΔOD (280 nm) in air, on the other hand, decreases rapidly until 30 min and then increases with time. These results strongly indicate that CTA plays an important role not only in the in situ coloration but also in the post coloration of the CTA dosimeter.

Figure 1 shows the ΔOD (280 nm) values at 3 min after irradiation and the minima against irradiation dose for the CTA film dosimeter and pure CTA films. The ΔOD (280 nm) values for pure CTA have been normalized to those of 105 μm thickness by taking into account that the CTA dosimeter of 125 μm contains 85% by weight of CTA. As may be seen from the figure, the in situ coloration of the CTA dosimeter arises not only from TPP but also from CTA, the contribution of CTA amounting to from 30% to 60% depending on irradiation dose and time after irradiation. In addition, it is evident that the contribution of the unstable component, which corresponds to the difference between ΔOD (280 nm) at 3 min and minimum of ΔOD (280 nm), is

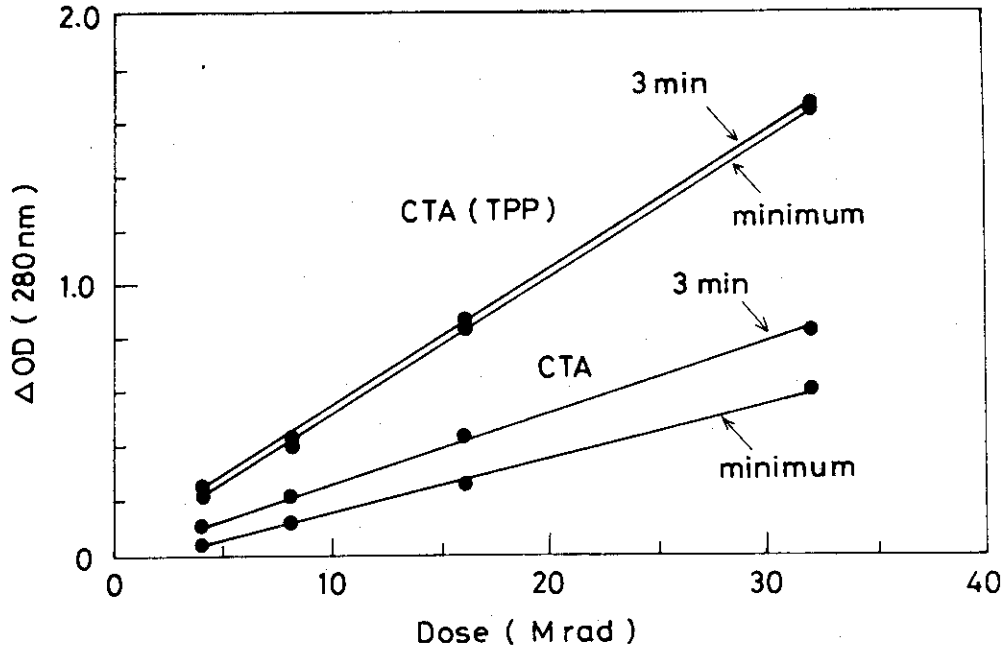

Fig. 1. Optical density change at 280 nm for the CTA film dosimeter and pure CTA film.

much higher in pure CTA than in the CTA dosimeter. This fact indicates that color centers produced not in TPP but CTA are responsible for the unstable component of the in situ coloration.

Next, species responsible for each of the three components contributing to the coloration, unstable and stable components of in situ coloration, and post coloration, are discussed. Species for the unstable component are discussed first.

The CTA film dosimeter after irradiation in vacuo at room temperature gives rise to the ESR spectrum quite similar to that of pure CTA films irradiated in the same condition. Therefore, radicals giving rise to the spectra are produced in CTA and not in TPP. When irradiation is carried out in air, the spectrum observed is analogous to the one observed in vacuo but decays rapidly with time. The half life of the spectrum in air was estimated to be about 12 min, in good agreement with the value of the unstable component obtained by optical density measurement.

It is further found that the decay of the CTA radicals proceeds through reaction with O_2 to produce peroxy radicals which we have successfully observed. Therefore, we may conclude that the unstable component of the in situ coloration is due to the CTA radicals. Most probable assignment of the CTA radicals would be to the radicals produced by H atom abstraction from C_1 in CTA molecules.

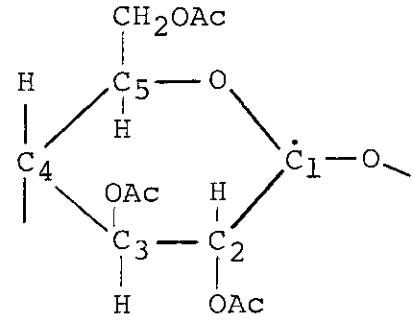

We turn to the second problem; what species give rise to the stable component of the in situ coloration? It was already shown that both CTA and TPP contribute to the stable component.

It was found that the values of ΔOD (280 nm) for pure CTA films agree with those of ΔOD (280 nm) for cellulose films up to the irradiation dose of 20 Mrad. Thus it is reasonably assumed that radiolysis products giving rise to the optical density at 280 nm are the same for CTA and cellulose. According to the extensive studies of radiation effects on cellulose by Arthur et al.[2], irradiation of cellulose produces carbonyl groups and acids as principal products. It is highly probable that these products give rise to optical density near 280 nm. We have made no further efforts to this point.

Product analysis by gaschromatography for TPP irradiated to 100 Mrad indicates that phenol and biphenyl are formed as major products with their approximate G values of 0.12 and 0.05, respectively.

On the basis of this result a model experiment was carried out to see if phenol and biphenyl detected by gaschromatograph play a role in ΔOD for the CTA dosimeter. The CTA dosimeter

and pure CTA films were irradiated to 100 Mrad and dissolved into methylene chloride, and the ΔOD values of the resultant solutions were measured. The difference of the two values was compared with the ΔOD of a methylene chloride solution containing phenol and biphenyl, concentrations of which had been determined on the basis of the GC analysis. Although the result was not fully satisfactory, it leads us to the conclusion that phenol and biphenyl produced from TPP certainly contribute to the coloration of the CTA dosimeter.

Finally we discuss the species giving rise to the post coloration. As mentioned already, the post coloration may arise from reaction of nitrogen oxides with CTA and TPP. Among nitrogen oxides, nitrogen dioxide appears to be the most likely candidate because of the higher reactivity. In fact, optical density at 280 nm for the CTA dosimeter as well as pure CTA films was found to increase when these films were exposed to nitrogen dioxide. Therefore, our explanation for the post coloration is that nitrogen dioxide produced by irradiation of air is adsorbed on the CTA dosimeter and reacts gradually with CTA and TPP to give products which show optical density at 280 nm. (K. Matsuda, S. Nagai)

1) K. Matsuda and S. Nagai, JAERI-M 7949, 102 (1978).
2) F. A. Blouin and J. C. Arthur, Jr., Textile Res. J., 28, 198 (1958).

3. Formation of Surface Charge on Polymer Films by Electron Irradiation

In the previous reports[1)], it was revealed that electric charge was produced on polymer film surface by electron irradiation of the polymer film placed on insulating material (PMMA). The surface charge density on the film surface was found to depend on the dose. It was, however, independent of the dose rate and electron accelerating voltage. Since the phenomenon seems to be applicable for estimating radiation

dose from the surface charge built-up on the film surface, we have continued the study in order to see whether the building-up of the charge on the film surface can be used as a simple method of dosimetry in the range of $10^3 \sim 3 \times 10^4$ rad where simple method of dosimetry such as film dosimeter is not established.

Two factors which are important for dosimeter were examined: one is the linearity between surface charge density on the film surface and dose and the other is the change of charge density during storage after irradiation.

The method of experiment was the same as those of the previous study [1]. Polyethylene terephthalate film (27 μm in thickness) and polypropylene film (32 μm in thickness) were obtained from Mitsubishi Kasei Co. as Diafoil and as Pylene from Toyobo Co., respectively.

Irradiation was carried out using a PMMA block of 1 cm thickness and irradiated on a conveyor 4 cm below the irradiation window for one way at a speed of 48 cm/min. Dose received by the film was altered by changing beam current.

Figure 1 shows the relationship between surface charge density and dose. It is evident from the figure that the surface charge density increases linearly with increasing dose in the dose range from 10^3 to 3×10^4 rad. Above 3×10^4 rad, the surface charge density shows no more linear change and reaches maximum at 10^5 rad and then decreases with increasing dose due to the break of insulation of a PMMA block. The reproducibility was within ±20%, which seems to be poor for that required for a dosimeter (±8%).

The decay of the surface charge density in atmosphere after irradiation is shown in Fig. 2 for the films which were irradiated at different doses; the time scale on the abscissa is expressed by minute up to 1500 minutes and after this time, by day. The curves were normalized so that the relative surface charge densities immediate after the irradiation come to fall on one point. The surface charge density decreases slowly with time after irradiation, and reaches a value which is practically independent of dose. The rate of decay of the

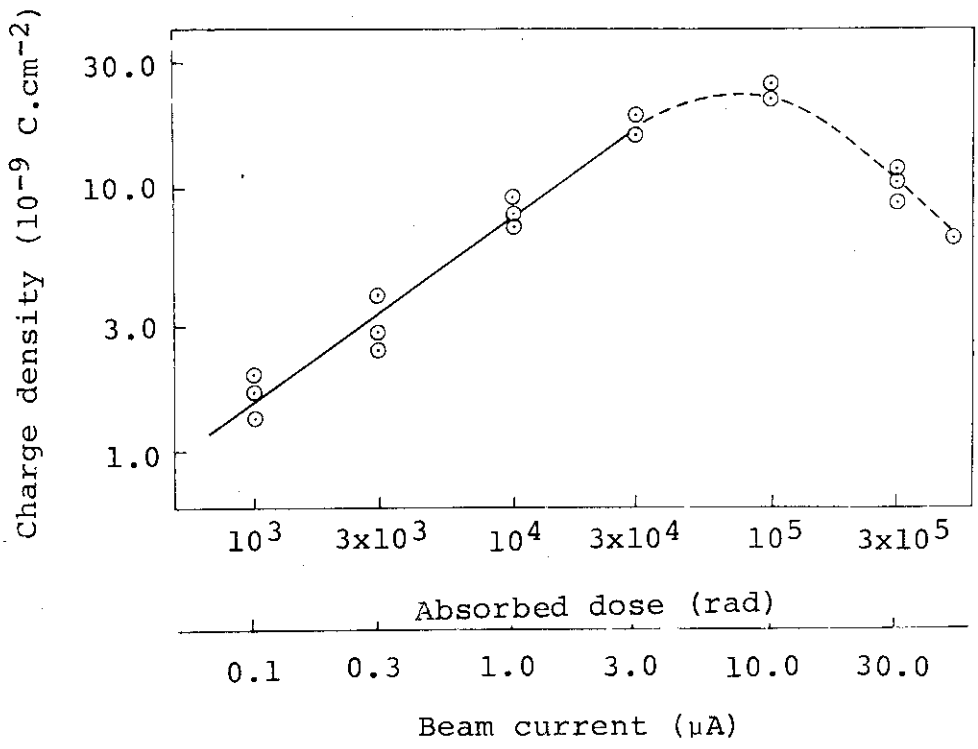

Fig. 1. Surface charge density on polyethylene terephthalate film as a function of dose: Electron accelerating voltage, 1.5 MV; the measurements were made 3 min after irradiation.

surface charge density, however, was higher as the dose absorbed by the film increases. The decay obtained in the present study is larger than those observed in the previous study [1], but the reason of this discrepancy is not clear regardless of extensive study carried out at different environments.

Similar curves of surface charge density against dose and decay of the surface charge density after irradiation were obtained for polypropylene film.

The results obtained above indicate that the surface charge density on the polymer film surface by electron irradiation is interesting in providing simple method of dosimetry at the dose range between 10^3 and 3×10^4 rad where simple method of dosimetry has not yet been established. For practical

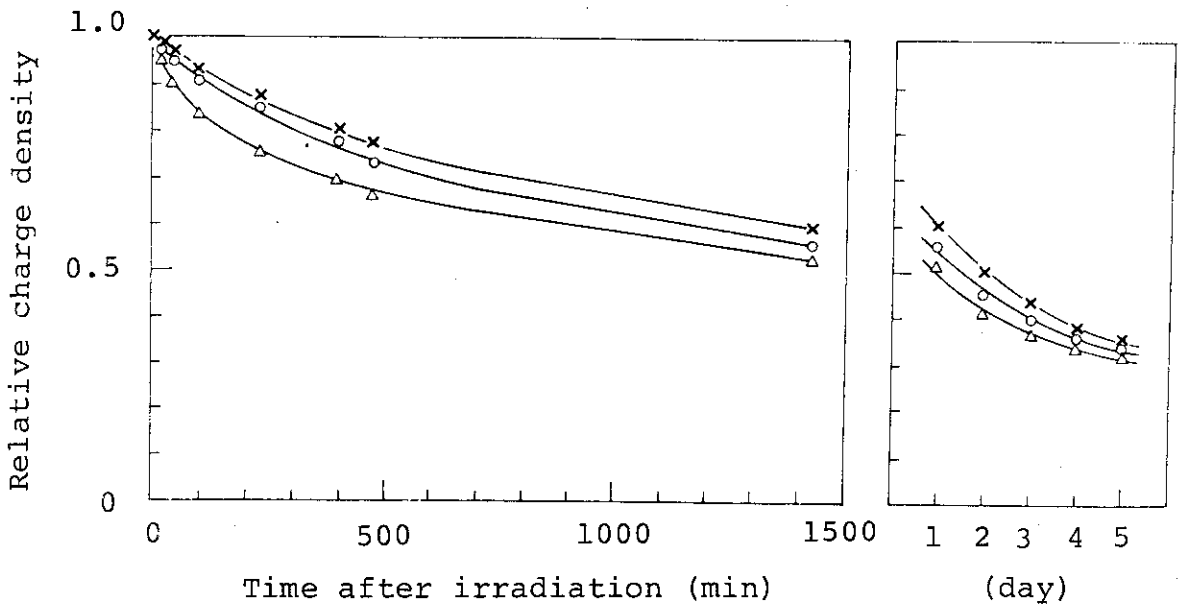

Fig. 3. Decay of surface charge density on polyethylene-terephthalate film after irradiation.
Dose: (×) 10^3 rad, (○) 10^4 rad, and (△) 10^5 rad.

purpose, however, it is necessary to solve the problem to improve the reproducibility, to diminish the decay of the surface charge density after the irradiation, and to extend the linear portion of the surface charge density vs. dose relationship. (M. Kajimaki, T. Takagaki, K. Matsuda)

1) M. Kajimaki and T. Okada, JAERI-M 7355, 52 (1977), JAERI-M 7949, 83 (1978).

III. LIST OF PUBLICATIONS

[1] Published Papers

1. S. Nagai, K. Matsuda, H. Arai, and M. Hatada, "Effects of Electron Beam Irradiation on Gas Mixture of Carbon Monoxide and Hydrogen in the Presence of Solid Catalysts", JAERI-M 7875 (1978).

2. S. Sugimoto, M. Nishii, and T. Sugiura, "Irradiation Effects on the Reaction of Mixture of Carbon Monoxide and Hydrogen. Part I", JAERI-M 7898 (1978).

3. S. Sugimoto and M. Nishii, "Irradiation Effects on the Reaction of Mixture of Carbon Monoxide and Hydrogen. Part II", JAERI-M 7899 (1978).

4. S. Nagai and T. Gillbro, "Electron Spin Resonance of Radicals Produced by γ-Irradiation of Thiophene in the Crystalline and Adsorbed State", J. Phys. Chem., 83, 402 (1979).

5. H. Arai and H. Hotta, "Self-Focussing of a Pulsed High-Intensity Electron Beam in a Low-Pressure Gas", Radiat. Res., 77, 405 (1979).

6. J. Takezaki, T. Okada, and I. Sakurada, "Radiation-Induced Polymerization of Water-Saturated Styrene in a Wide Range of Dose Rate", J. Appl. Polym. Sci., 22, 3311 (1978).

7. K. Kaji and T. Okada, "Radiation-Induced Chlorination of Polyester Fiber", Sen-i Gakkai-shi (J. of the Society of Fiber and Technology, Japan), 34, T-166 (1978).

8. K. Kaji, H. Ohkura, and T. Okada, "Preparation of Flame Retardant Polyethylene Terephthalate Fabrics by Electron-Induced Grafting of Oligomeric Vinyl Phosphonate", Sen-i Gakkai-shi (J. of the Society of Fiber and Technology, Japan), 35, T-80 (1979).

9. K. Kaji, T. Okada, and I. Sakurada, "Radiation Effects on Wholly Aromatic Polyamides", Sen-i Gakkai-shi (J. of the Society of Fiber and Technology, Japan), 34, T-545 (1979).

10. K. Kaji and T. Okada, "Alkali Treatment of Chlorinated Polyester Fiber", Sen-i Gakkai-shi (J. of the Society of Fiber and Technology, Japan), 34, T-331 (1978).

*　　*　　*　　*　　*

T. Kasamatsu, "Safety Control of Sealed Large Radiation Sources and Electron Accelerators", Nuclear Engineering (No. 7) 1978.

Y. Oshima and S. Machi, "On the Second International Meeting on Radiation Processing", J. of the Atomic Energy Soc. of Japan, 21, 175(1979).

T. Okada, "Radiation and Adhesion", Society of Applied Adhesion Technology, (1978).

T. Okada, "Radiation-Induced After Treatment of Textiles", Sen-i Gakkai-shi (J. of the Society of Fiber Science and Technology, Japan), 34, p-120 (1978).

Y. Ikada, "Characterization of Graft Copolymers", Advances in Polymer Sci., 29, 48 (1978).

Y. Ikada and T. Matsunaga, "Surface Energy of Polymers", Setchyaku Kyokai-shi (J. of the Adhesion Society of Japan), 14, 427 (1978), 15, 18, 91 (1979).

[2] Oral Presentation

1. S. Sugimoto, M. Nishii, and T. Sugiura, "Radiation Effects on the Reaction of Mixtures of Carbon Monoxide and Hydrogen (VII) Effect of Pressure", The 38th Annual Meeting of the Chemical Society of Japan. Apr. 2, 1978.

2. S. Sugimoto and M. Nishii, "Radiation Effects on the Reaction of Mixtures of Carbon Monoxide and Hydrogen (VIII) Effects of Composition and Temperature of Reactants under Elevated Pressures", The 21st Discussion Meeting on Radiation Chemistry, Oct. 30, 1978.

3. S. Nagai, H. Arai, K. Matsuda, and M. Hatada, "Effects of Electron Beam Irradiation on Gas Mixtures of Carbon Monoxide and Hydrogen in the Presence of a Fischer-Tropsch Catalyst", The 21st Discussion Meeting on Radiation Chemistry, Oct. 30, 1978.

4. H. Arai, S. Nagai, K. Matsuda, and M. Hatada, "Electron Beam Irradiation of Methane in a Flow System", The 21st Discussion Meeting on Radiation Chemistry, Oct. 30, 1978.

5. H. Arai and H. Hotta, "The Relation between the Breakdown Time of the Background Gas and the Degree of the Self-Focussing of High-Intensity Pulsed Electron Beam", Riken Symposium on Swarm Experiment and Gas Electronics, Nov. 1978.

6. J. Takezaki, T. Okada, and I. Sakurada, "Solution Polymerization of Styrene in the Presence of Halogen Containing Hydrocarbon by Electron Beams", The 27th Annual Meeting of the Polymer Society, Japan, May 26, 1978.

7. K. Hayashi, M. Tachibana, and S. Okamura, "Polymerization of Chloroprene by Electron Beams", The 21st Discussion Meeting on Radiation Chemistry, Oct. 30, 1978.

8. K. Hayashi, M. Tachibana, and S. Okamura, "Oligomerization of Isoprene by Electron Beams", The 27th Discussion Meeting of the Society of Polymer Science, Nov. 24, 1978.

9. K. Hayashi, M. Tachibana, and S. Okamura, "Polymerization of Isoprene by Electron Beams", The 27th Annual Meeting of the Polymer Society, Japan, May 26, 1978.

10. K. Kaji, T. Okada, and I. Sakurada, "Radiation Grafting of Vinyl Bromide onto Polyester Fabric and Flame-Retardance of the Graft Fabric", Annual Meeting of the Society of Fiber Science and Technology, Jun. 12, 1978.

11. K. Kaji, T. Okada, and I. Sakurada, "Radiation-Induced Grafting of Metallic Salt of Acrylic Acid onto Poly(Vinyl Chloride) Fibers", The 24th Regional Meeting of the

Society of Polymer Science (Kobe), Jul. 12, 1978.

12. Y. Kusama, T. Yagi, H. Yamada, and T. Okada, "Adhesion of Acrylic Acid Grafted Polyvinylchloride to Metal Surface", The 16th Annual Meeting on Adhesion, Jun. 15, 1978.

IV. LIST OF SCIENTISTS

(Mar. 31, 1979)

[1] Staff Members

Yunosuke OSHIMA	Dr., radiation physicist, Head
Tomomichi KASAMATSU*	Radiation physicist, The Former Head
Ichiro SAKURADA	Professor emeritus, Kyoto University, Ex-head
Seizo OKAMURA	Professor emeritus, Kyoto University
Toshio OKADA**	Dr., polymer chemist
Motoyoshi HATADA	Dr., physical chemist
Kanae HAYASHI	Dr., polymer chemist
Shun'ichi SUGIMOTO	Physical chemist
Koji MATSUDA	Radiation physicist
Jun'ichi TAKEZAKI	Physical chemist
Yasuo KUSAMA	Polymer chemist
Masanobu NISHII	Dr., polymer chemist
Siro NAGAI	Dr., physical chemist
Hidehiko ARAI	Physical chemist
Torao TAKAGAKI	Radiation physicist
Kanako KAJI	Polymer chemist
Toshiaki YAGI	Engineering chemist

[2] Advisors and Visiting Researchers

Isamu NITTA	Professor emeritus, Osaka University, Advisor
Shun'ichi OHNISHI	Professor, Kyoto University, Advisor
Yoshito IKADA	Assoc. Professor, Kyoto University, Advisor
Masao KAJIMAKI	Physicist, Duskin Co., Ltd. (May 1975 - Jun. 1978)

*) Appointed Establishment Director, Takasaki Radiation Chemistry Research Establishment.

**) Appointed Deputy Head, Pilot Scale Research Station, Takasaki Radiation Chemistry Research Establishment.